



The exploration of aza-quinolines as hematopoietic prostaglandin D synthase (H-PGDS) inhibitors with low brain exposure

Rodolfo Cadilla^a, David N. Deaton^{a,*}, Young Do^a, Patricia A. Elkins^b, Daniela Ennulat^b, Jeffrey H. Guss^b, Jason Holt^a, Michael R. Jeune^a, Andrew G. King^b, Jan C. Klapwijk^b, H. Fritz Kramer^a, Nicholas J. Kramer^b, Susan B. Laffan^b, Paresh I. Masuria^b, Alan V. McDougal^a, Paul N. Mortenson^d, Caterina Musetti^b, Gregory E. Peckham^a, Beth L. Pietrak^b, Chuck Poole^a, Daniel J. Price^a, Alan R. Rendina^b, Girish Sati^b, Gordon Saxty^d, Barry G. Shearer^a, Lisa M. Shewchuk^a, Helen F. Sneddon^c, Eugene L. Stewart^a, J. Darren Stuart^a, Dean N. Thomas^b, Stephen A. Thomson^a, Paris Ward^b, Joseph W. Wilson^a, Tiahshun Xu^a, Mark A. Youngman^b

^a GlaxoSmithKline, 5 Moore Drive, P.O. Box 13398, Research Triangle Park, NC 27709, USA

^b GlaxoSmithKline, 1250 South Collegeville Road, Collegeville, PA 19426, USA

^c GlaxoSmithKline, Gunnels Wood Road, Stevenage, Hertfordshire SG1 2NY, UK

^d Astex Pharmaceuticals, 436 Cambridge Science Park, Milton Road, Cambridge CB4 0QA, UK

ARTICLE INFO

Keywords:

Prostaglandin D₂
PGD₂
Hematopoietic prostaglandin D synthase
H-PGDS
H-PGDS inhibitor
CNS exposure

ABSTRACT

GlaxoSmithKline and Astex Pharmaceuticals recently disclosed the discovery of the potent H-PGDS inhibitor GSK2894631A **1a** (IC₅₀ = 9.9 nM) as part of a fragment-based drug discovery collaboration with Astex Pharmaceuticals. This molecule exhibited good murine pharmacokinetics, allowing it to be utilized to explore H-PGDS pharmacology *in vivo*. Yet, with prolonged dosing at higher concentrations, **1a** induced CNS toxicity. Looking to attenuate brain penetration in this series, aza-quinolines, were prepared with the intent of increasing polar surface area. Nitrogen substitutions at the 6- and 8-positions of the quinoline were discovered to be tolerated by the enzyme. Subsequent structure activity studies in these aza-quinoline scaffolds led to the identification of 1,8-naphthyridine **1y** (IC₅₀ = 9.4 nM) as a potent peripherally restricted H-PGDS inhibitor. Compound **1y** is efficacious in four *in vivo* inflammatory models and exhibits no CNS toxicity.

1. Introduction

Duchenne muscular dystrophy (DMD) is a degenerative skeletal muscle disease, resulting from exon deletions, insertions, point mutations, duplications, splicing errors, or small deletions in the dystrophin gene on Xp21.¹ The myocyte protein dystrophin helps connect the sarcolemma and the basal lamina of the extracellular matrix to the actin cytoskeleton contractile apparatus, supporting muscle strength and function. Lack of dystrophin results in destabilization of the glycoprotein complex of the sarcolemma with calcium influx, inflammation, and mitochondrial dysfunction, leading to muscle necrosis, fibrosis, and fat deposition.² As muscle repair and reconstruction fails to keep up with muscle deterioration and loss, this debilitating orphan disease results in

progressive loss of muscle function, loss of ambulation, respiratory insufficiency, and cardiomyopathy, leading to a life expectancy of ~ 30 years due to cardiorespiratory complications.³ Dystrophin is the third largest gene in the human genome, containing 79 exons. With over 7,000 identified mutations, it is the most common cause of dystrophinopathy. Due to its X chromosomal linkage, it is primarily a male disease, affecting approximately 1 in 5000 male births. There is no cure for DMD, although treatments, including corticosteroids, cardiovascular drugs (ACE inhibitors and β -blockers), osteoporosis drugs, ventilation, and physical therapy, have delayed disease progression, prolonged life expectancy, and improved quality of life.^{4–5} With its high unmet medical need and associated costs, numerous therapies are under investigation for DMD.^{6–7} Multiple gene therapies seek to target dystrophin directly,

* Corresponding author.

E-mail address: david.n.deaton@gsk.com (D.N. Deaton).

<https://doi.org/10.1016/j.bmc.2020.115791>

Received 25 April 2020; Received in revised form 18 September 2020; Accepted 24 September 2020

Available online 3 October 2020

0968-0896/© 2020 Elsevier Ltd. All rights reserved.

including AAV-delivered mini-dystrophins, stop codon readthrough agents, CRISPR/CAS9 corrective vectors, and exon skipping agents. Agents intended to affect muscle repair are also under consideration, such as myoblast transplant, utrophin modulators targeting cytoskeletal protein upregulation, and myostatin inhibitors. In addition, a host of indirect mechanisms are being explored including histone deacetylase inhibitors, anti-inflammatory agents, anti-fibrotic drugs, calcium rebalancing treatments, and supportive care drugs.

Several lines of evidence link the anti-inflammatory target hemato-poietic prostaglandin D synthase (H-PGDS, EC 5.3.99.2) to DMD.⁸ H-PGDS is induced in necrotic muscle fibers of DMD patients.⁹ Indeed a metabolite of PGD₂, 11,15-dioxo-9 α -hydroxy-2,3,4,5-tetranorprosta-1,20-dioic acid (tetranor-PGDM), is elevated in the urine of DMD patients and correlates with disease progression.^{10–11} Pharmacologically, a H-PGDS inhibitor, HQL-79, suppresses necrotic muscle volume in the mdx mouse model of DMD, as well as attenuating a loss in muscle strength.¹² As another H-PGDS inhibitor, TAS-205, dose-dependently decreased the total excretion of tetranor-PGDM in DMD boys in a phase I clinical trial, there is hope that the observation in rodents may translate to clinical efficacy.¹³

H-PGDS is a σ -class glutathione-S-transferase that converts prostaglandin PGH₂ to PGD₂ in inflammatory cells.^{14–15} It is expressed in mast cells, eosinophils, dendritic cells (DCs), megakaryocytes, and activated type 2 helper T lymphocytes (T_H2 cells), as well as tissue-resident macrophages such as Langerhans cells, Kupffer cells, and microglia. PGD₂ is a cyclic, oxygenated lipid derivative of the polyunsaturated fatty acid arachidonic acid that acts as an autocrine and paracrine factor to induce chemotaxis and stimulate cytokine production in T_H2 cells, mast cells, eosinophils and DCs. PGD₂ signaling is mediated through the seven transmembrane receptors DP₁ (G_s-coupled, stimulates cAMP production and Ca²⁺ release) and DP₂ (Chemoattractant Receptor-homologous molecule expressed on T_H2 cells receptor (CRTH2), G_i-coupled, mobilizes Ca²⁺).¹⁶ Inhibiting H-PGDS attenuates PGD₂ production/signaling and reduces inflammation. H-PGDS has also been implicated in asthma,¹⁷ allergic rhinitis,¹⁸ and Krabbe disease.¹⁹ PGD₂ is also produced by the evolutionarily unrelated, but functionally convergent enzyme, lipocalin prostaglandin D synthase (L-PGDS).²⁰ Selective H-PGDS inhibition is expected to provide anti-inflammatory benefits, without side effects from ablation of all PGD₂ signaling via pan-PGDS inhibition or direct antagonism of DP₁ and/or DP₂.

As a consequence of the roles of PGD₂ in the biology of inflammatory diseases, researchers have exerted significant efforts to discover H-PGDS

inhibitors and study their effects in animal models. A number of companies, including Osaka (HQL-79),²¹ Evotec,²² AstraZeneca,²³ Pfizer,²⁴ and Sanofi (SAR191801B)²⁵ have published their efforts, with some of this work being recently reviewed.²⁶ Furthermore, Taiho has entered the clinic with TAS-205 to treat Duchenne muscular dystrophy patients.¹³ The structures of several representative H-PGDS tool compounds are depicted in Fig. 1. Although these developments are promising, attempts to translate efficacious tool compounds in animal models into safe and effective approved drugs in humans encounter many difficulties. These difficulties include interspecies alterations in pharmacokinetics related to plasma protein binding differences,^{27–28} phase 1 metabolism inequalities, due to variations in enzyme expression, activity, and drug affinity,²⁹ phase 2 conjugation distinctions,³⁰ gut microbiome colonization disparities,³¹ and drug metabolite discrepancies. Furthermore, in humans, pharmacokinetics and pharmacodynamics can vary due to age,³² sex,^{33–34} and ethnicity,³⁵ as well as between healthy volunteers and diseased patient populations.³⁶ Moreover, animal disease models may not translate to human efficacy in diseased patients.³⁷ All of these complications can make translations from preclinical species to humans troublesome, potentially leading to poor human exposure,^{38–40} human toxicity, and/or lack of efficacy in humans. Due to these high attrition rates, maximizing the probability of clinical success in treating diseases with aberrant PGD₂ production requires the progression of multiple H-PGDS chemotypes into human studies to ultimately discover a H-PGDS medicine, necessitating continued efforts to discover and develop new H-PGDS agents.

These authors recently disclosed the discovery of the H-PGDS tool compound GSK2894631A **1a**, which was elaborated from a ligand efficient fragment, quinoline-3-carbonitrile (IC₅₀ = 220,000 nM, LE = 0.43), as part of a larger fragment-based drug discovery collaboration^{41–42} between Astex Therapeutics and GlaxoSmithKline.⁴³ The tool compound **1a** (IC₅₀ = 9.9 nM, LE = 0.42) is a potent, competitive, and reversible inhibitor of H-PGDS, as measured in a RapidFire™ mass spectrometry assay determining the inhibition of the conversion of PGH₂, generated *in situ* by COX-2 from arachidonic acid, to PGD₂. In addition, compound **1a** exhibited good H-PGDS cellular activity (RBL IC₅₀ = 160 nM) in a rat basophilic leukemia (RBL) cell PGD₂ production assay. An X-ray co-crystal structure of **1a** bound to hH-PGDS and the glutathione cofactor (PDB Code #6N4E) reveals several key contributions to this high potency, including hydrogen bonds between the basic quinoline nitrogen and an enzyme-bound, structural water molecule and between the carboxamide NH and thiol of the glutathione cofactor, as

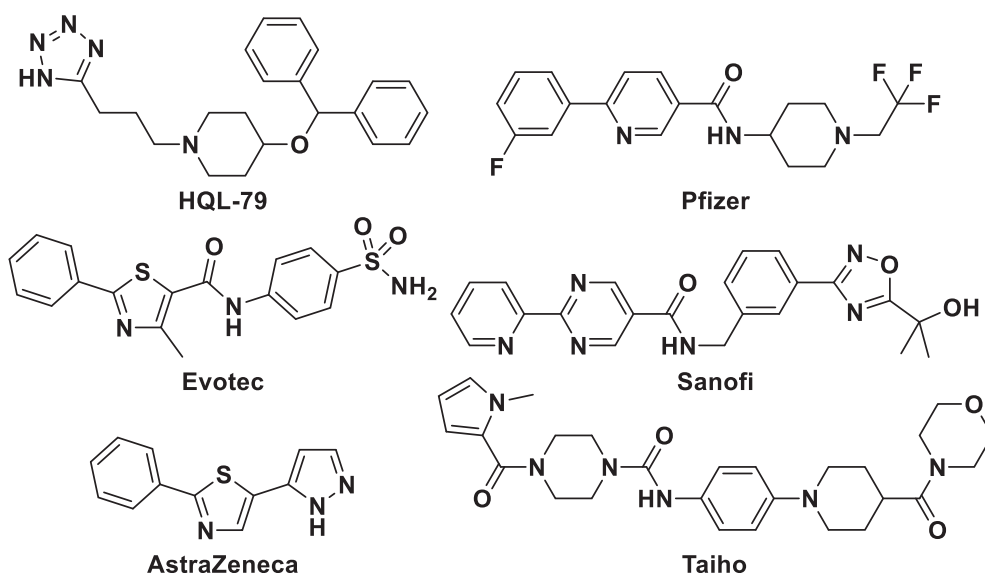


Fig. 1. H-PGDS Tool Compounds.

well as a face-to-face π - π stacking interaction between the quinoline ring and the indole of ¹⁰⁴Trp. In addition, compound **1a** had a low *i.v.* clearance ($C_l = 5.6$ mL/min/kg), moderate *i.v.* steady state volume of distribution ($V_{SS} = 1.7$ l/kg), long *i.v.* terminal half-life ($t_{1/2} = 3.8$ hr), and good oral exposure (*p.o.* DNAUC = 1800 ng/hr/mL, $F = 61\%$) in mice, making it suitable for exploring PGD₂ *in vivo* biology. Indeed, compound **1a** attenuated PGD₂ production in an acute *in vivo* murine mast cell degranulation model ($ED_{50} = 0.032$ mg/kg, $EC_{50} = 21$ nM) of inflammation.

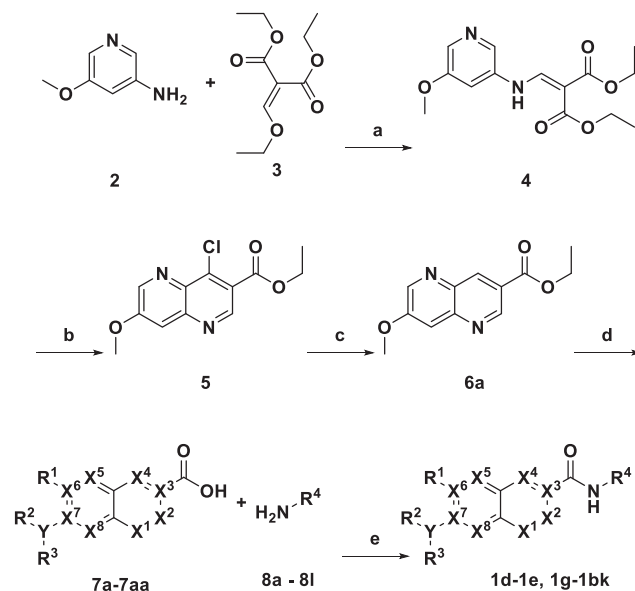
Unfortunately, at higher doses (≥ 10 mg/kg) in a chronic eccentric muscle damage model (*vide infra* Fig. 6) in mice, **1a**-treated animals exhibited seizure-like activity at day four of dosing, precluding its further development. No adverse effects were seen in lower dose groups (≤ 6 mg/kg) at up to 60 days of treatment. Furthermore, another quinoline H-PGDS inhibitor, with a higher brain to plasma ratio than **1a**, showed seizure symptoms earlier, at day two of dosing (10 mg/kg), in this same muscle damage model. Even though **1a** did not exhibit activity in a broad panel of over 40 protein assays at concentrations of 10,000 nM, the seizure-like symptoms were likely off-target, as they were also seen in the chronic eccentric muscle damage model dosed in H-PGDS (-/-) mice. H-PGDS inhibitor **1a** crosses the blood:brain barrier and has a brain to blood ratio of 0.59. Thus, elevated CNS concentrations of **1a**, at higher doses and prolonged exposures, are presumed to induce these adverse events. Under this hypothesis, one strategy to circumvent this toxicity is to limit brain penetration of the H-PGDS inhibitor, thus preventing interference with any putative CNS protein.

There are several chemical strategies for lowering brain exposure,⁴⁴ including increasing hydrogen bond donors,⁴⁵ lowering intrinsic permeability/lipophilicity,⁴⁶ adding negative charges,⁴⁷ increasing active brain transporter (e.g. P-glycoprotein) efflux,⁴⁸ and increasing polar surface area (PSA)⁴⁹ in the inhibitor template. The latter tactic, increasing the PSA of the quinoline template, was explored. Generally, molecules with PSAs greater than 90 Å² are poorly brain penetrant.⁵⁰ Substituting a nitrogen atom for a carbon atom in the quinoline ring results in 13 Å² increase in calculated topological polar surface area (tPSA) (e.g. **1c** tPSA = ~ 71 Å² \rightarrow **1e** tPSA = 84 Å²).

It was recognized that the strategy of inflating tPSA, via introduction of additional nitrogens in the quinoline heterocycle, has several ramifications on protein-ligand interactions, creating some challenges in intentional design. Calculated pK_a 's for N1 for several prospective heterocycles (data not shown) confirmed the supposition that N1 basicity could be significantly modulated, and as a result, hydrogen-bond strengths with both a structural, protein-bound water, and with water in bulk solution would be affected. To what extent modulating these interactions would cancel was unclear *a priori*. Desolvation of an addition hydrogen-bond acceptor was expected to be a factor in binding potency as well. Furthermore, the heterocycle's dipole, quadrupole, and inducible dipole moments that contribute to π - π stacking strength could be affected and conceivably alter the strength of interactions with ¹⁰⁴Trp in the binding site. Finally, introducing electron density in proximity to substitution, in particular the central amide, could impact conformational preference and therefore the energy required to adopt the bound conformation. Given the complicated balance of energetics at play, a deliberate and methodical exploration of aza-quinolines, derived from compound **1c**, was implemented to explore their effects on H-PGDS inhibition, CNS exposure, and other drug properties.

2. Chemistry

The aza-quinolines could be prepared as shown in Schemes 1–4. The 1,5-naphthyridine **6a** was synthesized as depicted in Scheme 1. First, thermal condensation of aniline **2** with diethyl 2-(ethoxymethylene) malonate **3**, via 1,4-aza-Michael addition, followed by β -elimination of ethanol, afforded the aminomethylenemalonate **4**. Then, phosphorus oxychloride catalyzed Friedel-Craft acylation of **4** yielded the 4-chloro-aza-quinoline **5**. Subsequent palladium catalyzed dechlorination of **5**,



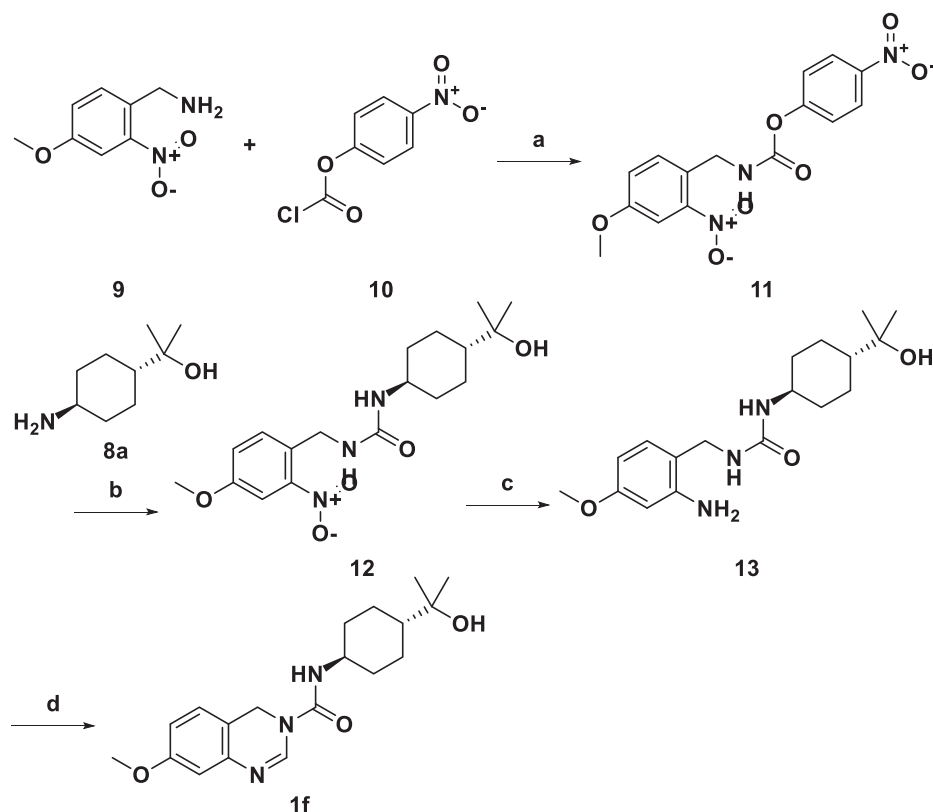
$X^1 = N, CH$; $X^2 = N, CH$; $X^3 = N, C, CH$; $X^4 = N, CH, CH_2$; $X^5 = N, CH$; $X^6 = N, C$; $X^7 = N, C$; $X^8 = N, CH$; $Y = O, S, SO, N, CH, Cl$; $R^1 = H, Cl$; $R^2, R^3 = H, CH_3, CF_3CH_2, CF_2HCH_2, -(CH_2)_2, -(CH_2)_3, -CH(CH_3)CH_2CH_2, -CH_2CH_2CH_2-$.

Scheme 1. Synthesis of aza-quinolines. Reagents and conditions: a) EtOH, 80 °C, 84%; b) POCl₃, μ W, 160 °C, 55%; c) Pd(PPh₃)₂Cl₂, Et₃SiH, MeCN, 70 °C, 46%; d) LiOH, THF, EtOH, H₂O, 50 °C, 99%; e) T3P® or HATU, iPr₂NEt, DMF, 21–90%.

employing triethylsilane as the reductant, yielded the aza-quinoline ester **6a**. Some carboxylic acid precursors, such as 6-methoxy-2-naphthoic acid **7a**, 7-methoxycinnoline-3-carboxylic acid **7b**, or 1,7-naphthyridine-3-carboxylic acid **7f**, were commercially available, while others, such as 6-methoxyquinoxaline-2-carboxylic acid **7c**, were prepared via literature procedures, and the rest, such as **7d-7e** and **7g-7aa** were synthesized according to Schemes 1, 3, or 4. Thus, lithium hydroxide catalyzed hydrolysis of ester **6a** provided 7-methoxy-1,5-naphthyridine-3-carboxylic acid **7d**. These carboxylic acids **7a-7aa** were coupled to various amines, either commercially available (**8a-8e**, **8j**, and **8l**) or known in the chemical literature (**8f-8i** and **8k**),^{43,51–53} to give the target compounds **1d-1e**, and **1g-1bk**.

The 7-methoxyquinazoline-3(4*H*)-carboxamide **1f** was prepared as shown in Scheme 2. First, the amine **9** was coupled to the chloroformate **10** to afford the carbamate **11**. Then, displacement of the *para*-nitrophenol moiety of activated carbamate **11**, with amine **8a**, gave the urea **12**. Subsequent palladium catalyzed reduction of the nitro group of urea **12**, employing hydrogen as the reductant, provided the aniline **13**. Finally, condensation of aniline **13** with triethylorthoformate, followed by ring closure, and loss of ethanol afforded the quinazoline **1f**.

The 7-methoxy-1,6-naphthyridine-3-carboxylic acid **7e** was synthesized as illustrated in Scheme 3. First, ytterbium catalyzed condensation of aniline **14** with acetal **15**, followed by cyclization, and dehydration afforded the 3-bromo-1,6-naphthyridine **16a**. Then, palladium catalyzed carbonylation of bromide **16a**, with carbon monoxide, afforded ethyl 7-chloro-1,6-naphthyridine-3-carboxylate **17a**. Finally, methoxide displacement of chloride **17a** and subsequent ester hydrolysis gave 1,6-naphthyridine-3-carboxylic acid **7e**. Alternatively, 7-methoxy-1,8-naphthyridine-3-carboxylic acid **7g** was prepared from pyridine-2,6-diamine **18**. First, phosphoric acid catalyzed condensation of aniline **18** with 2-bromomalonadehyde **19**, followed by Friedel-Craft cyclization and dehydration provided 6-bromo-1,8-naphthyridin-2-amine **16b**. Then, carbonylation of bromide **16b**, catalyzed by palladium, yielded the ester



Scheme 2. Synthesis of the 7-methoxyquinazoline-3(4H)-carboxamide **1f**. Reagents and conditions: a) $i\text{Pr}_2\text{NEt}$, THF, 88%; b) $i\text{Pr}_2\text{NEt}$, THF, 79%; c) $\text{H}_2/\text{Pd-C}$, MeOH, 100%; d) $(\text{EtO})_3\text{CH}$, 102 °C, 31%.

17b. Subsequent diazotization of aniline **17b** provided the 7-hydroxy-1,8-naphthyridine, which was converted to the chloride **17c** via phosphorus oxychloride. Finally, methoxide displacement of chloride **17c** and subsequent ester hydrolysis gave 1,8-naphthyridine-3-carboxylic acid **7g**. Furthermore, aniline **16b** was chlorinated with concentrated hydrochloric acid and hydrogen peroxide to afford 6-bromo-3-chloro-1,8-naphthyridin-2-amine **16c**. Then, carbonylation of **16c**, in a similar manner as above, gave the ester **17f**. Conversion of the aniline **17f** to the hydroxyl **17g**, via *in situ* generated nitrous acid, then transformation to the chloride provided dichloride **17h**. Treatment of the chloride **17h** with sodium methoxide afforded the ester **6o**, whereas, treatment of the chloride **17h** with sodium 2,2,2-trifluoroethan-1-ol led to carboxylic acid **7m**, via *in situ* hydrolysis. Moreover, chlorides **17a**, **17c**, and **17h** were converted to 7-amino/oxy derivatives **6c-6e**, **6g-6k**, and **6p-6q** or 7-alkyl derivatives **6f**, **6l-6n**, and **6r**, via $\text{S}_{\text{N}}\text{Ar}$ displacement with nucleophiles or Suzuki/Negishi couplings with boronic acids/zinc reagents, respectively. Upon hydrolysis, these esters, as well as esters **6b**, **6s**, and **6t** prepared according to Scheme 4, afforded carboxylic acids **7h-7l** and **7n-7aa**.

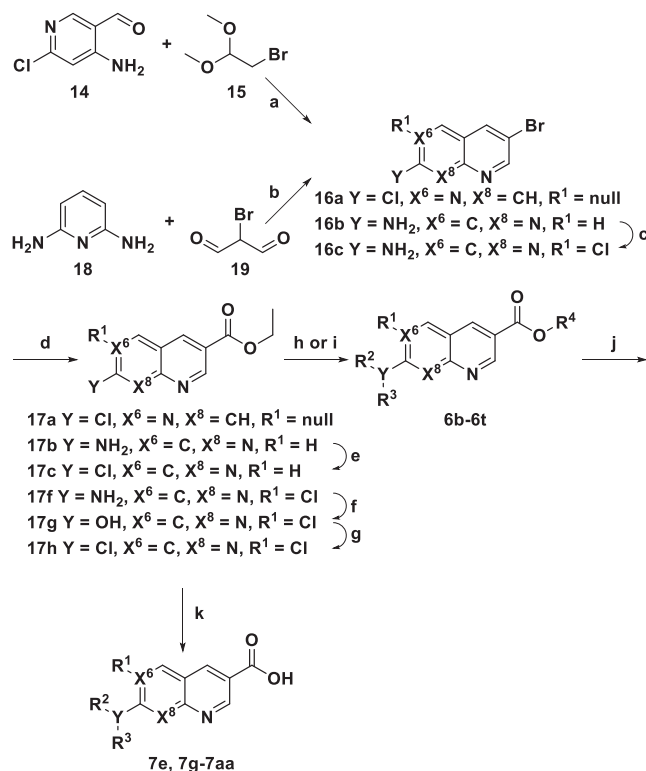
The ethyl 2-methoxyprido[2,3-*d*]pyrimidine-6-carboxylate **6b** was synthesized as shown in Scheme 4. First, aldol condensation of aldehyde **20** with malonate **21**, followed by dehydration and cyclization, afforded the 7-oxo-7,8-dihydropyrido[2,3-*d*]pyrimidine **22**. Then, treatment with phosphorus oxychloride provided the chloride **23**. Subsequent palladium catalyzed dechlorination of **23**, employing triethylsilane as the reductant, yielded the pyrido[2,3-*d*]pyrimidine **17d**. Oxidation of the sulfide **17d** with varying amounts of *meta*-chloroperoxybenzoic acid then afforded either the sulfoxide **17e** or the sulfone **17i**. Subsequent displacement of the oxidized sulfur moiety with oxygen or nitrogen nucleophiles, respectively, then gave the esters **6b** and **6s**. Furthermore, the 7-alkyl derivative **6t** was prepared from aniline **24**. First, acylation of aniline **24** with cyclopropanecarbonyl chloride gave the amide **25**. Then, condensation of aniline **25** with ammonia, followed by

cyclization, and elimination yielded the bromide **16d**. Then, carbonylation of bromide **16d**, under a carbon monoxide atmosphere, catalyzed by palladium, yielded the ester **6t**.

3. Results and discussion

3.1. Aza-quinoline template SAR

As mentioned above, a consequence of this strategy to inflate the tPSA of H-PGDS inhibitors with the introduction of additional ring nitrogens is that these substitutions in the quinoline template lead to alterations in the basicity of the ring as well as the hydrogen bonding acceptor capacity of the N1 nitrogen of these aza-analogs, compared with their corresponding quinolines (e.g. **1c** meas. $\text{pK}_{\text{A}} = 3.59$, calc. $\text{pK}_{\text{A}} = 3.38$ versus **1i** meas. $\text{pK}_{\text{A}} < 2.0$, calc. $\text{pK}_{\text{A}} = 0.87$). These property changes could affect the strength of a key hydrogen bond between the N1 nitrogen and the aforementioned structural water molecule that is observed crystallographically in the H-PGDS active site. They may also alter the π - π stacking interaction with ^{104}Trp and increase the desolvation penalty for an aza-quinoline relative to its corresponding quinoline. This initial structure/activity exploration was conducted with the 7-methoxy group to ease the synthesis of aza-analogs and avoid exposure to difluoromethanol which might be metabolically activated to toxic fluorophosgene. Initially, the contribution of the N1 hydrogen bond enzyme interaction to inhibitor binding was probed by replacing the quinoline nitrogen with a carbon atom, eliminating hydrogen bonding acceptor ability in the analog. As shown in Table 1, the non-basic naphthalene analog **1d** ($\text{IC}_{50} = 1300 \text{ nM}$) is almost 2 orders of magnitude less potent than quinoline **1c** ($\text{IC}_{50} = 25 \text{ nM}$) yet pays a lower desolvation cost than the quinoline. Thus, the N1 hydrogen bond likely affords at least 2.4 kcal/mol ($\Delta G = -RT\ln K_i$) to inhibitor binding energy, and any aza-quinoline analog that has reduced hydrogen bond acceptor capacity at its N1 nitrogen, should form an attenuated hydrogen bond

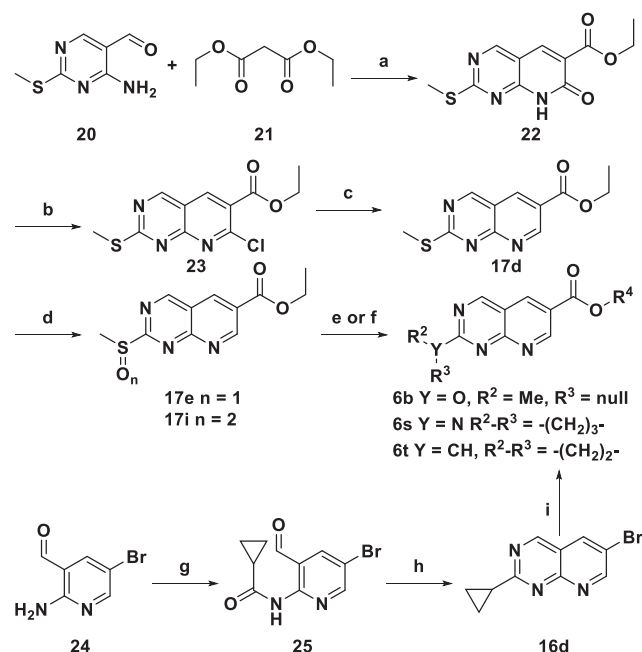


Scheme 3. Synthesis of 1,6-naphthyridine acids. Reagents and conditions: a) Yb(OTf)₃, MeCN, 80 °C, 35%; b) H₃PO₄, 120 °C, 38%; c) HCl, H₂O₂, 25%; d) Pd(dppf)Cl₂•CH₂Cl₂, CO, NEt₃, EtOH, 80 °C, 46–63%; e) NaNO₂, H₂SO₄, r.t.; iPr₂NEt, POCl₃, 80 °C, 55%; f) NaNO₂, H₂SO₄, r.t.; 64%; g) iPr₂NEt, POCl₃, dioxane, 80 °C, 52%; h) R²R³NH₂, iPr₂NEt, DMF or NMP, 100 °C, μW, 16–94%; i) R²R³YB(OH)₂ or R²R³YBZnBr, Pd₂(dba)₃/SPhos or Pd(dppf)Cl₂/CuI, Na₂CO₃, PhMe or THF, 60–110 °C, 21–91%; j) LiOH or NaOH, MeOH or THF, H₂O, 25–60 °C, 19–100%; k) NaOMe or NaOCH₂CF₃, MeOH, 60 °C, 98–100%.

with the protein, resulting in weaker binding of the aza-quinoline. For other templates explored in these laboratories, this hydrogen bond interaction can be less critical for potency.

Although the cinnoline analog **1e** (IC₅₀ 7900 nM) accomplishes design objectives of increasing tPSA (tPSA = 84 Å²), it is over two orders of magnitude less potent than quinoline **1c**. The cinnoline (meas. pK_A = <2.0, calc. pK_A = 0.55) is substantially less basic than its quinoline congener (meas. pK_A = 3.59, calc. pK_A = 3.38), yet its calculated N1 hydrogen bond acceptor strength (HBAS) (14.3 kcal/mol) is less than 2 kcal/mol less than the quinoline (16.1 kcal/mol). Thus, a weaker hydrogen bond and altered desolvation penalties are probably only partial contributors to the decreased binding. Another plausible explanation to account for the observed activity relies on ground state versus bound state energies. The cinnoline N2-nitrogen lone pair induces a preferred unbound conformation that results in an intramolecular hydrogen bond with the NH of the amide and this conformation differs geometrically – based on the H-PGDS ligand bound crystal structures – and energetically from the protein-bound conformation, which would prefer a conformation that allows formation of a hydrogen bond between the glutathione cofactor and the amide NH (*vide infra*). The preferred bound conformation would be energetically unfavorable because of lone pair:lone pair repulsion between the N2 nitrogen and the amide carbonyl oxygen, resulting in a lower observed binding affinity from this significant preorganization penalty in the form of the electrostatic clash, and likely accounts significantly for its > 300-fold loss in potency relative to **1c**.

Consistent with the assertion that the cinnoline N2 nitrogen steers the carbonyl oxygen away from the bound conformation, the quinoxaline **1g** should conversely promote the bound amide orientation, with its



Scheme 4. Synthesis of pyrido[2,3-d]pyrimidines. Reagents and conditions: a) K₂CO₃, NEt₃, DMF, 80 °C, 45%; b) POCl₃, 100 °C, 94%; c) Pd(PPh₃)₃Cl Et₃SiH, MeCN, 80 °C, 49%; d) m-CPBA, CH₂Cl₂, 0 °C, 73–78%. e) NaOMe, MeOH, 37%; f) azetidine, iPr₂NEt, NMP, 100 °C, μW, 11%; g) cPrCOCl, pyridine, CH₂Cl₂, 90%; h) NH₃, MeOH, sealed tube, 80 °C, 67%; i) Pd(dppf)Cl₂•CH₂Cl₂, CO, iPr₂NEt, EtOH, 80 °C, 65%.

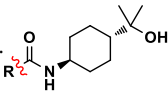
N4 nitrogen forming an intramolecular hydrogen bond with the amide NH. Indeed, the quinoxaline **1g** (IC₅₀ = 490 nM, tPSA = 84 Å²) is an order of magnitude more potent than the cinnoline, though, it still remains ~ 20-fold less potent than the original quinoline. The quinoxaline's calculated N1 HBAS (13.6 kcal/mol) is over 2 kcal/mol less than the quinoline (16.1 kcal/mol), while its basicity (meas. pK_A = <2.0, calc. pK_A = 0.62) is similar to the cinnoline **1e**. The quinoxaline's weaker hydrogen acceptor capacity, poorer π-π stacking alignment of ¹⁰⁴Trp indole and quinoxaline dipoles, and the increased desolvation cost, arising from the additional ring nitrogen, likely account for its reduced inhibitory activity relative to quinoline **1c**.

In contrast to the cinnoline **1e**, the 3,4-dihydroquinazoline analog **1f** (IC₅₀ = 890 nM, meas. pK_A = 4.31, calc. pK_A = 3.99, tPSA = 74 Å²) is slightly more basic than the parent quinoline **1c** and should form a stronger hydrogen bond with the H-PGDS protein (calc. HBAS = 15.7 kcal/mol). Its 35-fold reduced inhibition activity, despite its stronger hydrogen bonding potential, likely results from a reduced π-π stacking interaction (*vide infra*) between the indole of ¹⁰⁴Trp and the non-aromatic partially saturated dihydroquinazoline ring with its reduced planarity.

The N1 nitrogen of the 1,5-naphthyridine analog **1h** (IC₅₀ = 180 nM, tPSA = 84 Å²) is predicted to be slightly more basic (meas. pK_A = <2.0, calc. pK_A = 0.91) than the quinoxaline **1g** with a similar N1 nitrogen calculated HBAS (15.8 kcal/mol) to the quinoline **1c** and only loses 7-fold inhibitory potency relative to the parent quinoline **1c**, even though the rotamer of the amide is not conformationally biased. Furthermore, the N1 nitrogen of the 1,6-naphthyridine analog **1i** (IC₅₀ = 45 nM, tPSA = 84 Å²) is similar in basicity (meas. pK_A = <2.0, calc. pK_A = 0.87) to the 5-aza-quinoline analog **1h**, with lower N1 nitrogen calculated HBAS (14.2 kcal/mol) and yet is ~ 4-fold more active than **1h**. Intriguingly, ¹⁴Arg occupies two different rotamers in the two copies of the H-PGDS binding site in the asymmetric unit of another 1,6-naphthyridine **1m** (*vide infra*), with one conformation placing the electron-deficient guanidinium side chain in proximity to the N6 nitrogen. Even partial occupancy of this conformation for **1i** may minimize the

Table 1

H-PGDS enzyme inhibition data for aza-quinoline templates.



#	R	IC ₅₀ ± S.D. ^a nM	EC ₅₀ ± S.D. ^b nM	Meas. pK _A ^c	Calc. pK _A ^d
1a		9.9 ± 2.7	160 ± 160	2.43	3.03
1b		1800 ± 1100	30,000 ± 2,900	3.02	3.02
1c		25 ± 3.4	100 ± 60	3.59	3.38
1d		1300 ± 840	>50,000	–	–
1e		7900 ^e ± 2600	>50,000	<2.0	0.55
1f		890 ± 260	4300 ± 3500	4.31	3.99
1g		490 ± 260	3200 ± 620	<2.0	0.62
1h		180 ± 99	740 ± 190	<2.0	0.91
1i		45 ± 38	190 ± 69	<2.0	0.87
1j		7700 ^f ± 2600	39,000 ^g ± 16,000	2.74	2.5
1k		30 ± 30	150 ± 13	2.58	–0.24
1l		140 ± 69	2000 ± 1000	<2.0	–2.81

^a S.D. = standard deviation; mean ± S.D. All inhibitors were tested with N ≥ 4 in the H-PGDS RapidFire™ High Throughput Mass Spectrometry Assay.

^b S.D. = standard deviation; mean ± S.D. All inhibitors were tested with N ≥ 2 in the H-PGDS Rat Basophilic Leukemia (RBL) cell inhibition assay.

^c Measured basic pK_A.

^d Calculated basic pK_A. pK_As were calculated using the ChemAxon software program prediction.

^e Individual replicate pIC₅₀ = 5.16, 5.34, <5.0, <5.0. The mean was obtained by removing the < qualifier and averaging the values.

^f Individual replicate pIC₅₀ = 5.26, 5.27, <5.0, <5.0. The mean was obtained by removing the < qualifier and averaging the values.

^g Individual replicate pIC₅₀ = 4.57, <4.30. The mean was obtained by removing the < qualifier and averaging the values.

desolvation penalty associated with removing the N6 nitrogen from bulk solution and may distinguish this aza-regioisomer from the less potent quinoxaline **1g** and 1,5-naphthyridine **1h**. The pK_A of the N1 nitrogen of 1,8-naphthyridine **1k** (IC₅₀ = 30 nM, tPSA = 84 Å²) is ~ 1 order of magnitude less basic (meas. pK_A = 2.58, calc. pK_A = –0.24) than the quinoline **1c**, with lower calculated N1 nitrogen HBAS (13.6 kcal/mol), and yet these compounds have similar potency. Possibly, both the N1 and N8 nitrogens of the 1,8-naphthyridine **1k** can interact with the conserved water molecule and this dual polar interaction compensates for its reduced N1 acceptor strength. Finally, the N1 nitrogen of 1,7-naphthyridine **1j** is a weaker hydrogen bond acceptor (meas. pK_A = 2.74, calc. pK_A = 2.5, calc. HBAS = 13.5 kcal/mol) than the N1 nitrogen of its direct comparator quinoline **1b** and **1j** (IC₅₀ = 7,700 nM, tPSA = 75 Å²) is less potent than quinoline **1b** (IC₅₀ = 1,800 nM, meas. pK_A = 3.02, calc. pK_A = 3.02, HBAS = 14.8 kcal/mol, tPSA = 62 Å²).

Since the 6-aza and 8-aza-quinoline analogs **1i** and **1k** were both potent H-PGDS inhibitors, the more polar pyrido[2,3-*d*]pyrimidine analog **1l** (IC₅₀ = 140 nM, meas. pK_A = <2.0, calc. pK_A = –2.81, HBAS = 12.3 kcal/mol, tPSA = 97 Å²) was also prepared, in an effort to further

attenuate brain penetration through increased tPSA. The slightly lower potency of this compound likely results from the increased binding desolvation cost of an additional heteroatom in the 6,8-diazaquinoline template.

Desiring to identify aza-quinoline inhibitors with similar or better properties than previous tool compounds as potential development candidates, structure/activity relationships (SAR) in the quinoline series were used to set analog advancement criteria for the aza-quinoline templates. These learnings revealed that compounds with H-PGDS Rapid-Fire™ mass spectroscopy inhibition assay IC₅₀ ≤ 100 nM, artificial membrane permeability assay permeabilities P_{App} ≥ 30 nm/sec, and protein binding ≤ 95%, usually exhibited good cell potency in a rat basophilic leukemia (RBL) cell H-PGDS inhibition assay. Furthermore, analogs with RBL IC₅₀ ≤ 300 nM, good solubility (FaS-SIF solubility ≥ 0.025 mg/mL), and acceptable murine pharmacokinetics (*p.o.* DNAUC ≥ 1000 ng/hr/mL) usually were efficacious *in vivo* in the chronic murine eccentric muscle damage model. The most potent of these aza-quinoline analogs in the enzyme assay, the 1–6 and 1,8-naphthyridines **1i** (RBL IC₅₀ = 190 nM) and **1k** (RBL IC₅₀ = 150 nM), were also potent inhibitors of PGD₂ production in the RBL cellular assay, so it was decided to focus further research efforts on these templates.

An early read on metabolic stability, surprisingly revealed that the 7-methoxy-1,6-naphthyridine **1i** (t_{1/2} = >3 hr) and 7-methoxy-1,8-naphthyridine **1k** (t_{1/2} = >3 hr) had long half-lives in an *in vitro* mouse liver microsome assay, as shown in Table 2. However, and not unexpectedly, **1i** (*p.o.* DNAUC = 104 ng/hr/mL) and **1k** (*p.o.* DNAUC = 64.9 ng/hr/mL) exhibited poor oral exposure in a mouse pharmacokinetic study, likely due to *O*-dealkylation of the 7-methoxy methyl group. Because of this poor oral exposure, compound concentrations in the brain were not determined. Since both ligand-bound protein crystal structures and exhaustive SAR of the quinoline template revealed flexibility in substitution at the 6 and 7-positions of that scaffold, those learnings were applied to the 6- and 7-positions of the naphthyridine scaffolds in an attempt to alter their chemical properties toward improved pharmacokinetics.

3.2. Aza-quinoline substitution SAR

Previous SAR revealed that small alkyl groups and small heterocycles projecting from the seven position of the quinoline are tolerated, so these modifications were incorporated into the 1,6-naphthyridine template. As shown in Table 3, the 7-azetidine derivative **1m** (IC₅₀ = 3.9 nM, tPSA = 78 Å²) is ~ 11-fold more potent than its 7-methoxy comparator **1i**. The π-electron-rich azetidine ring nitrogen donates its electrons into the aromatic π-system of the naphthyridine ring, enhancing both its π-π stacking with ¹⁰⁴Trp and the hydrogen bond to the structural water molecule in the active site of the protein via modulation of the N1 nitrogen basicity. These reinforced interactions, as well as hydrophobic contributions of the propylene to the binding affinity, likely account for its substantial increase in inhibitory activity. Like the methoxy analog **1i**, the azetidine derivative **1m** was moderately stable to mouse liver microsomes (t_{1/2} = 2.7 hr) but had poor oral exposure (*p.o.* DNAUC = 41.0 ng/hr/mL).

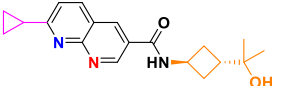
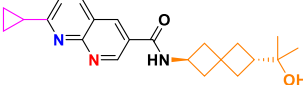
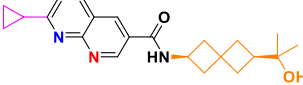
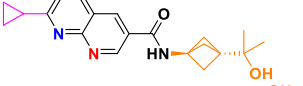
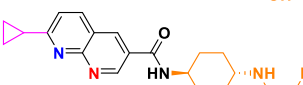
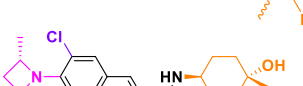
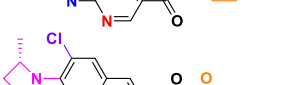
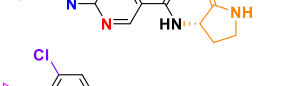
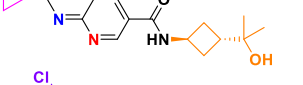
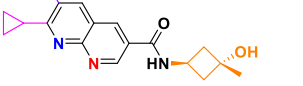
The 3-fluoro and 2-methyl azetidine derivatives **1n** (IC₅₀ = 12 nM, tPSA = 78 Å²), **1o** (IC₅₀ = 160 nM, tPSA = 78 Å²) and **1p** (IC₅₀ = 4.8 nM, tPSA = 78 Å²) were prepared in an effort to eliminate potential metabolism of the azetidine ring either through electronic or steric alterations. The electron withdrawing nature of the fluorine substituent in **1n** attenuates the electron donation capabilities of the azetidine nitrogen, lowering the compound's potency relative to the naked azetidine **1m**, while the (*S*)-methyl analog **1p** maintains similar activity to **1m**. In contrast, the (*R*)-methyl azetidine **1o** is substantially less active than the unsubstituted analog **1m**. This (*R*)-enantiomer is likely sterically encumbering to the protein, and thus substantially reduces its relative potency. Unfortunately, these modifications did not improve drug properties, as the (*S*)-methylazetidine **1p** (t_{1/2} = 0.98 hr) was quickly

Table 2
H-PGDS drug property data for aza-quinolines.

#	Structure	AMP ^a P _{APP} nm/s	FaS-SIF ^b mg/mL	mLM ^c t _{1/2} min	PB ^d %	DNAUC ^e ng•kg•hr/mL/mg
1a		240	0.070	>180 ^f	88	1820
1i		61	0.085	>180	67	104
1k		–	0.024	>180	73	64.9
1m		78	0.011	161 ^f	79	41.0
1n		–	0.013	>180 ^f	73	19.3
1q		165	0.027	>180 ^f	84	1040
1s		23	0.003	>180 ^f	80	72.5
1v		25	0.270	>180 ^f	78	73.7
1y		44	0.140	>180	80	1320
1af		<10	0.210	146	54	23.4
1ag		22	–	>180	64	204
1ah		38	0.460	>180 ^f	52	46.9
1ai		<10	0.400	>180 ^f	59	250
1aj		14	0.630	>180	56	715
1ak		130	0.280	>180	76	45.3
1an		30	0.430	147	43	262
1ao		180	0.100	>180	–	693
1ap		270	>1.000	>180	–	358
1at		–	0.100	>180	74	77.5

(continued on next page)

Table 2 (continued)

#	Structure	AMP ^a P _{APP} nm/s	FaS-SIF ^b mg/mL	mLM ^c t _{1/2} min	PB ^d %	DNAUC ^e ng•kg•hr/mL/mg
1au		45	0.035	>180 ^f	86	477
1av		54	0.034	>180 ^f	86	441
1aw		34	0.40	>180	69	285
1ba		170	>1.000	>180	82	681
1bf		110	0.740	>180	87	132
1bg		<3	>1.000	>180	81	86.2
1bh		280	0.046	>180	88	452
1bi		150	0.700	>180	86	362
1bj		220	0.031	>180	87	152
1bk		30	0.120	>180	81	252

^a Artificial membrane permeability assay at pH = 7.4 (P_{APP} = apparent permeability).^b Fasted state-simulated intestinal fluid solubility assay at pH = 6.5.^c Mouse liver microsome metabolism assay.^d Human serum albumin protein binding assay, % compound bound.^e Dose normalized area under the curve observed for the blood concentration versus time plot for an oral dose of 3.0 mg/kg in mice.^f Mouse S9 fraction assay.^g Tested as the racemate.

metabolized by mouse liver microsomes, and, although the 2-fluoroazetidine **1n** (t_{1/2} = >3 hr) was more stable in mouse liver microsomes, it had poor oral exposure in mice (*p.o.* DNAUC = 19.3 ng/hr/mL).

The 7-cyclopropyl analog **1q** (IC₅₀ = 14 nM, tPSA = 75 Å²) is less electron donating compared to the 7-methoxy compound **1i** and therefore provides a less basic compound that likely forms a weaker hydrogen bond with the structural water molecule in the active site, yet it has greater H-PGDS inhibitory activity than **1i**. Presumably, the hydrophobic contribution of the cyclopropyl group to binding compensates for the reduced hydrogen bonding interactions. In contrast to the methoxy and azetidine derivatives, **1q** had good *in vitro* metabolic stability and excellent oral exposure in mice (mLM t_{1/2} = > 3.0 hr, *p.o.* DNAUC =

1040 ng/hr/mL).

Small substitutions at the 7-position of the 1,8-naphthyridine template were also investigated. As shown in Table 3, the 2,2,2-trifluoroethoxy analog **1r** (IC₅₀ = 350 nM, tPSA = 78 Å²), prepared to prevent *O*-dealkylation, was an order of magnitude less potent than the parent 7-methoxy-1,8-naphthyridine **1k**. Although some of this activity loss could result from the reduced hydrogen bond acceptor capacity of the N1-nitrogen, likely steric clashes of the trifluoroethyl group with the protein prevent favorable binding to the H-PGDS protein.

In addition, the 7-azetidino analogs **1s** (IC₅₀ = 5.3 nM, meas. pK_A = 5.03, HBAS = 13.6 kcal/mol, tPSA = 78 Å²), **1t** (IC₅₀ = 13 nM, tPSA = 78 Å²), **1u** (IC₅₀ = 310 nM, tPSA = 78 Å²), and **1v** (IC₅₀ = 4.4 nM, tPSA

Table 3

H-PGDS enzyme inhibition data for aza-quinoline

#	R	IC ₅₀ ± S.D. ^a , nM	EC ₅₀ ± S.D. ^b , nM
1m		3.9 ± 0.7	24 ± 2.7
1n		12 ± 2.9	170 ± 36
1o		160 ± 110	450 ± 58
1p		4.8 ± 2.3	50 ± 8.2
1q		14 ± 5.8	94 ± 20
1r		350 ± 230	1100 ± 260
1s		5.3 ± 1.8	75 ± 12
1t		13 ± 12	1000 ± 120
1u		310 ± 170	3000 ± 1200
1v		4.4 ± 1.6	14 ± 4.8
1w		690 ± 91	9600 ± 2600
1x		150 ± 49	12,000 ± 8200
1y		9.4 ± 2.9	42 ± 18
1z		8.5 ± 5.6	64 ± 5.2
1aa		10 ± 9.3	120 ± 23
1ab		6.6 ± 3.1	22 ± 1.8
1ac		2.4 ± 0.4	3.9 ^c ± 1.4
1ad		3.8 ± 1.6	3.9 ± 0.3
1ae		4.7 ± 0.9	5.2 ± 0.8
1af		12 ± 5.0	340 ± 500

Table 3 (continued)

#	R	IC ₅₀ ± S.D. ^a , nM	EC ₅₀ ± S.D. ^b , nM
1ag		6.4 ± 7.1	170 ± 140

^a S.D. = standard deviation; mean ± S.D. All inhibitors were tested with N ≥ 4 in the H-PGDS RapidFire™ High Throughput Mass Spectrometry Assay.

^b S.D. = standard deviation; mean ± S.D. All inhibitors were tested with N ≥ 2 in the H-PGDS Rat Basophilic Leukemia (RBL) cell inhibition assay.

^c Individual replicate pIC₅₀ = 8.24, >8.6, 8.40, 8.47. The mean was obtained by removing the > qualifier and averaging the values.

= 78 Å²) exhibited similar SAR trends as their corresponding congeners in the 1,6-naphthyridine template. Moreover, the 2,2,2-trifluoroethylamino- and 2,2-difluoroethylamino- derivatives **1w** (IC₅₀ = 690 nM, tPSA = 87 Å²) and **1x** (IC₅₀ = 150 nM, tPSA = 87 Å²) lost inhibitory potency, similar to 2,2,2-trifluoroethoxy analog **1r**, with the smaller and less electron withdrawing analog **1x** showing the least reduction in activity. In addition, the two analogs **1s** (*p.o.* DNAUC = 72.5 ng/hr/mL) and **1v** (*p.o.* DNAUC = 73.7 ng/hr/mL) that met the progression criteria to murine pharmacokinetic studies exhibited poor oral exposure.

Similar to the cyclopropyl 1,6-naphthyridine analog **1q**, small 7-alkyl substitutions in the 1,8-naphthyridine series, like the cyclopropyl **1y** (IC₅₀ = 9.4 nM, meas. pK_A = 3.10, HBAS = 13.6 kcal/mol, tPSA = 75 Å²), the isopropyl **1z** (IC₅₀ = 8.5 nM, tPSA = 75 Å²), and the cyclobutyl **1aa** (IC₅₀ = 10 nM, tPSA = 75 Å²) are potent H-PGDS inhibitors. Although the cyclobutyl analog **1aa** (mLM t_{1/2} = 0.63 hr) is rapidly metabolized *in vitro*, like **1q**, the cyclopropyl derivative **1y** has good oral exposure (mLM t_{1/2} = > 3.0 hr, *p.o.* DNAUC = 1320 ng/hr/mL).

Quinoline SAR further revealed that halogens, such as chloro- and bromo-, appended to the 6-position of the quinoline template formed a halogen bond with the side chain carboxylate of ⁹⁶Asp to enhance H-PGDS inhibitory potency. Thus, 6-chloro derivatives in the 1,8-naphthyridine were prepared to explore their effect on enzyme inhibition. As shown in Table 3, the combination 6-chloro-7-methoxy analog **1ab** (IC₅₀ = 6.6 nM, meas. pK_A = <2.0, HBAS = 13.0 kcal/mol, tPSA = 84 Å²) is a 6-fold better H-PGDS inhibitor than its deschloro derivative **1i**. In contrast, the 6-chloro-7-azetidino derivatives **1ac** (IC₅₀ = 2.4 nM, tPSA = 78 Å²) and **1ad** (IC₅₀ = 3.8 nM, tPSA = 78 Å²), as well as the 6-chloro-7-cyclopropyl analog **1ae** (IC₅₀ = 4.7 nM, tPSA = 75 Å²), do not have as dramatic increases in potency, relative to **1s**, **1v**, and **1y**, respectively. Possibly the chloro substituent prevents the bulkier 7-substituents from accessing the optimal bound conformation. Furthermore, the combination analogs, involving the addition of the chlorine to the 1,8-naphthyridine scaffold, exhibit reduced FASSIF solubility of < 15 µg/mL in all cases, thereby limiting progression.

7-Substituted pyrido[2,3-*d*]pyrimidine analogs were also prepared, with both the 7-azetidino analog **1af** (IC₅₀ = 12 nM, tPSA = 97 Å²) and the 7-cyclopropyl analog **1ag** (IC₅₀ = 6.4 nM, tPSA = 97 Å²) being more potent H-PGDS inhibitors than the corresponding methoxy derivative **1l**. Yet, despite good *in vitro* metabolic stability (**1af** mLM t_{1/2} = 2.4 hr; **1ag** mLM t_{1/2} = > 3 hr), neither analog had good oral exposure (**1af** *p.o.* DNAUC = 23.4 ng/hr/mL; **1ag** *p.o.* DNAUC = 204 ng/hr/mL) in mice.

3.3. Aza-quinoline amide SAR

After the exploration of 6- and 7-ring substitutions, the best aza-quinoline scaffolds were combined with optimal amines from the quinoline template, in an effort to produce 3-carboxamide aza-quinolines with improved drug properties. These amines when integrated into the quinoline series had demonstrated improvements in potency (e.g. 2-(6-aminospiro[3.3]heptan-2-yl)propan-2-ol included in

1au and 2-(3-aminobicyclo[1.1.1]pentan-1-yl)propan-2-ol included in **1aw**, solubility (e.g. (*R*)-2-((*trans*-4-aminocyclohexyl)amino)-3,3,3-trifluoropropan-1-ol included in **1ao**, *trans*-4-(3-fluoroazetidin-1-yl)cyclohexan-1-amine included in **1ap**, and *trans*-N1-(1,1-difluoropropan-2-yl)cyclohexane-1,4-diamine included in **1ba**), and size (e.g. 3-amino-1-methylcyclobutanol included in **1ay**, (*S*)-3-aminopyrrolidin-2-one included in **1az** and 2-(*trans*-3-aminocyclobutyl)propan-2-ol included in **1at**). Although the azetidino analogs, such as **1m**, **1s**, and **1af**, are potent H-PGDS inhibitors, these compounds exhibit low oral exposure in mice relative to quinoline **1a**. Other amines that might provide better oral exposures were combined with these templates. As shown in Table 4, the 7-azetidino-1,6-naphthyridine derivatives, 3-methyl-3-hydroxycyclobutyl **1ah** (IC_{50} = 56 nM), and γ -lactams **1ai** (IC_{50} = 12 nM), and **1aj** (IC_{50} = 37 nM), are less potent H-PGDS inhibitors than **1m**. Although **1ai** and **1aj** have better oral exposure in mice (**1ah** *p.o.* DNAUC = 46.9 ng/hr/mL; **1ai** *p.o.* DNAUC = 250 ng/hr/mL; **1aj** *p.o.* DNAUC = 715 ng/hr/mL) than **1m**, these compounds do not meet the progression criteria of ≥ 1000 ng/hr/mL. Furthermore, the corresponding 1,8-naphthyridine analogs **1ar** (IC_{50} = 140 nM) and **1as** (IC_{50} = 71 nM) are less potent than **1s**, and their permeability (P_{app} = < 10 nm/sec) is too low for passive oral absorption, precluding pharmacokinetic studies. In contrast, the more potent 6-chloro-7-(2-methylazetidiny)-1,8-naphthyridine analogs, (cyclobutyl)propan-2-ol **1bc** (IC_{50} = 3.1 nM), 3-methyl-3-hydroxycyclobutyls **1bd** (IC_{50} = 5.0 nM) and **1be** (IC_{50} = 5.0 nM), 4-methyl-4-hydroxycyclohexyl **1bf** (IC_{50} = 4.6 nM), and γ -lactam **1bg** (IC_{50} = 5.1 nM), have higher permeabilities, possibly due to their increased lipophilicities. Yet, **1bc** ($t_{1/2}$ = 16 min), **1bd** ($t_{1/2}$ = 24 min), and **1be** ($t_{1/2}$ = 63 min) have low *in vitro* metabolic stability, and **1bf** ($t_{1/2}$ > 180 min, *p.o.* DNAUC = 132 ng/hr/mL) and **1bg** ($t_{1/2}$ > 180 min, *p.o.* DNAUC = 86.2 ng/hr/mL) have poor oral exposure. Thus, no acceptable improvements in oral exposure were realized in the 7-azetidiny-aza-quinolines.

The amine replacements in the 7-cyclopropyl aza-quinolines were also explored. The 1,6-naphthyridine **1q** has good oral exposure (*p.o.* DNAUC = 1040 ng/hr/mL), but limited solubility (FaS-SIF = 0.027 mg/mL). Thus, several analogs with solubility-enhancing amines - identified from the quinoline series - were synthesized. As shown in Table 4, these 6-aza-quinoline compounds, (cyclobutyl)propan-2-ol **1ak** (IC_{50} = 65 nM, FaS-SIF = 0.283 mg/mL), bicycle **1al** (IC_{50} = 38 nM, FaS-SIF = 0.43 mg/mL), 3-methyl-3-hydroxycyclobutyl **1am** (IC_{50} = 290 nM, FaS-SIF = 0.097 mg/mL), γ -lactam **1an** (IC_{50} = 110 nM, FaS-SIF = 0.420 mg/mL), and 4-aminocyclohexyls **1ao** (IC_{50} = 31 nM, FaS-SIF = 0.104 mg/mL), **1ap** (IC_{50} = 35 nM, FaS-SIF > 1.000 mg/mL), and **1aq** (IC_{50} = 14 nM, FaS-SIF = 0.011 mg/mL), are slightly less potent than **1q**, but are generally more soluble. Yet, the four compounds that were progressed into PK studies have lower oral exposures than **1q** (**1ak** *p.o.* DNAUC = 45.3 ng/hr/mL), **1an** (*p.o.* DNAUC = 262 ng/hr/mL), **1ao** (*p.o.* DNAUC = 693 ng/hr/mL), **1ap** (*p.o.* DNAUC = 358 ng/hr/mL) in mice.

Since the 1,8-naphthyridine **1y** also has good oral exposure (*p.o.* DNAUC = 1,320 ng/hr/mL), additional amine analogs were prepared to further probe the pharmacokinetic properties of this template. Of the tertiary alcohol derivatives synthesized, the spiro enantiomers **1au** (IC_{50} = 3.9 nM, FaS-SIF = 0.035 mg/mL) and **1av** (IC_{50} = 4.9 nM, FaS-SIF = 0.034 mg/mL) are the most potent, while the shorter (cyclobutyl)propan-2-ol **1at** (IC_{50} = 36 nM, FaS-SIF = 0.100 mg/mL), and bicyclic **1aw** (IC_{50} = 17 nM, FaS-SIF = 0.401 mg/mL) are less potent. The shortest 3-methyl-3-hydroxycyclobutyl diastereomers **1ax** (IC_{50} = 300 nM, FaS-SIF = 0.88 mg/mL) and **1ay** (IC_{50} = 160 nM, FaS-SIF = 0.13 mg/mL) are the least potent. The SAR within this series of amines are consistent with the general understanding that potency can be achieved by increasing hydrophobic surface area, driven by the entropic benefits of transferring the ligand from bulk solution. The oral exposures of the four most potent tertiary alcohols were determined in mice (**1at** (FaS-SIF = 0.100 mg/mL, *p.o.* DNAUC = 77.5 ng/hr/mL), **1au** (FaS-SIF = 0.035 mg/mL, *p.o.* DNAUC = 477 ng/hr/mL), **1av** (FaS-SIF = 0.034 mg/mL, *p.o.* DNAUC = 441 ng/hr/mL), **1aw** (FaS-SIF = 0.401 mg/mL, *p.o.*

Table 4

#	R ¹	R ²	IC ₅₀ ± S.D. ^a , nM	EC ₅₀ ± S.D. ^b , nM
1ah			56 ^c ± 3.7	450 ± 15
1ai			12 ^c ± 2.9	110 ± 87
1aj			37 ± 6.8	260 ± 140
1ak			65 ± 36	280 ± 63
1al			38 ± 19	210 ± 60
1am			290 ± 100	910 ± 59
1an			110 ± 64	260 ± 17
1ao			31 ± 9.7	310 ± 61
1ap			35 ± 11	280 ± 0.0
1aq			14 ± 14	88 ± 4.3
1ar			140 ± 58	17,000 ± 11,000
1as			71 ± 42	6000 ± 3300
1at			36 ± 14	280 ± 88
1au			3.9 ± 1.0	32 ± 16
1av			4.9 ± 0.3	29 ± 5.5
1aw			17 ± 9.3	230 ± 0.0
1ax			300 ± 180	7400 ± 1800
1ay			160 ± 66	1300 ± 41
1az			44 ± 10	640 ± 220
1ba			11 ± 7.3	28 ± 7.6

(continued on next page)

Table 4 (continued)

#	R ¹	R ²	IC ₅₀ ± S.D. ^a , nM	EC ₅₀ ± S.D. ^b , nM
1bb			14 ± 6.6	50 ± 7.1
1bc			3.1 ± 1.2	<2.5
1bd			5.0 ± 2.3	4.7 ± 0.2
1be			5.0 ± 1.5	<2.5
1bf			4.6 ± 2.2	3.7 ± 0.2
1bg			5.1 ± 2.7	3.8 ± 0.2
1bh			3.9 ± 2.2	11 ± 2.3
1bi			6.4 ± 6.3	190 ± 6.2
1bj			7.1 ± 4.9	54 ± 6.7
1bk			4.6 ± 1.4	14 ± 2.3

^a S.D. = standard deviation; mean ± S.D. All inhibitors were tested with N ≥ 4 in the H-PGDS RapidFire™ High Throughput Mass Spectrometry Assay.

^b S.D. = standard deviation; mean ± S.D. All inhibitors were tested with N ≥ 2 in the H-PGDS Rat Basophilic Leukemia (RBL) cell inhibition assay.

^c N = 2.

DNAUC = 285 ng/hr/mL), but dose normalized areas under the curve are lower than **1y**. Like the 3-methyl-3-hydroxycyclobutyl diastereomers **1ax** and **1ay**, the γ -lactam **1az** (IC₅₀ = 44 nM) does not meet the cell potency criteria for further progression, likely due to its limited permeability (P_{APP} < 10 nm/sec). In contrast, the amino derivatives **1ba** (IC₅₀ = 11 nM) and **1bb** (IC₅₀ = 14 nM) are potent H-PGDS inhibitors, yet the one analog progressed to a PK study in mice, **1ba** (FaS-SIF > 1.00 mg/mL, *p.o.* DNAUC = 681 ng/hr/mL), has a DNAUC < 1000 ng/hr/mL.

Furthermore, 6-chloro derivatives of the less potent and more polar derivatives **1at**, **1ax**, **1ay**, and **1az** were prepared, with the aim of increasing inhibitory activity and permeability. These analogs, **1bh** (IC₅₀ = 3.9 nM, P_{APP} = 280 nm/sec), **1bi** (IC₅₀ = 6.4 nM, P_{APP} = 150 nm/sec), **1bj** (IC₅₀ = 7.1 nM, P_{APP} = 220 nm/sec), and **1bk** (IC₅₀ = 4.6 nM, P_{APP} = 30 nm/sec), were substantially more potent and had higher P_{APP} values, yet none of them (**1bh** (*p.o.* DNAUC = 452 ng/hr/mL), **1bi** (*p.o.* DNAUC = 362 ng/hr/mL), **1bj** (*p.o.* DNAUC = 152 ng/hr/mL), **1bk** (*p.o.* DNAUC = 252 ng/hr/mL)) have oral exposures in mice better than **1y**.

As only aza-quinolines **1q** and **1y** met the oral DNAUC progression criteria, these compounds were subjected to more complete pharmacokinetic profiling. As shown in Table 5, the 1,6-naphthyridine **1q** has a low *i.v.* clearance (C_l = 22 mL/min/kg), moderate steady state volume of

Table 5

H-PGDS inhibitor pharmacokinetic data.^a

#	Species	t _{1/2} , h	C _l , mL/min/kg	V _{SS} , L/kg	F, %	B:B ^b
1a	mouse	3.8	5.6	1.7	61	0.59
1q	mouse	1.1	22	1.6	130	0.17
1y	mouse	2.9	9.0	1.6	71	0.06
1y	rat	5.1	4.5	1.6	100	–
1y	dog	6.2	1.9	1.0	92	–

^a Mice were dosed at 1 mg/kg *i.v.* and 3 mg/kg *p.o.* with an N = 2; rats were dosed at 0.4 mg/kg *i.v.* and 2.4 mg/kg *p.o.* with an N = 3; dogs were dosed at 0.5 mg/kg *i.v.* and 1 mg/kg *p.o.* with an N = 3.

^b Brain: blood ratio (B:B).

distribution (V_{SS} = 1.6 L/kg), and moderate terminal half-life (t_{1/2} = 1.1 h), with excellent oral bioavailability (F = 130%). The 1,8-naphthyridine **1y** has a lower *i.v.* clearance (C_l = 9.0 mL/min/kg), similar steady state volume of distribution (V_{SS} = 1.6 L/kg), and longer terminal half-life (t_{1/2} = 2.9 h), as well as high oral bioavailability (F = 71%). More importantly, both **1q** and **1y** have lower brain penetration with blood:brain ratios of 0.17 for **1q** and 0.06 for **1y**, supporting the hypothesis that increasing the PSA of these inhibitors would attenuate CNS exposure. As **1y** has very low brain exposures, its pharmacokinetics was also profiled in rat and dog, where the compound also exhibited low clearances (rat C_l = 4.5 mL/min/kg, dog C_l = 1.9 mL/min/kg) and high oral bioavailabilities (rat F = 100%, dog F = 92%).

3.4. 1,8-Naphthyridine **1y** binding kinetics

As 1,8-naphthyridine **1y** had the best pharmacokinetics in these aza-quinoline inhibitor series, its binding kinetics were explored further. The equilibrium dissociation constant K_d for **1y** (K_d = 0.24 ± 0.051 nM) was measured in the presence of 1 mM glutathione by titration of the quenching of the indole intrinsic fluorescence of ¹⁰⁴Trp in the active site with **1y** excited at 285 nm.⁵⁴ Furthermore, the k_{on} of **1y** (k_{on} = 3.3 ± 0.07 × 10⁷ M⁻¹ sec⁻¹) was measured by stopped-flow spectrofluorimetry from the single exponential fits of intrinsic tryptophan quench time courses, and the k_{off} of **1y** (calculated k_{off} = 0.0079 ± 0.017 s⁻¹) was calculated from the values of K_d and k_{on} (K_d = k_{off}/k_{on}). Inhibitor **1y** rapidly binds to and releases from the enzyme. Because the IC₅₀ of **1y** is elevated due to prostaglandin substrate competition and active site titration of hH-PGDS in the activity assay, the K_d is a better reflection of the intrinsic potency of **1y**.

3.5. Aza-quinoline X-ray co-crystal structures

To gain further understanding of the binding mode of aza-quinoline H-PGDS inhibitors, protein co-crystal structures of inhibitors **1m** and **1y** bound with hH-PGDS and GSH were obtained. The co-crystal structure of the 1,6-naphthyridine **1m** (PDB #6W58) is shown in Fig. 2, overlaid with the co-crystal structure of the original 3-cyanoquinoline fragment (PDB #6N69). Not surprisingly, 1,6-naphthyridine **1m** binds in a similar manner to the 3-cyanoquinoline fragment, with both inhibitors forming face to face π - π stacking interactions with the indole side chain of ¹⁰⁴Trp (face of indole ¹⁰⁴Trp to face of quinoline **1m** distance = 3.6 Å). To accommodate the 7-azetidine moiety into a small hydrophobic pocket formed by ⁹⁹Met, ¹⁵⁵Ile, ¹⁵²Tyr, ¹⁵⁶Cys, and ¹³Gly, the 1,6-naphthyridine ring is shifted slightly towards the solvent exposed portion of the protein. This displacement also slightly alters the interaction of the N1-nitrogen of the 1,6-naphthyridine ring with the structural water molecule that - in turn - interacts with the protein via hydrogen bonding to the C-terminal carboxylic acid of ¹⁹⁹Leu, the hydroxyl side chain of ¹⁵⁹Thr, and another bound water molecule. This structural water molecule is key to maintaining the integrity of the protein fold and the formation of the binding site.⁵⁵ The increased basicity of the 7-azetidine derivative **1m** strengthens the hydrogen bonding interaction with the structural water molecule and, along with the increased hydrophobic

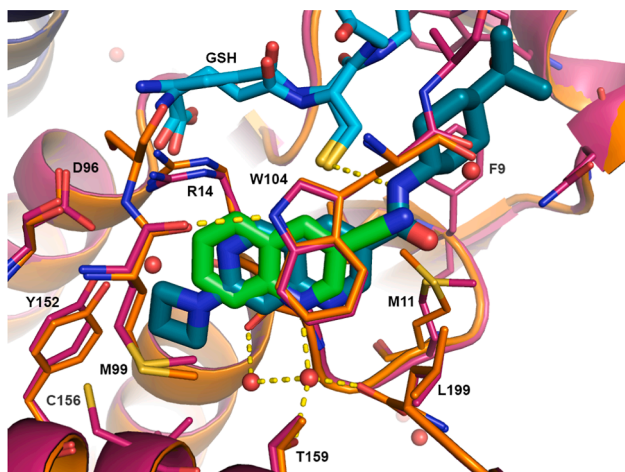


Fig. 2. Co-crystal structure of inhibitor **1m** bound to hH-PGDS with GSH superimposed on the co-crystal structure of 3-cyanoquinoline complexed with rH-PGDS and GSH. Ligand binding site of the X-ray co-crystal structure of **1m** complexed with hH-PGDS and GSH superimposed on the co-crystal structure of 3-cyanoquinoline complexed with rH-PGDS and GSH (PDB code 6N69). The hH-PGDS carbons are colored magenta while the rH-PGDS carbons are colored orange, inhibitor **1m** carbons colored dark green, the 3-cyanoquinoline carbons are colored light green, and both GSH carbons colored cyan. Hydrogen bonds are depicted as yellow dashed lines. The coordinates of hH-PGDS and GSH bound with **1m** have been deposited in the Brookhaven Protein Data Bank (PDB code 6W58). This figure was generated using PyMOL version 1.7.64.6 (The PyMOL Molecular Graphics System, Version 1.7.64 Schrodinger, LLC).

interactions of the azetidine group with the hH-PGDS protein, rationalizes the increased potency of **1m** relative to the 7-methoxy-1,6-naphthyridine **1i**.

The co-crystal structure of the 1,8-naphthyridine **1y** (PDB #6W8H) is shown in Fig. 3, with the co-crystal structure of quinoline **1a** (PDB #6N4E) overlaid with it. As with the 1,6-naphthyridine **1m**, the

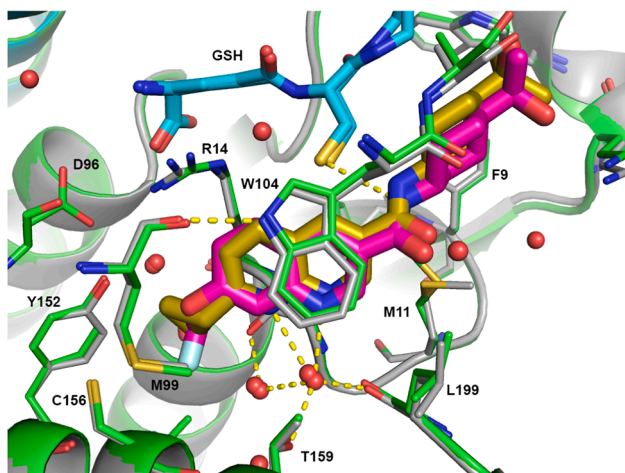


Fig. 3. Co-crystal structure of inhibitor **1y** bound to hH-PGDS with GSH superimposed on the co-crystal structure of **1a** complexed with hH-PGDS and GSH. Ligand binding site of the X-ray co-crystal structure of **1y** complexed with hH-PGDS and GSH superimposed on the co-crystal structure of **1a** complexed with hH-PGDS and GSH (PDB code 6N4E). The **1y** hH-PGDS carbons are colored green, while the **1a** hH-PGDS carbons are colored gray with inhibitor **1y** carbons colored gold, inhibitor **1a** carbons are colored magenta and both GSH carbons are colored cyan. Hydrogen bonds are depicted as yellow dashed lines. The coordinates of hH-PGDS and GSH bound with **1y** have been deposited in the Brookhaven Protein Data Bank (PDB code 6W8H). This figure was generated using PyMOL version 1.7.64.6 (The PyMOL Molecular Graphics System, Version 1.7.64 Schrodinger, LLC).

inhibitors **1a** and **1y** have shifted slightly relative to the 3-cyanoquinoline fragment to accommodate the 7-difluoromethoxy and 7-cyclopropyl moieties, respectively. However, the 1,8-naphthyridine is shifted slightly more than the quinoline and 1,6-naphthyridine rings, and one might speculate that this displacement allows both the N1 (structural water oxygen to N1 naphthyridine nitrogen distance = 2.9 Å) and N8 nitrogen (structural water oxygen to N8 naphthyridine nitrogen distance = 2.9 Å) of **1y** to maximally hydrogen bond to the structural water molecule, thus strengthening this interaction. As the 7-cyclopropyl derivative **1y** is less basic than the 7-methoxy-1,8-naphthyridine **1k** and therefore forms a comparably weaker hydrogen bond with the structural water, the increased potency of **1y** likely arises purely from hydrophobic interactions with the hH-PGDS protein. Moreover, none of these shifts, relative to the 3-cyanoquinoline fragment, dramatically alter the face to face π - π stacking interaction between the indole side chain of ¹⁰⁴Trp and the various aromatic rings (face of indole ¹⁰⁴Trp to face of quinoline/1,6-naphthyridine/1,8-naphthyridine distances all equal 3.6 Å); yet electronic perturbations by the 7-position substituents, 3-carboxamide group, and heteroatomic rearrangements in the ring systems, likely subtly adjust the strength of the π - π cloud interactions between each of these rings and the ¹⁰⁴Trp indole.

Like quinoline **1a**, inhibitors **1m** and **1y** also form hydrogen bonds between their 3-carboxamide NHs and the sulfur of the GSH. Furthermore, hydrophobic interactions of the chair conformation of the cyclohexyl moieties with the side chains of ¹⁰⁵Ala, ¹¹Met, and ⁹Phe enhance binding interactions with the enzyme. Thus, amide substituents with increased hydrophobic surface area, such as the spiro[3.3]heptane **1au**, exhibit enhanced potency relative to more polar and smaller amides, such as the 3-methyl-3-hydroxycyclobutane **1ax**. Although mostly solvent exposed and thus limiting its contributions to binding affinity, the tertiary alcohol increases water solubility of these analogs. These human H-PGDS co-crystal structures bound with ligand and cofactor help rationalize much of the SAR observed in the aza-quinoline carboxamide inhibitor series, as well as providing structural insight into the binding requirements of the enzyme and a blueprint for aiding design of other H-PGDS inhibitors.

3.6. 1,8-Naphthyridine **1y** cross screening

Since, in addition to H-PGDS, several other enzymes also utilize the substrate PGH₂ for production of prostanoids, the potency of 1,8-naphthyridine **1y** was determined against two other synthase enzymes in the prostanoid pathway, lipocalin prostaglandin D synthase (L-PGDS)²⁰ and microsomal prostaglandin E synthase (m-PGES),⁵⁶ to ensure that inhibition of these enzymes was not a factor in any pharmacodynamic study outcomes of inflammatory disease models. Because **1y** did not inhibit L-PGDS (IC₅₀ > 10,000 nM) or m-PGES (IC₅₀ > 100,000 nM) at the highest concentrations tested, the compound was deemed suitable for use *in vivo* to probe the protein specific effects of H-PGDS inhibition in inflammatory models.

Moreover, the general off-target liabilities of **1y** were also evaluated. Against a broad panel of proteins, including 7-TM G-protein coupled receptors (5HT_{1B}, 5HT_{2A}, 5HT_{2B}, 5HT_{2C}, α_{1B} , α_{2C} , β_2 , κ , μ , A_{2A}, CB₁, D₁, D₂, H₁, M₁, M₂, MRGPRX₂, NK₁, V_{1A}), ion channels (5HT₃, Cav1.2, GABA_A, Kv1.5, Kv7.1, Nav1.5), enzymes (AChE, COX-2, MAO-A, PDE_{3A}, PDE_{4B}), transcription factors (AhR, PXR), kinases (Aurora B, LCK, PI3K γ), and transporters (BSEP, NET, OATP_{1B1}, SERT), 1,8-naphthyridine **1y** did not exhibit any activity in these assays at concentrations up to 10,000 nM. Compound **1y** also did not inhibit cytochrome p450 3A4 monooxygenase enzyme (IC₅₀ > 100,000 nM) or block the human ether-a-go-go-related gene potassium ion channel (Kv11.1, IC₅₀ > 80,000 nM)⁵⁷ at the highest concentrations assayed. This selectivity profile, coupled with its high H-PGDS inhibitory potency and good pharmacokinetic characteristics, makes **1y** a suitable tool compound for studying the pharmacodynamic effects of H-PGDS inhibition.

3.7. 1,8-Naphthyridine 1y pharmacodynamics

Inhibitor **1y** was profiled in several *in vivo* inflammation models. First, to evaluate the acute effects of a H-PGDS inhibitor on mast cell release of PGD₂, 1,8-naphthyridine **1y** was evaluated in a murine mast cell degranulation model of inflammation.⁵⁸ Male C57BL/6J mice were administered *p.o.* with vehicle or H-PGDS inhibitor **1y** at various doses (0.003, 0.01, 0.03, 0.1, 0.3, and 1 mg/kg), then anesthetized and challenged one hour later with vehicle (PBS) or the *N*-methyl-*p*-methoxyphenethylamine/formaldehyde synthetic polymer 48/80 (*i.p.* 0.75 mg/mL) with abdomen massage. After seven minutes, blood was collected (**1y** analysis), the mice were euthanized, and lavage fluid was collected from the abdominal cavity (PGD₂ analysis). As shown in Fig 4, the mast cell secretagogue 48/80 induces production and release of PGD₂ into peritoneal lavage fluid versus phosphate buffered saline (PBS). H-PGDS inhibitor **1y** attenuates this PGD₂ release to baseline levels in a dose-dependent manner with an ED₅₀ = 0.009 mg/kg (**1y** blood EC₅₀ = 3.4 nM) in this acute inflammation model. Levels of the related prostaglandins PGE₂ and PGF_{1α} were not significantly different between **1y** treated and untreated animals after challenge with synthetic polymer 48/80.

Secondly, the acute effects of H-PGDS inhibition on lipopolysaccharide (LPS)-triggered PGD₂ production in mice were evaluated *in vivo*. The Gram-negative bacterial endotoxin LPS binds 7-TM pattern recognition receptors and activates NF-κB. These events initiate an inflammatory cascade that results in cytokine production and enzyme synthesis, including COX-mediated prostaglandin synthesis. Twelve-week-old C57BL6/N mice (n = 6/group) were dosed orally with vehicle, or **1y** at 0.003, 0.01, 0.03, 0.1, 0.3, or 1.0 mg/kg. One hour later, animals received intraperitoneal injection of PBS or 20 ng/kg LPS. Blood samples were withdrawn via cardiac puncture 30 min post LPS injection and animals were then euthanized and skeletal muscle tissues were isolated. Plasma and muscle prostaglandins and **1y** levels were determined using LC/MS/MS. In contrast to plasma which exhibits very low (90 pg/mL) prostanoid concentrations in the basal state, skeletal muscle exhibited a substantial amount of PGD₂ (0.6 ng/g) before LPS stimulation (Fig. 5). LPS induced a significant increase in PGD₂ levels in

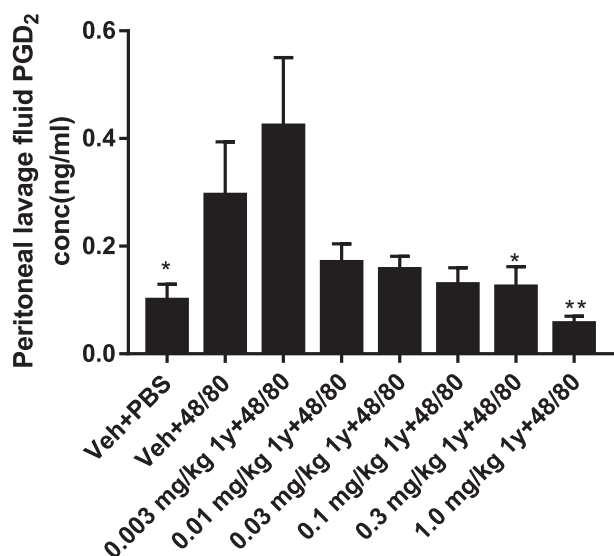


Fig. 4. H-PGDS inhibition blocks 48/80 challenge-induced PGD₂ production *in vivo*. Young adult male C57BL/6J mice were administered (*p.o.*) vehicle or the H-PGDS inhibitor **1y** at varying doses (from 0.003 mg/kg to 1.0 mg/kg). One hour later, mice were anesthetized, injected with (*i.p.*) 0.2 mL PBS or 48/80 (0.75 mg/mL), and peritoneal lavage fluid was collected after 7 min. (A) Data are presented as means (n = 7–8/group) ± S.E.M. and analyzed using ANOVA followed by Dunnett's comparing vehicle + 48/80 to respective treatment group (*p < 0.05; **p < 0.01 vs 48/80 + vehicle).

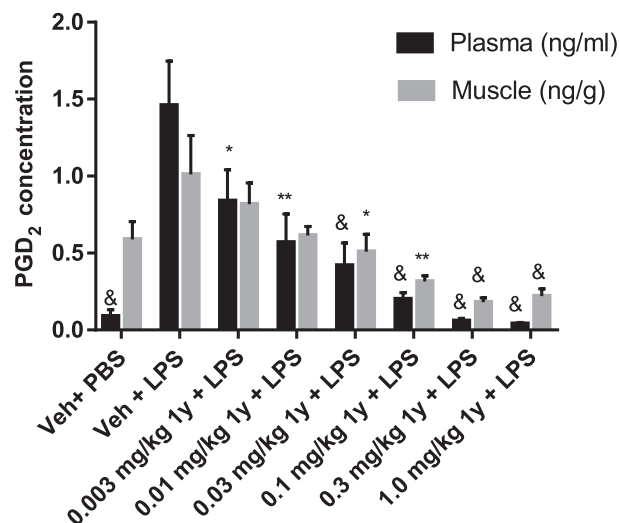


Fig. 5. H-PGDS inhibition blocks lipopolysaccharide challenge-induced PGD₂ production *in vivo*. Young adult male C57BL/6J mice were administered (*p.o.*) vehicle or the H-PGDS inhibitor **1y** at varying doses (from 0.003 mg/kg to 1.0 mg/kg) one hour prior to LPS or PBS injection. Blood samples were withdrawn via cardiac puncture 30 min post LPS injection and animals were then euthanized and skeletal muscle tissues were isolated. PGD₂ levels in plasma and skeletal muscle were determined using LC/MS/MS. Data are depicted as means ± S.E.M and analyzed using ANOVA followed by Dunnett's comparing vehicle + LPS to respective treatment group (*p < 0.05; **p < 0.01; &p < 0.001 vs. vehicle + LPS).

plasma (16-fold, p ≤ 0.001) and a modest increase in skeletal muscle (1.7-fold, p = 0.09) at 30 min after intraperitoneal administration. Inhibitor **1y** treatment inhibited LPS-induced PGD₂ increase in plasma and skeletal muscle in a dose-dependent manner. Significant PGD₂ inhibition were achieved at 0.003 mg/kg and 0.03 mg/kg for plasma and muscle, respectively. Plasma PGD₂ levels returned to baseline at 0.3 mg/kg. Muscle PGD₂ concentrations dropped below basal levels in the two high dose groups, suggesting both L-PGDS and H-PGDS contribute to basal PGD₂ production in skeletal muscle. There is a linear relationship between **1y** dose and drug levels in blood and skeletal muscle (data not shown). The estimated **1y** ED₅₀ for systemic and muscle specific H-PGDS inhibition of LPS-induced PGD₂ synthesis is 0.0031 mg/kg and 0.0138 mg/kg with an estimated EC₅₀ of 2.6 nM and 1.4 ng/g in plasma and skeletal muscle, respectively. Taken together, these results demonstrate that **1y** is a potent inhibitor of LPS-induced PGD₂ synthesis in mice. PGE₂ and PGF_{1α} were not significantly different between **1y** treated and untreated animals after challenge with LPS. The EC₅₀ values for **1y** in both the acute murine inflammatory models (MCD EC₅₀ = 3.4 nM, LPS EC₅₀ = 2.6 nM) are similar, but ~ 10-fold lower than the RBL cell EC₅₀ value (EC₅₀ = 42 nM). This difference could be due to intrinsic species-related differences in compound potency between mouse and rat H-PGDS inhibition and/or differences in species plasma protein binding.

H-PGDS inhibitor **1y** was also studied in two chronic eccentric contraction-induced muscle injury models. Male C57BL/6 mice (10–12 weeks-old, n = 7–8/group) were administered vehicle or **1y** at 1, 3, or 10 mg/kg orally before being anesthetized and challenged by unilateral eccentric contractions of the right hind limb for 10 min (Day 0), followed by 16 days of QD dosing with longitudinal measurements of isometric limb torque determined for each animal at Days 1, 9, and 16. Inhibitor **1y** significantly enhanced functional recovery of injured limbs, following eccentric contraction-induced muscle injury, at the top two doses as shown in Fig. 6. At least part of this response was due to dose-dependent protective effects of **1y**, as determined by the initially milder force deficit observed at Day 1 post-damage. More importantly, **1y** significantly hastened the time to full functional recovery of injured limb muscles, with maximal efficacy observed at ≥ 10 mg/kg QD. Using an

integrated measurement of limb recovery over time, the ED₅₀ for **1y** was determined to be 3 mg/kg, with an estimated AUC_{0-last} of 5300 hr•ng/mL, a C_{Max} of 1700 ng/mL, an estimated free AUC_{0-last} of 1200 hr•ng/mL, and a free C_{Max} of 370 ng/mL. Free blood concentrations reached or exceeded the cellular IC₅₀ at doses tested, although maximal efficacy was observed at the top (10 mg/kg) dose.

Duchenne muscular dystrophy (DMD) is a rare degenerative muscle disorder characterized by progressive muscle wasting, weakness, mobility loss, and premature death, resulting from mutations of the dystrophin gene. A commonly used preclinically model of DMD is the mdx mouse, which is deficient in dystrophin. Although the pathological severity of this model is milder than human DMD, by aging these mice (6 to 8 month-old) and stressing them with bouts of eccentric contractions (1 or more), its translatability to humans can be enhanced.⁵⁹ In a 5-point dose–response evaluation of **1y** in 8 month-old male mdx mice, animals (n = 7–8/group) received an initial oral dose of 0 (vehicle), 0.1, 0.3, 1, 3, or 10 mg/kg **1y** 10 min prior to damage-inducing eccentric contractions, and then daily (QD) thereafter for 43 days. Compared to vehicle alone, **1y**, at 1, 3, and 10 mg/kg, significantly improved functional recovery, following eccentric contraction-induced muscle injury in mdx mice as shown in Fig. 7. Whereas vehicle-treated mdx mice exhibited a ~ 25% loss of limb function (compared to pre-injury values) at study end, **1y** treated mice displayed near-complete (~90% to 100%) restoration of pre-injury function. An integrated measure of limb recovery over time (AUC) demonstrated significant reductions in total recovery time by **1y** treatment at doses ≥ 1.0 mg/kg and was used to calculate an ED₅₀ value of 1.1 mg/kg. The AUC_{0-last} associated with the ED₅₀ was estimated to be 1100 hr•ng/mL with an estimated C_{Max} of 260 ng/mL, an estimated free AUC_{0-last} of 200 hr•ng/mL, and a free C_{Max} of 49 ng/mL. Free blood concentrations reached or exceeded the cellular IC₅₀ at doses ≥ 0.3 mg/kg, while maximal efficacy occurred at 10 mg/kg. Steady state PGD₂ levels in gastrocnemius muscle were suppressed relative to vehicle treated animals, at all doses, and generally decreased with dose. Moreover, no seizure symptoms were observed in any of the mouse models upon dosing of H-PGDS inhibitor **1y**.

The diversity of these multiple inflammatory challenges models is reflected (to an extent) in the distinct **1y** treatment responses. MCD and LPS experiments are acute in nature and likely reflect C_{Max}-driven response profiles. In contrast, eccentric contraction-induced muscle injury is comprised of an acute phase of alarm/inflammation and cellular debris removal, followed by a chronic phase of myofibrillar remodeling and gross remodeling, depending on multiple, temporally-distinct interactions of the immune-, vascular- and neuromuscular systems. Compound **1y** efficacies in the more physiological and less contrived chronic model are likely driven by AUC values and require

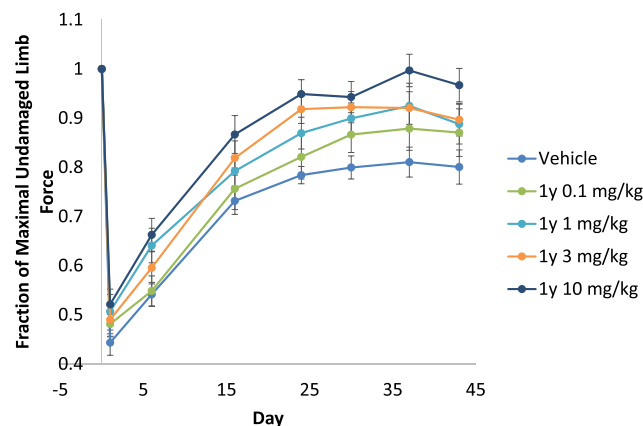


Fig. 7. H-PGDS inhibition attenuates muscle function loss and enhances recovery after eccentric muscle damage in mdx mice. Effect of different doses of an H-PGDS inhibitor, **1y**, on limb force following eccentric (lengthening) contraction-induced muscle injury in mdx mice. Doses were administered 10 min prior to damage and QD thereafter.

sufficient inhibitory exposures over many days/weeks for the resolution of muscle injury. The higher doses necessary for efficacy in the chronic eccentric contraction-induced muscle injury model might also reflect the lower muscle to plasma exposure of compound **1y** (muscle:plasma = 0.56) in mice.

3.8. 1,8-Naphthyridine **1y** safety assessment

To gain a better understanding of the development potential of **1y**, it was evaluated in a battery of non-clinical safety studies. H-PGDS inhibitor **1y** was negative in genetic toxicity *in vitro* screening tests; the bacterial reverse mutation assay (Ames test), both with and without metabolic activation and the mouse lymphoma assay. These results suggest that **1y** is unlikely to be carcinogenic as a result of drug-induced gene mutations or chromosomal aberrations.

After an oral pharmacokinetic rat study, demonstrated that a single 300 mg/kg dose of **1y** was well tolerated, **1y** was evaluated in a male Wistar Han rat oral, once daily, seven day repeat dose range finding study at dose levels of 10, 30, and 100 mg/kg/day in 0.5% hydroxypropylmethylcellulose with 0.1% TweenTM-80 (N = 4/dose). Systemic exposure (mean AUC and C_{Max} values) increased dose proportionally with increasing dose, and there was no marked change in systemic exposure after repeat dosing. Inhibitor **1y** was well tolerated at doses of 30 mg/kg/day, with no abnormal microscopic findings. Administration of 100 mg/kg/day was not tolerated, with rats found dead or terminated on day 7 prior to the scheduled necropsy. Rats given 100 mg/kg/day had microscopic findings in the heart (necrosis/inflammatory cell infiltrates), kidney (proximal tubular vacuolation and hyaline cast formation), adrenal gland (cortical hypertrophy) and thymus (increased lymphocytolysis). Day 7 AUC values at 10, 30, and 100 mg/kg/day were 120, 410, and 820 µg•hr/mL, respectively; respective C_{Max} values were 8.7, 24, and 57 µg/mL. Notably, there was no seizure-like activity or other CNS signs noted in this study, thus limiting brain exposure prevented manifestation of any off-target, adverse CNS events.

Furthermore, H-PGDS inhibitor **1y** was evaluated in a 4 day dog oral, once daily, dose range finding study at doses of 10, 30, and 75 mg/kg/day (n = 1/sex). Compound **1y** AUC and C_{Max} increased approximately proportionally on Day 1, but both AUC and C_{Max} values increased greater than proportionally on day 4, suggesting potential accumulation of **1y**. Inhibitor **1y** was well tolerated at dose levels up to 30 mg/kg/day with no abnormal microscopic findings; however, daily dosing of 75 mg/kg/day was not tolerated for the duration of the study based on deterioration in clinical condition/decreased body temperature and body weight loss. Macroscopically, dogs given 75 mg/kg/day had

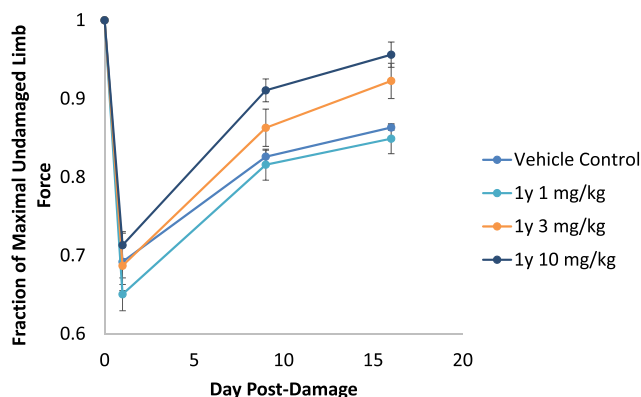


Fig. 6. H-PGDS inhibition attenuates muscle function loss and enhances recovery after eccentric muscle damage in wild-type mice. Effect of different doses of an H-PGDS inhibitor, **1y**, on limb force following eccentric (lengthening) contraction-induced muscle injury in normal C57Bl6/N mice. Doses were administered 10 min prior to damage and QD thereafter.

discoloration in the small intestine and esophagus (female), which correlated microscopically with diffuse degeneration/regeneration or multifocal erosion/ulceration. Additional microscopic findings were identified in the adrenal glands (degeneration of the zona glomerulosa, cytoplasmic alteration in the zona fasciculata, and hemorrhage of the zona fasciculata), and thymus (decreased cortical lymphoid cellularity consistent with stress). Clinical pathology changes included increased red cell mass due to hemoconcentration and increases in hepatobiliary parameters and cardiac troponin I concentrations. Day 4 AUC values in males and females given 10, 30, or 75 mg/kg/day were 120, 430, and 3600 $\mu\text{g}\cdot\text{hr}/\text{mL}$, respectively; respective C_{Max} values were 13, 34, and 210 $\mu\text{g}/\text{mL}$.

Although there was a margin of safety between the efficacious dose (ED_{50} , 3 mg/kg) and the non-tolerated dose (75 mg/kg), other H-PGDS inhibitors were discovered with improved safety profiles; therefore, **1y** was not advanced into GLP safety studies.

4. Conclusions

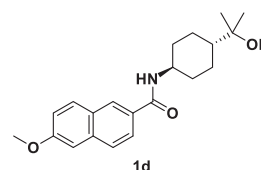
Desiring to explore the selective alteration of prostaglandin signaling for human disease intervention, GSK, in collaboration with Astex, used a fragment-based approach to discover H-PGDS inhibitors. These efforts resulted in the discovery of quinoline H-PGDS inhibitors, including **1a**. Quinoline **1a** is a potent H-PGDS inhibitor with good murine pharmacokinetic parameters. It was used to explore PGD_2 biology and attenuated mast cell degranulation in an acute inflammatory model, helping validate H-PGDS as a viable target for inflammatory diseases. Unfortunately, quinoline **1a** on repeat dosing at high concentrations caused CNS toxicity, precluding its further development. As the adverse effects were deemed to be off-target, a strategy was devised to limit CNS exposure in future H-PGDS inhibitors, and **1a** was utilized as a starting point to discover safer H-PGDS inhibitors. Tactically, a plan to limit brain exposure by increasing the PSA of inhibitors was devised. Specifically, PSA was increased by designing aza-quinolines. The preparation and testing of the aza-quinolines revealed that 1,6- and 1,8-naphthyridine inhibitors, such as **1i** and **1k**, were potent H-PGDS inhibitors. Further modifications to the 6- and 7- ring positions, as well as carboxamide amine substitutions, to improve H-PGDS inhibition and/or pharmacokinetic parameters resulted in the discovery of 1,8-naphthyridine **1y**. 1,8-Naphthyridine **1y** is a potent H-PGDS inhibitor with good selectivity versus other proteins, good pharmacokinetic parameters in mouse, rat, and dog, and minimal CNS exposure. Moreover, compound **1y** attenuated inflammatory exacerbations in two acute rodent models of inflammation and preserved muscle function in two chronic models of muscle injury. Finally, in rat and dog dose range finding safety studies, compound **1y** did not cause any CNS toxicity at doses significantly higher than its efficacious range, validating the strategy of limiting brain penetration to avoid adverse CNS effects. Thus, 1,8-naphthyridine **1y** is an excellent tool to explore PGD_2 biology and the potential therapeutic possibilities of H-PGDS inhibition.

5. Experimental section

All commercial chemicals and solvents were reagent grade and were used without further purification unless otherwise specified. The following abbreviations are utilized in the manuscript: tetrahydrofuran (THF), diethyl ether (Et_2O), dimethyl sulfoxide (DMSO), ethyl acetate (EtOAc), dichloromethane (CH_2Cl_2), trifluoroacetic acid (TFA), *N,N*-dimethylformamide (DMF), methanol (MeOH), dimethoxyethane (DME), *N*-methylpyrrolidine (NMP), acetonitrile (MeCN), chloroform (CHCl_3), phosphorus oxychloride (POCl_3), magnesium sulfate (MgSO_4), triethylamine (Et_3N), 2-propanol (*i*PrOH), *N,N*-diisopropylethylamine (*i*Pr₂NEt), sodium hydroxide (NaOH), *t*-butylmethyl ether (TBME), acetic acid (AcOH), ethanol (EtOH), di-*tert*-butyldicarbonate (BOC_2O), sodium sulfate (Na_2SO_4), *N,N*-dimethylacetamide (DMA), sodium bicarbonate (NaHCO_3), potassium carbonate (K_2CO_3), 1-[bis

(dimethylamino)-methylene]-1*H*-1,2,3-triazolo[4,5-*b*]pyridinium 3-oxid hexafluorophosphate (HATU), azobis(isobutyronitrile) (AIBN), 4-(2-hydroxyethyl)-piperazine-1-ethanesulfonic acid (HEPES), and dithiothreitol (DTT). All reactions except those in aqueous media were carried out with the use of standard techniques for the exclusion of moisture. Reactions were monitored by thin-layer chromatography (TLC) on 0.25 mm silica gel plates (60F-254, E. Merck) and visualized with UV light, iodine, iodoplatinate, potassium permanganate, cerium molybdate, or 5% phosphomolybdic acid in 95% ethanol. Final compounds were typically purified either by flash chromatography on silica gel (E. Merck 40–63 mm), radial chromatography on a Chromatotron™ using prepared silica gel plates, or on a Biotage Horizon or ISCO Combiflash® pump and fraction collection system utilizing prepacked silica gel. Analytical purity was assessed either by reversed-phase high performance liquid chromatography (RP-HPLC) using an Agilent 1100 system equipped with a diode array spectrometer (λ range 190–400 nm) or by the LC-MS method detailed below. The stationary phase was a Keystone Scientific BDS Hypersil™ C-18 column (5 μm , 4.6 mm \times 200 mm). The mobile phase employed 0.1% aqueous TFA with MeCN as the organic modifier and a flow rate of 1.0 mL/min. Analytical data are reported as retention time (t_R) in minutes and percent purity. All compounds were found to be $\geq 95\%$ pure unless otherwise indicated. ^1H NMR spectra were recorded on either a Varian Unityplus™ 400 MHz or a Bruker Avance™ III 400 MHz NMR spectrometer. Chemical shifts are reported in parts per million (ppm, δ units). Coupling constants are reported in units of hertz (Hz). Splitting patterns are designated as s, singlet; d, doublet; t, triplet; q, quartet; p, pentet; h, hextet; m, multiplet; or br, broad. Low-resolution mass spectra (MS) were recorded on a Waters SQD. High-resolution MS were recorded on a Waters (Micro-mass®) LCT time-of-flight mass spectrometer. Low-resolution mass spectra were obtained under electrospray ionization (ESI), atmospheric pressure chemical ionization (APCI), or fast atom bombardment (FAB) methods. All studies were conducted in accordance with the GSK Policy on the Care, Welfare and Treatment of Laboratory Animals and were reviewed by the Institutional Animal Care and Use Committee either at GSK or by the ethical review process at the institution where the work was performed.

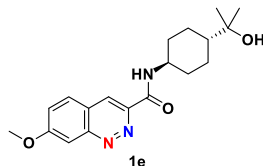
N-(*trans*-4-(2-Hydroxypropan-2-yl)cyclohexyl)-6-methoxy-2-naphthamide **1d**



N,N-Diisopropylethylamine (0.095 mL, 0.544 mmol) was added to a solution of 6-methoxy-2-naphthoic acid **7a** (50 mg, 0.247 mmol) in *N,N*-dimethylformamide (3 mL), followed by 1-[bis(dimethylamino)methylene]-1*H*-1,2,3-triazolo[4,5-*b*]pyridinium 3-oxide hexafluorophosphate (103 mg, 0.272 mmol) in portions. The reaction mixture was stirred for ~ 3 min and then 2-(*trans*-4-aminocyclohexyl)propan-2-ol **8a** (42.8 mg, 0.272 mmol, PharmaBlock) was added. After 40 min, LC-MS showed $\sim 50\%$ product. Additional 2-(*trans*-4-aminocyclohexyl)propan-2-ol **8a** (15.6 mg, 0.099 mmol) was added, and the reaction mixture was stirred for another 45 min. The reaction mixture is diluted with ethyl acetate and washed with saturated potassium carbonate solution (2X), 0.1 M hydrochloric acid (2X), and saturated sodium chloride (1X), dried over sodium sulfate, filtered, and concentrated. The residue was purified by silica gel chromatography, eluting with ethyl acetate:hexanes (0:1 to 7:3), then crystallized from dichloromethane:hexanes to give *N*-(*trans*-4-(2-hydroxypropan-2-yl)cyclohexyl)-6-methoxy-2-naphthamide **1d** (58 mg, 0.16 mol, 65% yield). ^1H NMR (400 MHz, CD_3SOCD_3) δ 1.04 (s, 6H), 1.06–1.24 (m, 3H), 1.33 (q, $J = 10$ Hz, 2H), 1.84 (br d, $J = 12$ Hz, 2H), 1.92 (br d, $J = 10$ Hz, 2H), 3.68–3.80 (m, 1H), 3.89 (s, 3H), 4.03 (s, 1H),

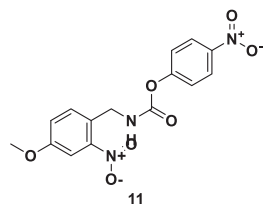
7.21 (dd, $J = 9, 2$ Hz, 1H), 7.36 (d, $J = 2$ Hz, 1H), 7.85 (d, $J = 9$ Hz, 1H), 7.87 (d, $J = 2$ Hz, 1H), 7.91 (d, $J = 9$ Hz, 1H), 8.24 (d, $J = 8$ Hz, 1H), 9.34 (s, 1H); LC-MS (LC-ES) $C_{21}H_{27}NO_3$ M + H = 342; $t_R = 0.75$ min, 100% purity.

N-(*trans*-4-(2-Hydroxypropan-2-yl)cyclohexyl)-7-methoxycinnoline-3-carboxamide **1e**



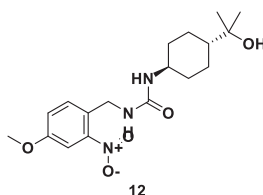
N,N-Diisopropylethylamine (0.474 mL, 2.72 mmol) was added to 7-methoxycinnoline-3-carboxylic acid **7b** (0.0924 g, 0.453 mmol) in 1,4-dioxane (2.263 mL) at room temperature. Then, 2-(*trans*-4-aminocyclohexyl)propan-2-ol **8a** (0.078 g, 0.498 mmol, PharmaBlock) was added and the reaction mixture was stirred for five minutes. Then, *n*-propylphosphonic acid anhydride (0.539 mL, 0.905 mmol) was added and the reaction mixture was stirred for sixty-four hours. The reaction mixture was poured into saturated sodium bicarbonate, extracted with ethyl acetate (3X), dried over magnesium sulfate, filtered, and concentrated. The residue was purified by silica gel chromatography, eluting with ethyl acetate to give *N*-(*trans*-4-(2-hydroxypropan-2-yl)cyclohexyl)-7-methoxycinnoline-3-carboxamide (0.0677 g, 0.187 mmol, 41.4% yield). 1H NMR (400 MHz, CD_3SOCD_3) δ 1.05 (s, 6H), 1.06–1.26 (m, 3H), 1.50 (q, $J = 12$ Hz, 2H), 1.84 (br d, $J = 12$ Hz, 2H), 1.91 (br d, $J = 10$ Hz, 2H), 3.86 (qt, $J = 8, 4$ Hz, 1H), 4.04 (s, 3H), 4.04 (s, 1H), 7.59 (dd, $J = 9, 3$ Hz, 1H), 7.87 (d, $J = 2$ Hz, 1H), 8.20 (d, $J = 9$ Hz, 1H), 8.72 (s, 1H), 9.02 (d, $J = 8$ Hz, 1H); LC-MS (LC-ES) $C_{19}H_{25}N_3O_3$ M + H = 344; $t_R = 0.69$ min, 100% purity.

4-Nitrophenyl 4-methoxy-2-nitrobenzylcarbamate **11**



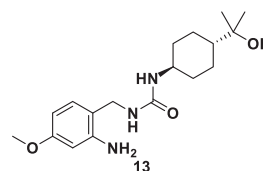
N,N-Diisopropylethylamine (1.220 mL, 6.99 mmol) was added to (4-methoxy-2-nitrophenyl)methanamine hydrochloride **9** (0.5092 g, 2.329 mmol) in tetrahydrofuran (11.64 mL) at room temperature. Then, 4-nitrophenyl chloroformate **10** (0.516 g, 2.56 mmol) was added and the reaction mixture was stirred for sixteen hours. 10% Citric acid was added to the reaction mixture and it was extracted with diethyl ether, washed with saturated sodium bicarbonate, dried over magnesium sulfate, filtered, and concentrated. The reaction mixture was purified by silica gel chromatography, eluting with ethyl acetate:hexanes (3:7) to give 4-nitrophenyl 4-methoxy-2-nitrobenzylcarbamate **11** (0.7470 g, 2.043 mmol, 88% yield). 1H NMR (400 MHz, CD_3SOCD_3) δ 3.85 (s, 3H), 4.52 (d, $J = 6$ Hz, 2H), 7.36 (dd, $J = 9, 3$ Hz, 1H), 7.41 (d, $J = 9$ Hz, 2H), 7.56 (d, $J = 6$ Hz, 1H), 7.57 (s, 1H), 8.26 (d, $J = 9$ Hz, 2H), 8.60 (br t, $J = 6$ Hz, 1H); LC-MS (LC-ES) M + H = 348.

1-(*trans*-4-(2-Hydroxypropan-2-yl)cyclohexyl)-3-(4-methoxy-2-nitrobenzyl)urea **12**



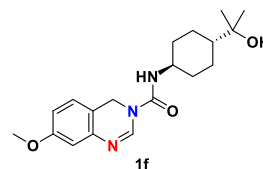
N,N-Diisopropylethylamine (0.238 mL, 1.363 mmol) was added to 4-nitrophenyl 4-methoxy-2-nitrobenzylcarbamate **11** (0.1578 g, 0.454 mmol) in tetrahydrofuran (4.54 mL) at room temperature. Then, 2-(*trans*-4-aminocyclohexyl)propan-2-ol **8a** (0.093 g, 0.591 mmol, PharmaBlock) was added and the reaction mixture was stirred for sixteen hours. 10% Citric acid was added to the reaction mixture and it was extracted with diethyl ether, washed with saturated sodium bicarbonate, dried over magnesium sulfate, filtered, and concentrated. The reaction mixture was purified by silica gel chromatography, eluting with methanol:ethyl acetate (0:1 to 1:19) to give 1-(*trans*-4-(2-hydroxypropan-2-yl)cyclohexyl)-3-(4-methoxy-2-nitrobenzyl)urea **12** (0.1373 g, 0.357 mmol, 79% yield). 1H NMR (400 MHz, CD_3SOCD_3) δ 1.00 (s, 6H), 0.94–1.16 (m, 5H), 1.70–1.78 (m, 2H), 1.78–1.86 (m, 2H), 3.14–3.28 (m, 1H), 3.82 (s, 3H), 3.98 (br s, 1H), 4.34 (d, $J = 6$ Hz, 2H), 5.91 (d, $J = 8$ Hz, 1H), 6.20 (br t, $J = 6$ Hz, 1H), 7.30 (dd, $J = 9, 3$ Hz, 1H), 7.43 (d, $J = 9$ Hz, 1H), 7.50 (d, $J = 3$ Hz, 1H); LC-MS (LC-ES) M + H = 366.

1-(2-Amino-4-methoxybenzyl)-3-(*trans*-4-(2-hydroxypropan-2-yl)cyclohexyl)urea **13**



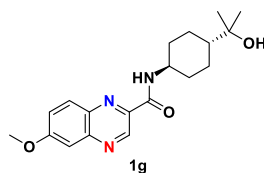
Palladium on carbon (3.75 mg, 0.035 mmol) was added to 1-(*trans*-4-(2-hydroxypropan-2-yl)cyclohexyl)-3-(4-methoxy-2-nitrobenzyl)urea **12** (0.1287 g, 0.352 mmol) in methanol (7.04 mL) at room temperature under nitrogen atmosphere. Then, the reaction vessel was fitted with a hydrogen balloon and the vessel was repeatedly evacuated and purged with hydrogen, then stirred for two hours. Then, the vessel was repeatedly evacuated and purged with nitrogen, filtered through Celite®, and concentrated. The residue was purified by silica gel chromatography, eluting with methanol:ethyl acetate (1:19) to give 1-(2-amino-4-methoxybenzyl)-3-(*trans*-4-(2-hydroxypropan-2-yl)cyclohexyl)urea **13** (0.1373 g, 0.389 mmol, 110% yield). 1H NMR (400 MHz, CD_3SOCD_3) δ 1.00 (s, 6H), 0.92–1.16 (m, 5H), 1.70–1.78 (m, 2H), 1.78–1.86 (m, 2H), 3.14–3.28 (m, 1H), 3.62 (s, 3H), 3.96 (d, $J = 6$ Hz, 2H), 3.98 (s, 1H), 5.21 (s, 2H), 5.70 (d, $J = 8$ Hz, 1H), 5.93 (br t, $J = 6$ Hz, 1H), 6.03 (dd, $J = 8, 3$ Hz, 1H), 6.14 (d, $J = 3$ Hz, 1H), 6.82 (d, $J = 8$ Hz, 1H); LC-MS (LC-ES) M + H = 336.

N-(*trans*-4-(2-Hydroxypropan-2-yl)cyclohexyl)-7-methoxyquinazoline-3(4*H*)-carboxamide **1f**



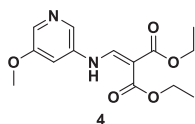
1-(2-Amino-4-methoxybenzyl)-3-(*trans*-4-(2-hydroxypropan-2-yl)cyclohexyl)urea **13** (0.0531 g, 0.158 mmol) was taken up in trimethyl orthoformate (1.732 mL, 15.83 mmol) at room temperature under nitrogen atmosphere and heated at 102 °C for two hours. Then, the vessel was cooled and concentrated. The residue was purified by silica gel chromatography, eluting with methanol:ethyl acetate (1:19) to give *N*-(*trans*-4-(2-hydroxypropan-2-yl)cyclohexyl)-7-methoxyquinazoline-3(4*H*)-carboxamide **1f** (0.0178 g, 0.049 mmol, 30.9% yield). 1H NMR (400 MHz, CD_3SOCD_3) δ 1.02 (s, 6H), 1.05 (q, $J = 10$ Hz, 2H), 1.08–1.20 (m, 1H), 1.24 (q, $J = 12$ Hz, 2H), 1.80 (br d, $J = 12$ Hz, 2H), 1.87 (br d, $J = 10$ Hz, 2H), 3.45 (qt, $J = 8, 4$ Hz, 1H), 3.72 (s, 3H), 4.02 (br s, 1H), 4.63 (s, 2H), 6.63 (d, $J = 3$ Hz, 1H), 6.70 (dd, $J = 8, 3$ Hz, 1H), 6.97 (d, $J = 8$ Hz, 1H), 7.21 (d, $J = 8$ Hz, 1H), 7.85 (s, 1H); LC-MS (LC-ES) $C_{19}H_{27}N_3O_3$ M + H = 346; $t_R = 0.49$ min, 96% purity.

N-(trans-4-(2-Hydroxypropan-2-yl)cyclohexyl)-6-methoxyquinoxaline-2-carboxamide **1g**



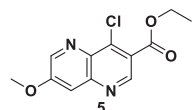
N,N-Diisopropylethylamine (0.066 mL, 0.377 mmol) was added to a solution of 6-methoxyquinoxaline-2-carboxylic acid **7c** (35 mg, 0.171 mmol) in *N,N*-dimethylformamide (3 mL), followed by 1-[bis(dimethylamino)methylene]-1*H*-1,2,3-triazolo[4,5-*b*]pyridinium 3-oxide hexafluorophosphate (71.7 mg, 0.189 mmol). After stirring for ~ 2 min, 2-(trans-4-aminocyclohexyl)propan-2-ol **8a** (29.7 mg, 0.189 mmol, PharmaBlock) was added in one portion. After 3 h, the reaction mixture is diluted with ethyl acetate and washed with diluted aqueous hydrochloric acid (1X), saturated potassium carbonate solution (2X), and saturated aqueous sodium chloride (1X). The organic phase was dried over sodium sulfate, filtered and concentrated. The residue was chromatographed over silica gel, eluting with ethyl acetate:hexanes (1:4 to 4:1), then repurified by silica gel chromatography, eluting with ethyl acetate:hexanes (1:4 to 4:1). The resulting material was dissolved in ethyl acetate with a little methanol and washed with water (4X) and saturated sodium chloride, dried over sodium sulfate, filtered, concentrated, and crystallized from dichloromethane:hexanes to give *N*-(trans-4-(2-hydroxypropan-2-yl)cyclohexyl)-6-methoxyquinoxaline-2-carboxamide **1g** (34 mg, 0.094 mmol, 55% yield) as a yellow solid. ¹H NMR (400 MHz, CD₃SOCD₃) δ 1.05 (s, 6H), 1.06–1.26 (m, 3H), 1.45 (q, *J* = 12 Hz, 2H), 1.85 (br d, *J* = 16 Hz, 2H), 1.90 (br d, *J* = 16 Hz, 2H), 3.72–3.86 (m, 1H), 4.00 (s, 3H), 4.06 (br s, 1H), 7.54 (d, *J* = 2 Hz, 1H), 7.61 (dd, *J* = 9, 2 Hz, 1H), 8.11 (d, *J* = 9 Hz, 1H), 8.60 (d, *J* = 8 Hz, 1H), 9.37 (s, 1H); LC-MS (LC-ES) C₁₉H₂₅N₃O₃ M + H = 344; *t*_R = 0.71 min, 100% purity.

Diethyl 2-(((5-methoxypyridin-3-yl)amino)methylene)malonate **4**



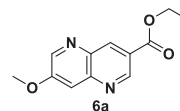
To a solution of 5-methoxypyridin-3-amine **2** (3 g, 24.17 mmol) in ethanol (150 mL) was added diethyl 2-(ethoxymethylene)malonate **3** (5.49 g, 25.4 mmol) and the reaction was heated at 80 °C for 24 h. The reaction mixture was concentrated under reduced pressure and the solid was placed under vacuum overnight to give diethyl 2-(((5-methoxypyridin-3-yl)amino)methylene)malonate **4** (6.0 g, 84% yield). LC-MS (LC-ES) M + H = 295.

Ethyl 4-chloro-7-methoxy-1,5-naphthyridine-3-carboxylate **5**



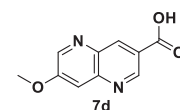
Diethyl 2-(((5-methoxypyridin-3-yl)amino)methylene)malonate **4** (500 mg, 1.699 mmol) was added to phosphorus oxychloride (3167 μL, 34.0 mmol). The reaction mixture was heated at 160 °C in a microwave for 3 h. The solution was diluted with ethyl acetate (150 mL), cooled to 0 °C in an ice bath, and pH adjusted to ~ 7 with saturated sodium bicarbonate. The organic layer was separated, the aqueous layer was reextracted with ethyl acetate (2X, 100 mL), and the combined organic layers were adsorbed to silica gel and purified by silica gel chromatography, eluting with ethyl acetate:hexanes (1:19 to 2:3) to give ethyl 4-chloro-7-methoxy-1,5-naphthyridine-3-carboxylate **5** (250 mg, 55% yield). LC-MS (LC-ES) M + H = 267.

Ethyl 7-methoxy-1,5-naphthyridine-3-carboxylate **6a**



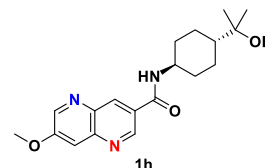
To a nitrogen degassed solution of ethyl 4-chloro-7-methoxy-1,5-naphthyridine-3-carboxylate **5** (250 mg, 0.937 mmol) in acetonitrile (10 mL) was added bis(triphenylphosphine)palladium(II) chloride (65.8 mg, 0.094 mmol) followed by triethylsilane (0.299 mL, 1.875 mmol). After heating 3 h at 70 °C, the reaction mixture was adsorbed to silica gel and purified by silica gel chromatography, eluting with methanol:dichloromethane (0:1 to 1:19) to give ethyl 7-methoxy-1,5-naphthyridine-3-carboxylate **6a** (100 mg, 46% yield). LC-MS (LC-ES) M + H = 233.

7-Methoxy-1,5-naphthyridine-3-carboxylic acid **7d**



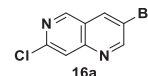
A solution of ethyl 7-methoxy-1,5-naphthyridine-3-carboxylate **6a** (50 mg, 0.215 mmol) in tetrahydrofuran (5 mL), and ethanol (5.00 mL) was treated with a solution of lithium hydroxide (25.8 mg, 1.076 mmol) in water (5 mL). The reaction mixture was heated at 50 °C for 45 min. The pH of the reaction was adjusted to ~ 6 and the solvent was removed under vacuum to give crude 7-methoxy-1,5-naphthyridine-3-carboxylic acid **7d** (44 mg, 100% yield). LC-MS (LC-ES) M + H = 205.

N-(trans-4-(2-Hydroxypropan-2-yl)cyclohexyl)-7-methoxy-1,5-naphthyridine-3-carboxamide **1h**



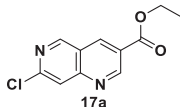
N,N-Diisopropylethylamine (0.171 mL, 0.980 mmol) was added to a solution of 7-methoxy-1,5-naphthyridine-3-carboxylic acid **7d** (50 mg, 0.245 mmol) in *N,N*-dimethylformamide (10 mL) at room temperature, followed by 2-(trans-4-aminocyclohexyl)propan-2-ol **8a** (38.5 mg, 0.245 mmol, PharmaBlock). Next, 2,4,6-tripropyl-1,3,5,2,4,6-trioxatriphosphinane 2,4,6-trioxide (50% in ethyl acetate) (312 mg, 0.490 mmol) was added by a slow dropwise addition and the reaction was allowed to stir at room temperature overnight. Saturated sodium bicarbonate solution was added to adjust the pH to ~ 8. The reaction mixture was repeatedly extracted with ethyl acetate until no product was in the organic layer as observed by thin layer chromatography (1:9 methanol:dichloromethane). The combined organic extracts were concentrated, adsorbed to silica gel, and purified by silica gel chromatography, eluting with methanol:dichloromethane (0:1 to 1:9) to give *N*-(trans-4-(2-hydroxypropan-2-yl)cyclohexyl)-7-methoxy-1,5-naphthyridine-3-carboxamide **1h** (35 mg, 0.102 mmol, 42% yield). ¹H NMR (400 MHz, CD₃SOCD₃) δ 1.04 (s, 6H), 1.04–1.24 (m, 3H), 1.34 (q, *J* = 12 Hz, 2H), 1.85 (br d, *J* = 12 Hz, 2H), 1.94 (br d, *J* = 10 Hz, 2H), 3.72–3.82 (m, 1H), 4.00 (s, 3H), 4.04 (s, 1H), 7.83 (d, *J* = 3 Hz, 1H), 8.61 (br d, *J* = 8 Hz, 1H), 8.79 (d, *J* = 2 Hz, 1H), 8.82 (d, *J* = 3 Hz, 1H), 9.29 (d, *J* = 2 Hz, 1H); LC-MS (LC-ES) C₁₉H₂₅N₃O₃ M + H = 344; *t*_R = 0.59 min, 100% purity.

3-Bromo-7-chloro-1,6-naphthyridine **16a**



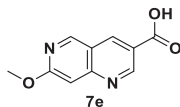
Ytterbium(III) trifluoromethanesulfonate (43.1 g, 69.5 mmol) was added to a solution of 4-amino-6-chloronicotinaldehyde **14** (50 g, 278 mmol, AstaTech) in acetonitrile (500 mL) at 0 °C under argon. Then, 2-bromo-1,1-dimethoxyethane **15** (98 mL, 833 mmol) was added and the resulting reaction mixture was heated to 80 °C and stirred for sixteen hours. On completion, the reaction mixture was filtered through a Celite® pad, the residue was washed with acetonitrile (500 mL) and the filtrate was evaporated under reduced pressure to give an impure material, which was purified via silica gel column chromatography, eluting with ethyl acetate:hexanes (1:4) to afford 3-bromo-7-chloro-1,6-naphthyridine **16a** (30 g, 98 mmol, 35% yield) as light yellow color solid. ¹H NMR (400 MHz, CDCl₃) δ 7.99 (s, 1H), 8.43 (m, 1H), 9.05 (s, 1H), 9.09 (d, *J* = 2 Hz, 1H); LC-MS (LC-ES) *M* + *H* = 243.

Ethyl 7-chloro-1,6-naphthyridine-3-carboxylate **17a**



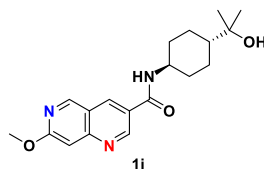
Triethylamine (17.69 mL, 127 mmol) was added to a solution of 3-bromo-7-chloro-1,6-naphthyridine **16a** (20 g, 63.4 mmol) in ethanol (400 mL) in an autoclave under carbon monoxide atmosphere (80 psi) at room temperature. Then, [1,1'-bis(diphenylphosphino)ferrocene] dichloropalladium(II) dichloromethane adduct (5.18 g, 6.34 mmol) was added and the reaction mixture was heated to 80 °C and stirred for 90 min. On completion, the reaction mixture was filtered through a Celite® pad, the residue was washed with ethanol (200 mL), and the solvent evaporated under reduced pressure to give an impure material, which was purified via silica gel column chromatography, eluting with ethyl acetate:hexanes (1:9) to afford ethyl 7-chloro-1,6-naphthyridine-3-carboxylate **17a** (10.7 g, 38.6 mmol, 61% yield) as an off white solid. ¹H NMR (400 MHz, CDCl₃) δ 1.48 (t, *J* = 7 Hz, 3H), 4.51 (q, *J* = 7 Hz, 2H), 8.06 (s, 1H), 8.88–9.03 (m, 1H), 9.21 (s, 1H), 9.62 (d, *J* = 2 Hz, 1H); LC-MS (LC-ES) *M* + *H* = 237.

7-Methoxy-1,6-naphthyridine-3-carboxylic acid **7e**



Sodium methoxide (25% in methanol, 1.15 mL, 5.03 mmol) was added to ethyl 7-chloro-1,6-naphthyridine-3-carboxylate **17a** (0.238 g, 1.006 mmol) in methanol (10 mL) at room temperature and the reaction mixture was heated to 60 °C for seven hours. The reaction mixture was concentrated, then water (10 mL) was added and the reaction was stirred for 90 min. The reaction mixture was filtered through a pad of Celite® and the filter cake rinsed with water. The pH was adjusted to ~5 with 1 N hydrochloric acid (4 mL). A fine, milky precipitate formed. An additional 1 N hydrochloric acid (1 mL) was added (pH = ~2). The solids were filtered off and rinsed with water (2X), air-dried, and then dried under vacuum to give 7-methoxy-1,6-naphthyridine-3-carboxylic acid **7e** (0.206 g, 1.009 mmol, 100% yield) as a pale yellow powder. ¹H NMR (400 MHz, CD₃SOCD₃) δ 4.02 (s, 3H), 7.29 (s, 1H), 9.07 (d, *J* = 2 Hz, 1H), 9.35 (s, 1H), 9.36 (d, *J* = 2 Hz, 1H), 13.54 (br s, 1H); LC-MS (LC-ES) *M* + *H* = 205.

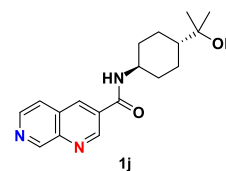
N-(*trans*-4-(2-Hydroxypropan-2-yl)cyclohexyl)-7-methoxy-1,6-naphthyridine-3-carboxamide **1i**



7-Methoxy-1,6-naphthyridine-3-carboxylic acid **7e** (0.110 g, 0.539

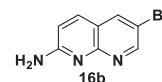
mmol) was added to 2-(*trans*-4-aminocyclohexyl)propan-2-ol **8a** (0.079 g, 0.502 mmol, PharmaBlock) in *N,N*-dimethylformamide (5 mL) at room temperature. Then, *N,N*-diisopropylethylamine (0.22 mL, 1.263 mmol) was added, followed by 1-[bis(dimethylamino)methylene]-1*H*-1,2,3-triazolo[4,5-*b*]pyridinium 3-oxide hexafluorophosphate (0.232 g, 0.610 mmol) and the reaction mixture was stirred for 150 min. The reaction mixture was concentrated and the resulting residue was purified by silica gel chromatography, eluting with (ethyl acetate:ethanol (3:1)):hexanes (0:1 to 1:0) to give a residue which was triturated/sonicated with ethyl acetate and filtered to give *N*-(*trans*-4-(2-hydroxypropan-2-yl)cyclohexyl)-7-methoxy-1,6-naphthyridine-3-carboxamide **1i** (0.123 g, 0.358 mmol, 71.3% yield) as a pale yellow powder. ¹H NMR (400 MHz, CD₃SOCD₃) δ 1.04 (s, 6H), 1.06–1.24 (m, 3H), 1.31 (q, *J* = 10 Hz, 2H), 1.84 (br d, *J* = 12 Hz, 2H), 1.94 (br d, *J* = 10 Hz, 2H), 3.68–3.80 (m, 1H), 4.01 (s, 3H), 4.06 (s, 1H), 7.27 (s, 1H), 8.58 (d, *J* = 8 Hz, 1H), 8.90 (dd, *J* = 2, 1 Hz, 1H), 9.25 (d, *J* = 1 Hz, 1H), 9.34 (d, *J* = 2 Hz, 1H); LC-MS (LC-ES) C₁₉H₂₅N₃O₃ *M* + *H* = 344; *t*_R = 0.68 min, 100% purity.

N-(*trans*-4-(2-Hydroxypropan-2-yl)cyclohexyl)-1,7-naphthyridine-3-carboxamide **1j**



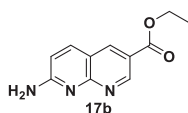
N,N-Diisopropylethylamine (0.604 mL, 3.46 mmol) was added to 1,7-naphthyridine-3-carboxylic acid **7f** (0.1003 g, 0.576 mmol, Enamine) in 1,4-dioxane (2.88 mL) at room temperature. Then, 2-(*trans*-4-aminocyclohexyl)propan-2-ol **8a** (0.109 g, 0.691 mmol, PharmaBlock) was added and the reaction mixture was stirred for five minutes. Then, *n*-propylphosphonic acid anhydride (0.686 mL, 1.152 mmol) was added and the reaction mixture was stirred for sixteen hours. The reaction mixture was poured into saturated sodium bicarbonate, extracted with ethyl acetate (3X), dried over magnesium sulfate, filtered, and concentrated. The residue was purified by silica gel chromatography, eluting with methanol:ethyl acetate (1:8) to give *N*-(*trans*-4-(2-hydroxypropan-2-yl)cyclohexyl)-1,7-naphthyridine-3-carboxamide **1j** (0.0552 g, 0.167 mmol, 29.1% yield). ¹H NMR (400 MHz, CD₃SOCD₃) δ 1.05 (s, 6H), 1.06–1.24 (m, 3H), 1.32 (q, *J* = 12 Hz, 2H), 1.84 (br d, *J* = 12 Hz, 2H), 1.96 (br d, *J* = 10 Hz, 2H), 3.76 (qt, *J* = 8, 4 Hz, 1H), 4.05 (s, 1H), 8.02 (d, *J* = 6 Hz, 1H), 8.69 (d, *J* = 6 Hz, 1H), 8.71 (d, *J* = 8 Hz, 1H), 8.83 (d, *J* = 2 Hz, 1H), 9.36 (d, *J* = 2 Hz, 1H), 9.46 (s, 1H); LC-MS (LC-ES) C₁₈H₂₃N₃O₂ *M* + *H* = 314; *t*_R = 0.50 min, 100% purity.

6-Bromo-1,8-naphthyridin-2-amine **16b**



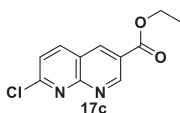
Phosphoric acid (60 mL, 183 mmol) was added to a mixture of pyridine-2,6-diamine **18** (20 g, 183 mmol) and 2-bromomalonaldehyde **19** (27.7 g, 183 mmol) at 0 °C under nitrogen. The resulting reaction mixture was heated to 120 °C and stirred for sixteen hours. On completion, the reaction mixture was quenched with 2 M aqueous sodium hydroxide solution (150 mL). The precipitate was filtered, washed with water (1000 mL), and dried to give an impure material. This material was purified via neutral alumina column chromatography, eluting with methanol:dichloromethane (1:9) to afford 6-bromo-1,8-naphthyridin-2-amine **16b** (20 g, 69.4 mmol, 38% yield) as a yellow solid. ¹H NMR (400 MHz, CD₃SOCD₃) δ 6.85 (d, *J* = 9 Hz, 1H), 6.98 (br s, 2H), 7.90 (d, *J* = 9 Hz, 1H), 8.32 (s, 1H), 8.68 (s, 1H); LC-MS (LC-ES) *M* + *H* = 224.

Ethyl 7-amino-1,8-naphthyridine-3-carboxylate **17b**



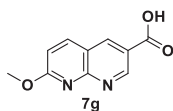
Triethylamine (19.33 mL, 139 mmol) was added to a solution of 6-bromo-1,8-naphthyridine-2-amine⁶² **16b** (20 g, 69.4 mmol) in ethanol (200 mL) in an autoclave under carbon monoxide atmosphere (100 psi). Then, [1,1'-bis(diphenylphosphino)ferrocene]dichloropalladium(II) (5.07 g, 6.94 mmol) was added and the reaction mixture was heated to 100 °C and stirred for five hours. On completion, the reaction mixture was filtered through a Celite® pad that was washed with ethanol (500 mL). The filtrate was evaporated under reduced pressure to give a residue, which was purified via neutral alumina column chromatography, eluting with methanol:dichloromethane (1:9) to afford ethyl 7-amino-1,8-naphthyridine-3-carboxylate **17b** (10 g, 43.8 mmol, 63% yield) as an off white solid. ¹H NMR (400 MHz, CD₃SOCD₃) δ 1.35 (t, *J* = 7 Hz, 3H), 4.36 (q, *J* = 7 Hz, 2H), 6.89 (d, *J* = 9 Hz, 1H), 7.29 (s, 2H), 8.09 (d, *J* = 9 Hz, 1H), 8.60 (d, *J* = 2 Hz, 1H), 9.12 (d, *J* = 2 Hz, 1H); LC-MS (LC-ES) *M* + *H* = 218.

Ethyl 7-chloro-1,8-naphthyridine-3-carboxylate **17c**



Sodium nitrite (1.210 g, 17.53 mmol) was added to ethyl 7-amino-1,8-naphthyridine-3-carboxylate **17b** (2 g, 8.77 mmol) at room temperature. Then, concentrated sulfuric acid (4.77 mL, 88 mmol) was added dropwise and the reaction mixture was stirred for sixteen hours. On completion, the reaction mixture was diluted with ice water (50 mL) and stirred for 10 min. The precipitate was filtered, washed with pentane (10 mL) and diethyl ether (10 mL), and dried under vacuum to afford ethyl 7-hydroxy-1,8-naphthyridine-3-carboxylate (1.8 g, 63% yield) as off white solid (¹H NMR (400 MHz, CD₃SOCD₃) δ 1.22–1.52 (t, *J* = 7 Hz, 3H), 4.37 (q, *J* = 7 Hz, 2H), 6.44–6.79 (m, 1H), 7.86–8.17 (m, 1H), 8.52–8.76 (m, 1H), 8.92–9.09 (m, 1H), 12.39–12.71 (br s, 1H); LC-MS (LC-ES) *M* + *H* = 219). *N,N*-Diisopropylethylamine (2.3 mL, 13.33 mmol) was added to a solution of ethyl 7-hydroxy-1,8-naphthyridine-3-carboxylate (1.8 g, 6.67 mmol) in 1,4-dioxane (18 mL) at 0 °C. Then, phosphorus oxychloride (2.48 mL, 26.7 mmol) was added and the resulting reaction mixture was heated to 80 °C and stirred for sixteen hours. On completion, the reaction mixture was diluted with ice cold water (50 mL) and extracted with ethyl acetate (2 X 50 mL). The combined organic layers were washed with brine (50 mL), dried over anhydrous sodium sulfate, filtered, and evaporated under reduced pressure to give an impure material, which was purified via neutral alumina column chromatography, eluting with ethyl acetate:petroleum ether (2:3) to afford ethyl 7-chloro-1,8-naphthyridine-3-carboxylate **17c** (900 mg, 3.66 mmol, 55% yield) as an off white solid. ¹H NMR (400 MHz, CDCl₃) δ 1.37–1.52 (t, *J* = 7 Hz, 3H), 4.48–4.59 (q, *J* = 7 Hz, 2H), 7.58 (d, *J* = 9 Hz, 1H), 8.26 (d, *J* = 9 Hz, 1H), 8.88 (d, *J* = 2 Hz, 1H), 9.66 (d, *J* = 2 Hz, 1H); LC-MS (LC-ES) *M* + *H* = 237.

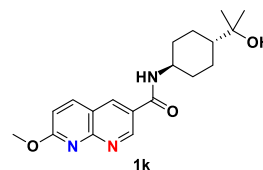
7-Methoxy-1,8-naphthyridine-3-carboxylic acid **7g**



Sodium methoxide (25% in methanol, 1.15 mL, 5.03 mmol) was added to ethyl 7-chloro-1,8-naphthyridine-3-carboxylate **17c** (0.238 g, 1.006 mmol) in methanol (10 mL) at room temperature and the reaction mixture was heated at 60 °C for two hours. The reaction mixture was concentrated and water (10 mL) was added. The reaction mixture was

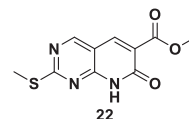
stirred for 75 min, then the reaction mixture was filtered through a pad of Celite® and the filter cake rinsed with water. The pH was adjusted to ~ 4–5 with 1 N hydrochloric acid (4 mL). A fine, milky precipitate formed. An additional 1 N hydrochloric acid (1 mL) was added (pH = ~2), and the solids were filtered off and rinsed twice with water, air dried, then dried under vacuum to give 7-methoxy-1,8-naphthyridine-3-carboxylic acid **7g** (0.202 g, 0.989 mmol, 98% yield) as a tan powder. ¹H NMR (400 MHz, CD₃SOCD₃) δ 4.05 (s, 3H), 7.23 (d, *J* = 9 Hz, 1H), 8.50 (d, *J* = 9 Hz, 1H), 8.95 (d, *J* = 2 Hz, 1H), 9.31 (d, *J* = 2 Hz, 1H), 13.46 (br s, 1H); LC-MS (LC-ES) *M* + *H* = 205.

N-(*trans*-4-(2-Hydroxypropan-2-yl)cyclohexyl)-7-methoxy-1,8-naphthyridine-3-carboxamide **1k**



7-Methoxy-1,8-naphthyridine-3-carboxylic acid **7g** (0.110 g, 0.539 mmol) was added to 2-(*trans*-4-aminocyclohexyl)propan-2-ol **8a** (0.081 g, 0.515 mmol, PharmaBlock) in *N,N*-dimethylformamide (5 mL) at room temperature. Then, *N,N*-diisopropylethylamine (0.23 mL, 1.320 mmol) was added, followed by 1-[bis(dimethylamino)methylene]-1*H*-1,2,3-triazolo[4,5-*b*]pyridinium 3-oxide hexafluorophosphate (0.235 g, 0.618 mmol) and the reaction mixture was stirred for 150 min. The reaction mixture was concentrated and the resulting residue was purified by silica gel chromatography, eluting with (ethyl acetate:ethanol (3:1)):hexanes (0:1 to 1:0) to give a residue which was triturated/sonicated with ethyl acetate and filtered to give *N*-(*trans*-4-(2-hydroxypropan-2-yl)cyclohexyl)-7-methoxy-1,8-naphthyridine-3-carboxamide **1j** (0.127 g, 0.370 mmol, 71.8% yield) as an off-white powder. ¹H NMR (400 MHz, CD₃SOCD₃) δ 1.04 (s, 6H), 1.06–1.24 (m, 3H), 1.31 (q, *J* = 12 Hz, 2H), 1.83 (br d, *J* = 12 Hz, 2H), 1.93 (br d, *J* = 10 Hz, 2H), 3.68–3.80 (m, 1H), 4.03 (s, 3H), 4.06 (s, 1H), 7.19 (d, *J* = 9 Hz, 1H), 8.40 (d, *J* = 9 Hz, 1H), 8.54 (d, *J* = 8 Hz, 1H), 8.78 (d, *J* = 2 Hz, 1H), 9.27 (d, *J* = 2 Hz, 1H); LC-MS (LC-ES) C₁₉H₂₅N₃O₃ *M* + *H* = 344; *t*_R = 0.66 min, 100% purity.

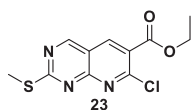
Ethyl 2-(methylthio)-7-oxo-7,8-dihydropyrido[2,3-*d*]pyrimidine-6-carboxylate **22**



Diethyl malonate **20** (2.40 mL, 15.73 mmol) was added to a stirred solution of 4-amino-2-(methylthio)pyrimidine-5-carbaldehyde **21** (2.00 g, 11.82 mmol, AstaTech) in *N,N*-dimethylformamide (40 mL). Then, potassium carbonate (2.000 g, 14.47 mmol) was added and the reaction mixture was heated to 85 °C and stirred overnight. As starting material was still present, triethylamine (1.00 mL, 7.17 mmol) was added to the mixture with stirring continued overnight. Additional triethylamine (1.00 mL, 7.17 mmol) was added to the mixture and stirring was continued for 8 h. Additional diethyl malonate (0.5 mL, 525 mg, 3.28 mmol) was added to the mixture and stirring was continued overnight. The reaction temperature was increased to 100 °C and stirring was continued for 1 h. Additional diethyl malonate (0.5 mL, 525 mg, 3.28 mmol) was added, followed by triethylamine (1.00 mL, 7.17 mmol) and stirring was continued for 5 h. Then the mixture was cooled to room temperature, poured into water (400 mL) and acidified with acetic acid (6 mL) to ~ pH = 4. Some solid precipitated and was collected via vacuum filtration. The filtrate was extracted with ethyl acetate (3X) and the combined organic layers were washed with brine, dried over sodium sulfate, filtered, and concentrated to give an orange solid. This material

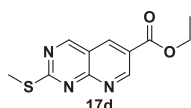
was combined with the previously collected tan solid and recrystallized from ethanol to give ethyl 2-(methylthio)-7-oxo-7,8-dihydropyrido[2,3-*d*]pyrimidine-6-carboxylate **22** (903 mg, 3.40 mmol, 29% yield) as a tan solid. The mother liquor from the recrystallization was evaporated under reduced pressure. The remaining material was dissolved in a minimal amount of dichloromethane and purified via silica gel chromatography, eluting with ethyl acetate:hexanes (1:19 to 1:1) to give recovered starting material (230 mg) as a yellow solid. The aqueous layer from the previous workup contained solid material. This solid was collected via vacuum filtration, washed with water and dried in vacuo to give ethyl 2-(methylthio)-7-oxo-7,8-dihydropyrido[2,3-*d*]pyrimidine-6-carboxylate **22** (496 mg, 1.87 mmol, 16% yield) as a tan solid. ¹H NMR (400 MHz, CD₃SOCD₃) δ 1.29 (t, *J* = 7 Hz, 3H), 2.57 (s, 3H), 4.26 (q, *J* = 7 Hz, 2H), 8.51 (s, 1H), 8.99 (s, 1H), 12.66 (br s, 1H); LC-MS (LC-ES) *M* + *H* = 266.

Ethyl 7-chloro-2-(methylthio)pyrido[2,3-*d*]pyrimidine-6-carboxylate **23**



A slurry of ethyl 2-(methylthio)-7-oxo-7,8-dihydropyrido[2,3-*d*]pyrimidine-6-carboxylate **22** (0.795 g, 3.00 mmol) in phosphorus oxychloride (6 mL, 64.4 mmol) was heated to 100 °C and stirred for 4 h. The mixture was still not homogeneous. Stirring was continued for 1 h and the mixture became homogeneous. After cooling to room temperature, the mixture was carefully pipetted into rapidly stirring ice cold saturated aqueous sodium bicarbonate and carefully and slowly adjusted to ~ pH = 5 with saturated aqueous sodium bicarbonate. The mixture was stirred for ~ 5 min and the resulting precipitate was collected via vacuum filtration, washed with water and dried in vacuo to give ethyl 7-chloro-2-(methylthio)pyrido[2,3-*d*]pyrimidine-6-carboxylate (681 mg, 2.40 mmol, 80% yield) as a tan solid. The filtrate was extracted with ethyl acetate (2X), washed with brine, dried over sodium sulfate, filtered, and concentrated to give ethyl 7-chloro-2-(methylthio)pyrido[2,3-*d*]pyrimidine-6-carboxylate **23** (117 mg, 0.412 mmol, 14% yield) as a yellow solid. ¹H NMR (400 MHz, CD₃SOCD₃) δ 1.36 (t, *J* = 7 Hz, 3H), 2.65 (s, 3H), 4.40 (q, *J* = 7 Hz, 2H), 9.10 (s, 1H), 9.51 (s, 1H); LC-MS (LC-ES) *M* + *H* = 284.

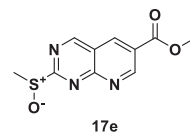
Ethyl 2-(methylthio)pyrido[2,3-*d*]pyrimidine-6-carboxylate **17d**



Acetonitrile (10 mL) was added to ethyl 7-chloro-2-(methylthio)pyrido[2,3-*d*]pyrimidine-6-carboxylate **23** (678 mg, 2.390 mmol) and bis(triphenylphosphine)palladium(II) chloride (85 mg, 0.121 mmol) and the mixture was degassed by sparging with nitrogen for ~ 15 min. Then, triethylsilane (0.50 mL, 3.13 mmol) was added to the mixture and it was heated to 80 °C and stirred overnight. After stirring at 80 °C for 19 h, the mixture was cooled to room temperature and a solid precipitated. The solid was collected by vacuum filtration, washed with hexane and dried in vacuo to give ethyl 2-(methylthio)pyrido[2,3-*d*]pyrimidine-6-carboxylate (237 mg, 0.951 mmol, 39.8% yield) as a tan solid. The filtrate was evaporated to dryness, dissolved in a minimal amount of dichloromethane, containing enough methanol for complete solubilization, and purified by silica gel chromatography, eluting with ethyl acetate:hexanes (1:19 to 2:3) to give ethyl 2,7-bis(methylthio)pyrido[2,3-*d*]pyrimidine-6-carboxylate (101 mg, 0.342 mmol, 14% yield) as a yellow solid and ethyl 2-(methylthio)pyrido[2,3-*d*]pyrimidine-6-carboxylate **17d** (52 mg, 0.209 mmol, 9% yield) as a yellow solid. ¹H NMR (400 MHz, CD₃SOCD₃) δ 1.38 (t, *J* = 7 Hz, 3H), 2.66 (s, 3H), 4.41 (q, *J* = 7 Hz, 2H), 9.13 (d, *J* = 2 Hz, 1H), 9.51 (d, *J* = 2 Hz, 1H), 9.65 (s,

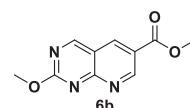
1H); LC-MS (LC-ES) *M* + *H* = 250.

Ethyl 2-(methylsulfinyl)pyrido[2,3-*d*]pyrimidine-6-carboxylate **17e**



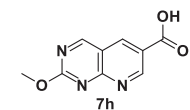
To a stirred, cooled (0 °C) solution of ethyl 2-(methylthio)pyrido[2,3-*d*]pyrimidine-6-carboxylate **17d** (200 mg, 0.802 mmol) in dichloromethane (10 mL) was added 3-chloroperoxybenzoic acid (370 mg, 1.651 mmol). The mixture was stirred for 30 min. The mixture was poured into saturated aqueous sodium bicarbonate and extracted with dichloromethane (2X). The combined organic layers were washed with brine, dried over sodium sulfate, filtered, and concentrated to give crude ethyl 2-(methylsulfinyl)pyrido[2,3-*d*]pyrimidine-6-carboxylate, containing some ethyl 2-(methylsulfonyl)pyrido[2,3-*d*]pyrimidine-6-carboxylate **17e** (155 mg, 73% yield) which was carried forward to the next reaction. ¹H NMR (400 MHz, CD₃SOCD₃) δ 1.40 (t, *J* = 7 Hz, 3H), 3.00 (s, 3H), 4.46 (q, *J* = 7 Hz, 2H), 9.36 (d, *J* = 2 Hz, 1H), 9.73 (d, *J* = 2 Hz, 1H), 10.04 (s, 1H); LC-MS (LC-ES) *M* + *H* = 266.

Methyl 2-methoxyxyrido[2,3-*d*]pyrimidine-6-carboxylate **6b**



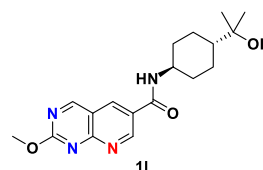
To a stirred solution of crude ethyl 2-(methylsulfinyl)pyrido[2,3-*d*]pyrimidine-6-carboxylate **17e** (154 mg, 0.581 mmol) in methanol (5 mL) was added 25% sodium methoxide (1 mL, 4.37 mmol) in methanol. A precipitate formed immediately upon addition of the sodium methoxide. The mixture was stirred for 20 min, then filtered and the collected solid was washed with a small amount of methanol and dried in vacuo to give methyl 2-methoxyxyrido[2,3-*d*]pyrimidine-6-carboxylate **6b** (47 mg, 0.214 mmol, 37% yield) as a white solid. ¹H NMR (400 MHz, CD₃SOCD₃) δ 3.10 (s, 3H), 3.25 (s, 3H), 8.32 (d, *J* = 2 Hz, 1H), 8.66 (d, *J* = 2 Hz, 1H), 8.88 (s, 1H); LC-MS (LC-ES) *M* + *H* = 220.

2-Methoxyxyrido[2,3-*d*]pyrimidine-6-carboxylic acid **7h**



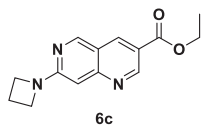
To a stirred suspension of methyl 2-methoxyxyrido[2,3-*d*]pyrimidine-6-carboxylate **6b** (45 mg, 0.205 mmol) in tetrahydrofuran (1.5 mL) and methanol (0.5 mL) was added 1 M aqueous lithium hydroxide (0.25 mL, 0.250 mmol). The mixture eventually became homogeneous and was stirred for 1 h. The solvent was removed under reduced pressure. The remaining material was suspended in water, acidified with 1 N aqueous hydrochloric acid and extracted with ethyl acetate (2X). The combined organic layers were washed with brine, dried over sodium sulfate, filtered, and concentrated to give 2-methoxyxyrido[2,3-*d*]pyrimidine-6-carboxylic acid **7h** (18 mg, 0.088 mmol, 43% yield) as a white solid. ¹H NMR (400 MHz, CD₃SOCD₃) δ 4.09 (s, 3H), 9.10 (d, *J* = 2 Hz, 1H), 9.49 (d, *J* = 2 Hz, 1H), 9.71 (s, 1H), 13.68 (br s, 1H); LC-MS (LC-ES) *M* + *H* = 206.

N-((trans)-4-(2-Hydroxypropan-2-yl)cyclohexyl)-2-methoxyxyrido[2,3-*d*]pyrimidine-6-carboxamide **11**



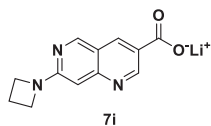
To a thick, stirred suspension of 2-methoxypyrido[2,3-*d*]pyrimidine-6-carboxylic acid **7h** (16 mg, 0.078 mmol) and 2-((trans-4-aminocyclohexyl)propan-2-yl) **8a** (15 mg, 0.095 mmol, PharmaBlock) in *N,N*-dimethylformamide (1 mL) was added *N,N*-diisopropylethylamine (0.050 mL, 0.286 mmol), followed by *n*-propylphosphonic acid anhydride (0.095 mL, 0.161 mmol). The mixture quickly became homogeneous and was allowed to stir overnight and concentrated. The mixture was purified by reverse phase chromatography, eluting with acetonitrile–water with 0.1% ammonium hydroxide (0:1 to 7:3) to give *N*-((trans-4-(2-hydroxypropan-2-yl)cyclohexyl)-2-methoxypyrido[2,3-*d*]pyrimidine-6-carboxamide **1k** (10 mg, 0.029 mmol, 37%) as a white solid. ¹H NMR (400 MHz, CD₃SOCD₃) δ 1.04 (s, 6H), 1.04–1.24 (m, 3H), 1.31 (q, *J* = 12 Hz, 2H), 1.84 (br d, *J* = 12 Hz, 2H), 1.94 (br d, *J* = 11 Hz, 2H), 3.68–3.80 (m, 1H), 4.08 (s, 3H), 8.65 (d, *J* = 8 Hz, 1H), 8.96 (d, *J* = 2 Hz, 1H), 9.47 (d, *J* = 2 Hz, 1H), 9.64 (s, 1H); LC-MS (LC-ES) C₁₈H₂₄N₄O₃ M + H = 345; t_R = 0.59 min, 100% purity.

Ethyl 7-(azetidin-1-yl)-1,6-naphthyridine-3-carboxylate **6c**



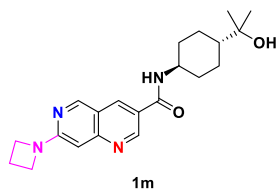
N,N-Diisopropylethylamine (1.502 mL, 8.62 mmol) was added to ethyl 7-chloro-1,6-naphthyridine-3-carboxylate **17a** (0.5102 g, 2.156 mmol) in *N*-methyl-2-pyrrolidone (7.19 mL) at room temperature. Then, azetidine hydrochloride (0.605 g, 6.47 mmol) was added and the reaction mixture was heated at 100 °C in the microwave for five hours. The reaction mixture was diluted in dichloromethane, washed with saturated sodium bicarbonate, dried over magnesium sulfate, filtered, and concentrated. The resulting residue was purified by RP HPLC, eluting with acetonitrile:water with 0.1% ammonium hydroxide (5:95 to 100:0), then further purified by silica gel chromatography, eluting with ethyl acetate:hexanes (3:7 to 4:1) to give ethyl 7-(azetidin-1-yl)-1,6-naphthyridine-3-carboxylate **6c** (0.2198 g, 0.812 mmol, 37.6% yield). ¹H NMR (400 MHz, CD₃SOCD₃) δ 1.35 (t, *J* = 7 Hz, 3H), 2.40 (p, *J* = 7 Hz, 2H), 4.10 (t, *J* = 7 Hz, 4H), 4.35 (q, *J* = 7 Hz, 2H), 6.53 (s, 1H), 8.83 (s, 1H), 9.15 (s, 1H), 9.17 (s, 1H); LC-MS (LC-ES) M + H = 258.

7-(Azetidin-1-yl)-1,6-naphthyridine-3-carboxylic acid lithium salt **7i**



Lithium hydroxide (0.061 g, 2.56 mmol) was added to ethyl 7-(azetidin-1-yl)-1,6-naphthyridine-3-carboxylate **6c** (0.2198 g, 0.854 mmol) in methanol (3.42 mL) and water (0.854 mL) at room temperature and the reaction mixture was stirred sixteen hours at 60 °C. Then, the reaction mixture was concentrated to give 7-(azetidin-1-yl)-1,6-naphthyridine-3-carboxylic acid lithium salt **7i** (0.2291 g, 0.854 mmol, 100% yield). ¹H NMR (400 MHz, CD₃SOCD₃) δ 2.36 (p, *J* = 7 Hz, 2H), 4.02 (t, *J* = 7 Hz, 4H), 6.51 (s, 1H), 8.50 (s, 1H), 8.96 (s, 1H), 9.25 (s, 1H); LC-MS (LC-ES) M–H = 230.

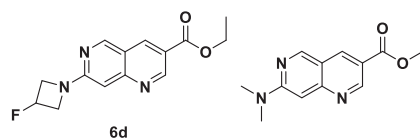
7-(Azetidin-1-yl)-*N*-(trans-4-(2-hydroxypropan-2-yl)cyclohexyl)-1,6-naphthyridine-3-carboxamide **1m**



N,N-Diisopropylethylamine (0.265 mL, 1.517 mmol) was added to 7-(azetidin-1-yl)-1,6-naphthyridine-3-carboxylic acid lithium salt **7i**

(0.0597 g, 0.253 mmol) in *N,N*-dimethylformamide (0.843 mL) at room temperature. Then, 2-(trans-4-aminocyclohexyl)propan-2-ol **8a** (0.048 g, 0.303 mmol, PharmaBlock) was added and the reaction mixture was stirred for five minutes. Then, *n*-propylphosphonic acid anhydride (0.301 mL, 0.506 mmol) was added and the reaction mixture was stirred for sixteen hours. The reaction mixture was concentrated. The resulting residue was purified by RP HPLC, eluting with acetonitrile:water with 0.1% ammonium hydroxide (5:95 to 100:0), then further purified by silica gel chromatography, eluting with methanol:ethyl acetate (0:1 to 3:7) to give 7-(azetidin-1-yl)-*N*-(trans-4-(2-hydroxypropan-2-yl)cyclohexyl)-1,6-naphthyridine-3-carboxamide **1n** (0.0514 g, 0.133 mmol, 52.4% yield). ¹H NMR (400 MHz, CD₃SOCD₃) δ 1.04 (s, 6H), 1.04–1.24 (m, 3H), 1.29 (q, *J* = 12 Hz, 2H), 1.83 (br d, *J* = 12 Hz, 2H), 1.91 (br d, *J* = 12 Hz, 2H), 2.39 (p, *J* = 7 Hz, 2H), 3.64–3.78 (m, 1H), 4.03 (s, 1H), 4.08 (t, *J* = 7 Hz, 4H), 6.54 (s, 1H), 8.38 (d, *J* = 7 Hz, 1H), 8.69 (s, 1H), 9.04 (s, 1H), 9.17 (s, 1H); LC-MS (LC-ES) C₂₁H₂₈N₄O₂ M + H = 369; t_R = 0.55 min, 100% purity.

Ethyl 7-(3-fluoroazetidin-1-yl)-1,6-naphthyridine-3-carboxylate **6d** and Ethyl 7-(dimethylamino)-1,6-naphthyridine-3-carboxylate

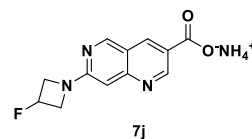


N,N-Diisopropylethylamine (1.259 mL, 7.23 mmol) was added to ethyl 7-chloro-1,6-naphthyridine-3-carboxylate **17a** (0.4278 g, 1.808 mmol) in *N,N*-dimethylformamide (6.03 mL) at room temperature. Then 3-fluoroazetidin-1-ium chloride (0.605 g, 5.42 mmol) was added and the reaction mixture was heated at 100 °C in the microwave for three hours. The reaction mixture was diluted in dichloromethane, washed with saturated sodium bicarbonate, dried over magnesium sulfate, filtered, and concentrated. The residue was purified by silica gel chromatography, eluting with ethyl acetate:hexanes (2:3 to 4:1), then further purified by RP HPLC, eluting with acetonitrile:water with 0.1% ammonium hydroxide (30:70 to 80:20) and shaving fractions to give some pure ethyl 7-(3-fluoroazetidin-1-yl)-1,6-naphthyridine-3-carboxylate **6d** (0.0831 g, 0.287 mmol, 15.86% yield) as well as some impure material and some pure ethyl 7-(dimethylamino)-1,6-naphthyridine-3-carboxylate (0.0419 g, 0.162 mmol, 8.98% yield).

Ethyl 7-(3-fluoroazetidin-1-yl)-1,6-naphthyridine-3-carboxylate **6d**
¹H NMR (400 MHz, CD₃SOCD₃) δ 1.35 (t, *J* = 7 Hz, 3H), 4.18 (br dd, *J* = 24, 11 Hz, 2H), 4.36 (q, *J* = 7 Hz, 2H), 4.38–4.50 (m, 2H), 5.44–5.70 (m, 1H), 6.69 (s, 1H), 8.91 (s, 1H), 9.21 (s, 1H), 9.23 (s, 1H); LC-MS (LC-ES) M + H = 276.

Ethyl 7-(dimethylamino)-1,6-naphthyridine-3-carboxylate
¹H NMR (400 MHz, CD₃SOCD₃) δ 1.35 (t, *J* = 7 Hz, 3H), 3.18 (s, 6H), 4.35 (q, *J* = 7 Hz, 2H), 6.81 (s, 1H), 8.82 (s, 1H), 9.17 (s, 2H); LC-MS (LC-ES) M + H = 246.

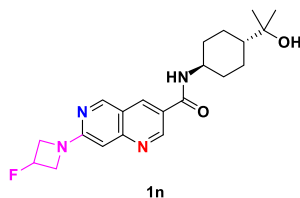
7-(3-Fluoroazetidin-1-yl)-1,6-naphthyridine-3-carboxylic acid ammonia salt **7j**



Lithium hydroxide (0.022 g, 0.906 mmol) was added to ethyl 7-(3-fluoroazetidin-1-yl)-1,6-naphthyridine-3-carboxylate **6d** (0.0831 g, 0.302 mmol) in methanol (1.20 mL) and water (0.30 mL) at room temperature and the reaction mixture was stirred sixteen hours at 60 °C. The reaction mixture was concentrated. The reaction mixture was purified by RP HPLC, eluting with acetonitrile:water with 0.1% ammonium hydroxide (0:100 to 60:40) to give 7-(3-fluoroazetidin-1-yl)-1,6-naphthyridine-3-carboxylic acid ammonia salt **7j** (0.0579 g, 0.208 mmol,

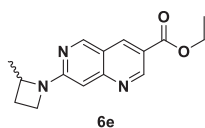
69.0% yield). ^1H NMR (400 MHz, CD_3SOCD_3) δ 4.09 (br dd, $J = 25, 10$ Hz, 2H), 4.02–4.44 (m, 2H), 5.42–5.66 (m, 1H), 6.65 (s, 1H), 8.54 (s, 1H), 9.01 (s, 1H), 9.28 (s, 1H); LC-MS (LC-ES) $M + H = 248$.

7-(3-Fluoroazetidin-1-yl)-*N*-(*trans*-4-(2-hydroxypropan-2-yl)cyclohexyl)-1,6-naphthyridine-3-carboxamide **1n**



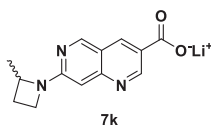
N,N-Diisopropylethylamine (0.230 mL, 1.315 mmol) was added to 7-(3-fluoroazetidin-1-yl)-1,6-naphthyridine-3-carboxylic acid ammonia salt **7j** (0.0579 g, 0.219 mmol) in *N,N*-dimethylformamide (0.730 mL) at room temperature. Then, 2-(*trans*-4-aminocyclohexyl)propan-2-ol **8a** (0.041 g, 0.263 mmol, PharmaBlock) was added and the reaction mixture was stirred for five minutes. Then, *n*-propylphosphonic acid anhydride (0.261 mL, 0.438 mmol) was added and the reaction mixture was stirred for sixty-four hours. The reaction mixture was concentrated. The resulting residue was purified by RP HPLC, eluting with acetonitrile: water with 0.1% ammonium hydroxide (5:95 to 100:0), then further purified by silica gel chromatography, eluting with methanol:ethyl acetate (0:1 to 1:4) to give 7-(3-fluoroazetidin-1-yl)-*N*-(*trans*-4-(2-hydroxypropan-2-yl)cyclohexyl)-1,6-naphthyridine-3-carboxamide **1n** (0.0622 g, 0.153 mmol, 69.8% yield). ^1H NMR (400 MHz, CD_3SOCD_3) δ 1.04 (s, 6H), 1.06–1.24 (m, 3H), 1.30 (q, $J = 13$ Hz, 2H), 1.83 (br d, $J = 12$ Hz, 2H), 1.92 (br d, $J = 12$ Hz, 2H), 3.64–3.78 (m, 1H), 4.03 (s, 1H), 4.14 (br dd, $J = 24, 10$ Hz, 2H), 4.34–4.48 (m, 2H), 5.38–5.68 (m, 1H), 6.70 (s, 1H), 8.42 (d, $J = 7$ Hz, 1H), 8.73 (s, 1H), 9.09 (s, 1H), 9.21 (s, 1H); LC-MS (LC-ES) $\text{C}_{21}\text{H}_{27}\text{FN}_4\text{O}_2$ $M + H = 387$; $t_R = 0.58$ min, 100% purity.

Ethyl 7-(2-methylazetidin-1-yl)-1,6-naphthyridine-3-carboxylate **6e**



N,N-Diisopropylethylamine (1.361 mL, 7.81 mmol) was added to ethyl 7-chloro-1,6-naphthyridine-3-carboxylate **17a** (0.4622 g, 1.953 mmol) in *N*-methyl-2-pyrrolidone (6.51 mL) at room temperature. Then 2-methylazetidine hydrochloride (0.420 g, 3.91 mmol) was added and the reaction mixture was heated at 100 °C in the microwave for four hours. The reaction mixture was diluted in dichloromethane, washed with saturated sodium bicarbonate, dried over magnesium sulfate, filtered, and concentrated. The resulting residue was purified by RP HPLC, eluting with acetonitrile:water with 0.1% ammonium hydroxide (5:95:100:0), then further purified by silica gel chromatography, eluting with ethyl acetate:hexanes (1:4 to 3:2) to give ethyl 7-(2-methylazetidin-1-yl)-1,6-naphthyridine-3-carboxylate **6e** (0.2731 g, 0.956 mmol, 49.0% yield). ^1H NMR (400 MHz, CD_3SOCD_3) δ 1.35 (t, $J = 7$ Hz, 3H), 1.51 (d, $J = 6$ Hz, 3H), 2.04 (p, $J = 8$ Hz, 1H), 2.50 (p, $J = 8$ Hz, 1H), 3.90 (q, $J = 8$ Hz, 1H), 4.06 (q, $J = 5$ Hz, 1H), 4.35 (q, $J = 7$ Hz, 2H), 4.48 (h, $J = 7$ Hz, 1H), 6.53 (s, 1H), 8.83 (s, 1H), 9.15 (s, 1H), 9.17 (s, 1H); LC-MS (LC-ES) $M + H = 272$.

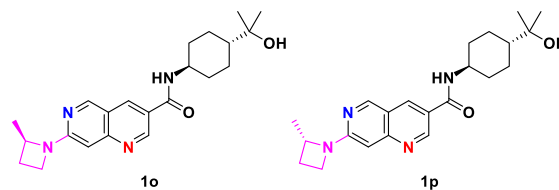
Lithium 7-(2-methylazetidin-1-yl)-1,6-naphthyridine-3-carboxylic acid **k**



Lithium hydroxide (0.072 g, 3.02 mmol) was added to ethyl 7-(2-

methylazetidin-1-yl)-1,6-naphthyridine-3-carboxylate **6e** (0.2731 g, 1.007 mmol) in methanol (4.03 mL) and water (1.007 mL) at room temperature and the reaction mixture was stirred three hours at 60 °C. The reaction mixture was concentrated to give lithium 7-(2-methylazetidin-1-yl)-1,6-naphthyridine-3-carboxylic acid **7k** (0.2551 g, 0.969 mmol, 96% yield). ^1H NMR (400 MHz, CD_3SOCD_3) δ 1.49 (d, $J = 6$ Hz, 3H), 2.03 (p, $J = 9$ Hz, 1H), 2.36–2.48 (m, 1H), 3.80 (q, $J = 8$ Hz, 1H), 3.98 (q, $J = 8$ Hz, 1H), 4.36 (h, $J = 7$ Hz, 1H), 6.51 (s, 1H), 8.51 (s, 1H), 8.97 (s, 1H), 9.25 (s, 1H); LC-MS (LC-ES) $M + H = 244$.

N-(*trans*-4-(2-Hydroxypropan-2-yl)cyclohexyl)-7-((*R*)-2-methylazetidin-1-yl)-1,6-naphthyridine-3-carboxamide **1o** and *N*-(*trans*-4-(2-Hydroxypropan-2-yl)cyclohexyl)-7-((*S*)-2-methylazetidin-1-yl)-1,6-naphthyridine-3-carboxamide **1p**



N,N-Diisopropylethylamine (0.426 mL, 2.441 mmol) was added to 7-(2-methylazetidin-1-yl)-1,6-naphthyridine-3-carboxylic acid lithium salt **7k** (0.1018 g, 0.407 mmol) in *N,N*-dimethylformamide (1.36 mL) at room temperature. Then, 2-(*trans*-4-aminocyclohexyl)propan-2-ol **8a** (0.077 g, 0.488 mmol, PharmaBlock) was added and the reaction mixture was stirred for five minutes. Then, *n*-propylphosphonic acid anhydride (0.484 mL, 0.814 mmol) was added and the reaction mixture was stirred for sixteen hours. The reaction mixture was concentrated. The resulting residue was purified by RP HPLC, eluting with acetonitrile: water with 0.1% ammonium hydroxide (5:95 to 100:0), then further purified by silica gel chromatography, eluting with methanol:ethyl acetate (0:1 to 1:9) to give racemic *N*-(*trans*-4-(2-hydroxypropan-2-yl)cyclohexyl)-7-(2-methylazetidin-1-yl)-1,6-naphthyridine-3-carboxamide (0.1064 g, 0.264 mmol, 64.9% yield). ^1H NMR (400 MHz, CD_3SOCD_3) δ 1.04 (s, 6H), 1.04–1.24 (m, 3H), 1.30 (q, $J = 12$ Hz, 2H), 1.50 (d, $J = 6$ Hz, 3H), 1.83 (br d, $J = 12$ Hz, 2H), 1.92 (br d, $J = 11$ Hz, 2H), 2.04 (p, $J = 9$ Hz, 1H), 2.42–2.54 (m, 1H), 3.66–3.78 (m, 1H), 3.86 (q, $J = 8$ Hz, 1H), 4.02 (s, 1H), 4.04 (q, $J = 6$ Hz, 1H), 4.44 (h, $J = 7$ Hz, 1H), 6.54 (s, 1H), 8.38 (d, $J = 7$ Hz, 1H), 8.69 (s, 1H), 9.05 (s, 1H), 9.17 (s, 1H); LC-MS (LC-ES) $\text{C}_{22}\text{H}_{30}\text{N}_4\text{O}_2$ $M + H = 383$. Racemic *N*-(*trans*-4-(2-hydroxypropan-2-yl)cyclohexyl)-7-(2-methylazetidin-1-yl)-1,6-naphthyridine-3-carboxamide (0.0971 g, 0.254 mmol) was separated into its enantiomers on a chiral IC column eluting with methanol:hexanes (3:2) with 1% diethylamine to give *N*-(*trans*-4-(2-hydroxypropan-2-yl)cyclohexyl)-7-((*R*)-2-methylazetidin-1-yl)-1,6-naphthyridine-3-carboxamide **1o** (0.0201 g, 0.050 mmol, 19.67% yield) as the first diastereomer (>99% ee) to elute and *N*-(*trans*-4-(2-hydroxypropan-2-yl)cyclohexyl)-7-((*S*)-2-methylazetidin-1-yl)-1,6-naphthyridine-3-carboxamide **1p** (0.0230 g, 0.057 mmol, 22.50% yield) as the last diastereomer to elute (96.6% ee). The structures were assigned by analogy.

N-(*trans*-4-(2-Hydroxypropan-2-yl)cyclohexyl)-7-((*R*)-2-methylazetidin-1-yl)-1,6-naphthyridine-3-carboxamide **1o**

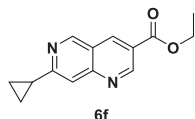
^1H NMR (400 MHz, CD_3SOCD_3) δ 1.04 (s, 6H), 1.04–1.24 (m, 3H), 1.30 (q, $J = 12$ Hz, 2H), 1.51 (d, $J = 6$ Hz, 3H), 1.83 (br d, $J = 12$ Hz, 2H), 1.92 (br d, $J = 12$ Hz, 2H), 2.04 (p, $J = 8$ Hz, 1H), 2.42–2.54 (m, 1H), 3.66–3.78 (m, 1H), 3.87 (q, $J = 8$ Hz, 1H), 4.01 (s, 1H), 4.04 (q, $J = 5$ Hz, 1H), 4.44 (h, $J = 6$ Hz, 1H), 6.54 (s, 1H), 8.38 (d, $J = 7$ Hz, 1H), 8.68 (s, 1H), 9.05 (s, 1H), 9.17 (s, 1H); LC-MS (LC-ES) $\text{C}_{22}\text{H}_{30}\text{N}_4\text{O}_2$ $M + H = 383$; $t_R = 0.62$ min, 100% purity.

N-(*trans*-4-(2-Hydroxypropan-2-yl)cyclohexyl)-7-((*S*)-2-methylazetidin-1-yl)-1,6-naphthyridine-3-carboxamide **1p**

^1H NMR (400 MHz, CD_3SOCD_3) δ 1.04 (s, 6H), 1.04–1.24 (m, 3H), 1.30 (q, $J = 12$ Hz, 2H), 1.50 (d, $J = 6$ Hz, 3H), 1.83 (br d, $J = 12$ Hz, 2H), 1.92 (br d, $J = 11$ Hz, 2H), 2.04 (p, $J = 9$ Hz, 1H), 2.42–2.54 (m,

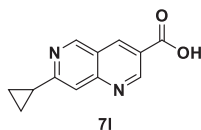
1H), 3.66–3.78 (m, 1H), 3.87 (q, $J = 8$ Hz, 1H), 4.02 (s, 1H), 4.04 (q, $J = 5$ Hz, 1H), 4.44 (h, $J = 6$ Hz, 1H), 6.54 (s, 1H), 8.38 (d, $J = 8$ Hz, 1H), 8.68 (s, 1H), 9.05 (s, 1H), 9.17 (s, 1H); LC-MS (LC-ES) $C_{22}H_{30}N_4O_2$ $M + H = 383$; $t_R = 0.62$ min, 100% purity.

Ethyl 7-cyclopropyl-1,6-naphthyridine-3-carboxylate **6f**



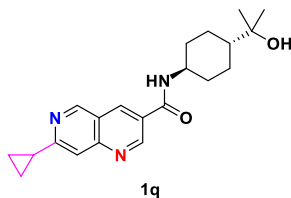
Cyclopropylboronic acid (17.42 g, 203 mmol) was added to a solution of ethyl 7-chloro-1,6-naphthyridine-3-carboxylate **17a** (20 g, 67.6 mmol) in toluene (600 mL) at room temperature under nitrogen. Then, 2-dicyclohexylphosphino-2',6'-dimethoxybiphenyl (SPHos) (0.638 g, 1.555 mmol) was added, followed by the addition of tris(dibenzylideneacetone)dipalladium(0) (3.65 g, 3.99 mmol) and 2 M aqueous sodium carbonate (42.3 mL, 85 mmol) and the reaction was purged with argon for 10 min. The reaction mixture was heated to 110 °C and stirred for sixteen hours. On completion, the reaction mixture was filtered through a Celite® pad, the residue was washed with ethyl acetate (200 mL), and the filtrate was evaporated under reduced pressure to give an impure material, which was purified via silica gel column chromatography, eluting with ethyl acetate:hexanes (1:4) to afford ethyl 7-cyclopropyl-1,6-naphthyridine-3-carboxylate **6f** (15 g, 61.4 mmol, 91% yield) as an off white solid. 1H NMR (400 MHz, $CDCl_3$) δ 1.05–1.24 (m, 4H), 1.46 (t, $J = 7$ Hz, 3H), 2.26–2.36 (m, 1H), 4.48 (q, $J = 7$ Hz, 2H), 7.78 (s, 1H), 8.84–8.93 (m, 1H), 9.21 (s, 1H), 9.54 (d, $J = 2$ Hz, 1H); LC-MS (LC-ES) $M + H = 243$.

7-Cyclopropyl-1,6-naphthyridine-3-carboxylic acid **7l**



A solution of sodium hydroxide (5.76 g, 144 mmol) in water (75 mL) was added to a solution of ethyl 7-cyclopropyl-1,6-naphthyridine-3-carboxylate **6f** (30 g, 120 mmol) in tetrahydrofuran (75 mL) at room temperature and the resulting reaction mixture was stirred for fifteen hours. On completion, the reaction mixture was concentrated (until tetrahydrofuran was removed) under vacuum, and then the reaction mixture was acidified with 1 M hydrochloric acid solution. The precipitate was filtered, washed with water (250 mL), pentane (500 mL) and diethyl ether (500 mL), and dried to afford 7-cyclopropyl-1,6-naphthyridine-3-carboxylic acid **7l** (18 g, 84 mmol, 70% yield) as an off white solid. 1H NMR (400 MHz, CD_3SOCD_3) δ 0.96–1.22 (m, 4H), 2.25–2.40 (m, 1H), 7.89 (s, 1H), 9.06 (dd, $J = 2, 1$ Hz, 1H), 9.43 (d, $J = 3$ Hz, 2H), 13.57 (br s, 1H); LC-MS (LC-ES) $M + H = 215$.

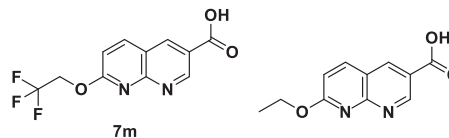
7-Cyclopropyl-*N*-((trans-4-(2-hydroxypropan-2-yl)cyclohexyl)-1,6-naphthyridine-3-carboxamide **1q**



To a stirring suspension of 7-cyclopropyl-1,6-naphthyridine-3-carboxylic acid **7l** (214 mg, 0.999 mmol) in *N,N*-dimethylformamide (13.3 mL) was added *N,N*-diisopropylethylamine (0.262 mL, 1.498 mmol) followed by 1-[bis(dimethylamino)methylene]-1*H*-1,2,3-triazolo[4,5-*b*]pyridinium 3-oxide hexafluorophosphate (475 mg, 1.249 mmol) in one portion. After ~ 5 min, 2-((trans-4-aminocyclohexyl)propan-2-ol

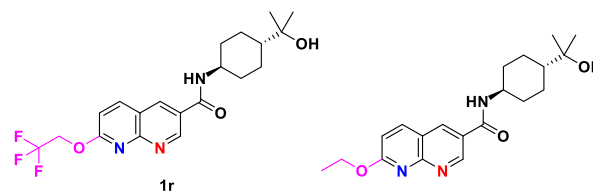
8a (236 mg, 1.498 mmol, PharmaBlock) and *N,N*-diisopropylethylamine (0.262 mL, 1.498 mmol) were added. The reaction was stirred at room temperature over the weekend. Water was added to the vessel in attempts to crash out the product, to no avail. The solution was concentrated in vacuo to give a crude solid. The residue was purified using silica gel chromatography, eluting with methanol:dichloromethane (0:1 to 1:9) to give 7-cyclopropyl-*N*-((trans-4-(2-hydroxypropan-2-yl)cyclohexyl)-1,6-naphthyridine-3-carboxamide **1q** (318 mg, 0.900 mmol, 90% yield). 1H NMR (400 MHz, CD_3OD) δ 1.09–1.53 (m, 15H), 1.92–2.19 (m, 4H), 2.26–2.43 (m, 1H), 3.85–3.99 (m, 1H), 7.80 (s, 1H), 8.65 (d, $J = 8$ Hz, 1H), 8.82–8.92 (m, 1H), 9.28 (s, 1H), 9.39 (d, $J = 2$ Hz, 1H); LC-MS (LC-ES) $C_{21}H_{27}N_3O_2$ $M + H = 354$; $t_R = 0.65$ min, 100% purity.

7-(2,2,2-Trifluoroethoxy)-1,8-naphthyridine-3-carboxylic acid **7m** and 7-Ethoxy-1,8-naphthyridine-3-carboxylic acid



2,2,2-Trifluoroethanol (0.18 mL, 2.470 mmol) was added to sodium hydride (60% in mineral oil, 0.121 g, 3.03 mmol) in tetrahydrofuran (10 mL) under nitrogen. It bubbled gently. After 30 min, ethyl 7-chloro-1,8-naphthyridine-3-carboxylate **17c** (0.241 g, 1.018 mmol) was added and the reaction mixture was stirred for nineteen hours. Water (2 mL) was added to the reaction mixture and it was allowed to stir for six hours. Then, the reaction mixture was partitioned between diethyl ether (25 mL) and water (15 mL) and the layers were separated. The aqueous layer was filtered through a pad of Celite®, gently concentrated to remove any remaining organics, and acidified with 1 N hydrochloric acid (2 mL, pH = ~3–4). The precipitate was collected by filtration, rinsed with water (2X), and air-dried, then dried under vacuum to give a mixture of 7-(2,2,2-trifluoroethoxy)-1,8-naphthyridine-3-carboxylic acid **7m** and 7-ethoxy-1,8-naphthyridine-3-carboxylic acid (0.231 g, ~65:35 ratio). LC-MS (LC-ES) $M + H = 219$ and LC-MS (LC-ES) $M + H = 273$.

N-((trans-4-(2-Hydroxypropan-2-yl)cyclohexyl)-7-(2,2,2-trifluoroethoxy)-1,8-naphthyridine-3-carboxamide **1r** and 7-Ethoxy-*N*-((trans-4-(2-hydroxypropan-2-yl)cyclohexyl)-1,8-naphthyridine-3-carboxamide



2-((trans-4-aminocyclohexyl)propan-2-ol **8a** (0.144 g, 0.916 mmol, PharmaBlock) was added to a mixture of 7-(2,2,2-trifluoroethoxy)-1,8-naphthyridine-3-carboxylic acid **7m** and 7-ethoxy-1,8-naphthyridine-3-carboxylic acid (0.249 g, 0.913 mmol) in *N,N*-dimethylformamide (10 mL) at room temperature. Then, *N,N*-diisopropylethylamine (0.40 mL, 2.296 mmol) was added, followed by 1-[bis(dimethylamino)methylene]-1*H*-1,2,3-triazolo[4,5-*b*]pyridinium 3-oxide hexafluorophosphate (0.418 g, 1.099 mmol) and the reaction mixture was stirred for four hours. The reaction mixture was concentrated, and the resulting residue was purified by silica gel chromatography, eluting with (ethyl acetate: ethanol (3:1)):hexanes (0:1 to 1:0). The mixed fractions were repurified by silica gel chromatography, eluting with (ethyl acetate: ethanol (3:1)):hexanes (0:1 to 3:1) and the mixed fractions were repurified by silica gel chromatography, eluting with (ethyl acetate: ethanol (3:1)):hexanes (0:1 to 3:1), then combined with the appropriate fractions to give residues which were triturated/sonicated with ethyl acetate and filtered to give

N-(*trans*-4-(2-hydroxypropan-2-yl)cyclohexyl)-7-(2,2,2-trifluoroethoxy)-1,8-naphthyridine-3-carboxamide **1r** (0.188 g, 0.457 mmol, 49.9% yield) as a white powder and 7-ethoxy-*N*-(*trans*-4-(2-hydroxypropan-2-yl)cyclohexyl)-1,8-naphthyridine-3-carboxamide (0.045 g, 0.126 mmol, 13.7% yield) as an off-white powder.

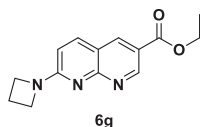
N-(*trans*-4-(2-Hydroxypropan-2-yl)cyclohexyl)-7-(2,2,2-trifluoroethoxy)-1,8-naphthyridine-3-carboxamide **1r**

¹H NMR (400 MHz, CD₃SOCD₃) δ 1.04 (s, 6H), 1.06–1.24 (m, 3H), 1.32 (q, *J* = 12 Hz, 2H), 1.84 (br d, *J* = 11 Hz, 2H), 1.94 (br d, *J* = 10 Hz, 2H), 3.68–3.80 (m, 1H), 4.06 (s, 1H), 5.21 (q, *J* = 9 Hz, 2H), 7.19 (d, *J* = 9 Hz, 1H), 8.40 (d, *J* = 9 Hz, 1H), 8.54 (d, *J* = 8 Hz, 1H), 8.78 (d, *J* = 2 Hz, 1H), 9.27 (d, *J* = 2 Hz, 1H); LC-MS (LC-ES) C₂₀H₂₄F₃N₃O₃ M + H = 412; t_R = 0.85 min, 97% purity.

7-Ethoxy-*N*-(*trans*-4-(2-hydroxypropan-2-yl)cyclohexyl)-1,8-naphthyridine-3-carboxamide

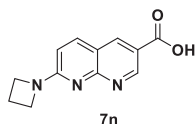
¹H NMR (400 MHz, CD₃SOCD₃) δ 1.04 (s, 6H), 1.06–1.24 (m, 3H), 1.31 (q, *J* = 12 Hz, 2H), 1.40 (t, *J* = 7 Hz, 3H), 1.83 (br d, *J* = 12 Hz, 2H), 1.93 (br d, *J* = 10 Hz, 2H), 3.68–3.80 (m, 1H), 4.06 (s, 1H), 4.51 (q, *J* = 7 Hz, 2H), 7.16 (d, *J* = 9 Hz, 1H), 8.39 (d, *J* = 9 Hz, 1H), 8.53 (d, *J* = 8 Hz, 1H), 8.76 (d, *J* = 2 Hz, 1H), 9.26 (d, *J* = 2 Hz, 1H); LC-MS (LC-ES) C₂₀H₂₇N₃O₃ M + H = 358.

Ethyl 7-(azetidin-1-yl)-1,8-naphthyridine-3-carboxylate **6g**



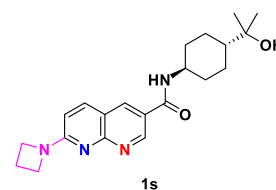
N,N-Diisopropylethylamine (1.35 mL, 7.75 mmol) was added to ethyl 7-chloro-1,8-naphthyridine-3-carboxylate **17c** (0.4588 g, 1.939 mmol) in *N*-methyl-2-pyrrolidone (6.46 mL) at room temperature. Then, azetidine hydrochloride (0.544 g, 5.82 mmol) was added and the reaction mixture was heated at 100 °C in the microwave for one hour. The reaction mixture was diluted in dichloromethane, washed with saturated sodium bicarbonate, dried over magnesium sulfate, filtered, and concentrated. The resulting residue was purified by RP HPLC, eluting with acetonitrile:water with 0.1% ammonium hydroxide (5:95 to 100:0) to give ethyl 7-(azetidin-1-yl)-1,8-naphthyridine-3-carboxylate **6g** (0.4469 g, 1.650 mmol, 85% yield). ¹H NMR (400 MHz, CD₃SOCD₃) δ 1.34 (t, *J* = 7 Hz, 3H), 2.39 (p, *J* = 7 Hz, 2H), 4.18 (t, *J* = 7 Hz, 4H), 4.34 (q, *J* = 7 Hz, 2H), 6.81 (d, *J* = 9 Hz, 1H), 8.17 (d, *J* = 9 Hz, 1H), 8.65 (s, 1H), 9.12 (s, 1H); LC-MS (LC-ES) M + H = 258.

7-(Azetidin-1-yl)-1,8-naphthyridine-3-carboxylic acid **7n**



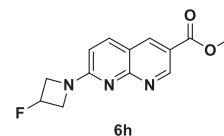
Lithium hydroxide (0.125 g, 5.21 mmol) was added to ethyl 7-(azetidin-1-yl)-1,8-naphthyridine-3-carboxylate **6g** (0.4469 g, 1.737 mmol) in methanol (6.95 mL) and water (1.737 mL) at room temperature and the reaction mixture was stirred three hours at 60 °C. The reaction mixture was concentrated. The reaction mixture was purified by RP HPLC eluting with acetonitrile:water with 0.1% ammonium hydroxide (5:95 to 100:0), then further purified by silica gel chromatography, eluting with methanol:ethyl acetate (1:9 to 4:1) to give 7-(azetidin-1-yl)-1,8-naphthyridine-3-carboxylic acid **7n** (0.4216 g, 1.696 mmol, 98% yield). ¹H NMR (400 MHz, CD₃SOCD₃) δ 2.37 (p, *J* = 7 Hz, 2H), 4.11 (t, *J* = 7 Hz, 4H), 6.69 (d, *J* = 9 Hz, 1H), 8.03 (d, *J* = 9 Hz, 1H), 8.37 (s, 1H), 9.13 (s, 1H); LC-MS (LC-ES) M – H = 230.

7-(Azetidin-1-yl)-*N*-(*trans*-4-(2-hydroxypropan-2-yl)cyclohexyl)-1,8-naphthyridine-3-carboxamide **1s**



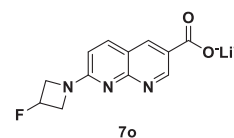
N,N-Diisopropylethylamine (0.298 mL, 1.707 mmol) was added to 7-(azetidin-1-yl)-1,8-naphthyridine-3-carboxylic acid **7n** (0.0672 g, 0.285 mmol) in *N,N*-dimethylformamide (0.948 mL) at room temperature. Then, 2-(*trans*-4-aminocyclohexyl)propan-2-ol **8a** (0.054 g, 0.341 mmol, PharmaBlock) was added and the reaction mixture was stirred for five minutes. Then, *n*-propylphosphonic acid anhydride (0.339 mL, 0.569 mmol) was added and the reaction mixture was stirred for sixty-six hours. The reaction mixture was concentrated. The resulting residue was purified by RP HPLC, eluting with acetonitrile:water with 0.1% ammonium hydroxide (5:95 to 100:0), then further purified by silica gel chromatography, eluting with methanol:ethyl acetate (0:1 to 1:4) to give 7-(azetidin-1-yl)-*N*-(*trans*-4-(2-hydroxypropan-2-yl)cyclohexyl)-1,8-naphthyridine-3-carboxamide **1s** (0.0648 g, 0.167 mmol, 58.7% yield). ¹H NMR (400 MHz, CD₃SOCD₃) δ 1.04 (s, 6H), 1.04–1.24 (m, 3H), 1.30 (q, *J* = 11 Hz, 2H), 1.83 (br d, *J* = 11 Hz, 2H), 1.92 (br d, *J* = 11 Hz, 2H), 2.39 (p, *J* = 7 Hz, 2H), 3.66–3.78 (m, 1H), 4.02 (s, 1H), 4.16 (t, *J* = 7 Hz, 4H), 6.78 (d, *J* = 9 Hz, 1H), 8.08 (d, *J* = 9 Hz, 1H), 8.31 (d, *J* = 7 Hz, 1H), 8.51 (s, 1H), 9.10 (s, 1H); LC-MS (LC-ES) C₂₁H₂₈N₄O₂ M + H = 369; t_R = 0.47 min, 100% purity.

Ethyl 7-(3-fluoroazetidin-1-yl)-1,8-naphthyridine-3-carboxylate **6h**



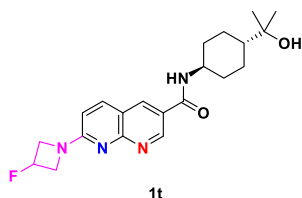
N,N-Diisopropylethylamine (1.23 mL, 7.09 mmol) was added to ethyl 7-chloro-1,8-naphthyridine-3-carboxylate **17c** (0.4194 g, 1.772 mmol) in *N*-methyl-2-pyrrolidone (5.91 mL) at room temperature. Then 3-fluoroazetidine hydrochloride (0.593 g, 5.32 mmol) was added and the reaction mixture was heated at 100 °C in the microwave for one hour. The reaction mixture was concentrated. The resulting residue was purified by RP HPLC, eluting with acetonitrile:water with 0.1% ammonium hydroxide (5:95 to 100:0), then further purified by silica gel chromatography, eluting with methanol:ethyl acetate (0:1 to 1:9) to give ethyl 7-(3-fluoroazetidin-1-yl)-1,8-naphthyridine-3-carboxylate **6h** (0.4561 g, 1.574 mmol, 89% yield). ¹H NMR (400 MHz, CD₃SOCD₃) δ 1.35 (t, *J* = 7 Hz, 3H), 4.25 (br dd, *J* = 24, 11 Hz, 2H), 4.35 (q, *J* = 7 Hz, 2H), 4.46–4.60 (m, 2H), 5.46–5.68 (m, 1H), 6.91 (d, *J* = 9 Hz, 1H), 8.25 (d, *J* = 9 Hz, 1H), 8.71 (s, 1H), 9.16 (s, 1H); LC-MS (LC-ES) + H = 276.

7-(3-Fluoroazetidin-1-yl)-1,8-naphthyridine-3-carboxylic acid lithium salt **7o**



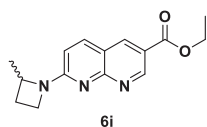
Lithium hydroxide (0.119 g, 4.97 mmol) was added to ethyl 7-(3-fluoroazetidin-1-yl)-1,8-naphthyridine-3-carboxylate **6h** (0.4561 g, 1.657 mmol) in methanol (6.6 mL) and water (1.7 mL) at room temperature and the reaction mixture was stirred three hours at 60 °C. The reaction mixture was concentrated to give 7-(3-fluoroazetidin-1-yl)-1,8-naphthyridine-3-carboxylic acid lithium salt **7o** (0.4332 g, 1.619 mmol, 98% yield). ¹H NMR (400 MHz, CD₃SOCD₃) δ 4.17 (br dd, *J* = 24, 10 Hz, 2H), 4.38–4.54 (m, 2H), 5.44–5.66 (m, 1H), 6.79 (d, *J* = 9 Hz, 1H), 8.11 (d, *J* = 9 Hz, 1H), 8.44 (s, 1H), 9.18 (s, 1H); LC-MS (LC-ES) M + H = 248.

7-(3-Fluoroazetidin-1-yl)-*N*-(*trans*-4-(2-hydroxypropan-2-yl)cyclohexyl)-1,8-naphthyridine-3-carboxamide **1t**



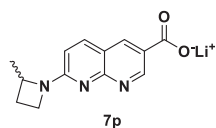
N,N-Diisopropylethylamine (0.278 mL, 1.591 mmol) was added to 7-(3-fluoroazetidin-1-yl)-1,8-naphthyridine-3-carboxylic acid lithium salt **7o** (0.0674 g, 0.265 mmol) in *N,N*-dimethylformamide (0.88 mL) at room temperature. Then, 2-(*trans*-4-aminocyclohexyl)propan-2-ol **8a** (0.050 g, 0.318 mmol, PharmaBlock) was added and the reaction mixture was stirred for five minutes. Then, *n*-propylphosphonic acid anhydride (0.316 mL, 0.530 mmol) was added and the reaction mixture was stirred for sixteen hours. The reaction mixture was concentrated. The resulting residue was purified by RP HPLC, eluting with acetonitrile: water with 0.1% ammonium hydroxide (5:95 to 100:0), then further purified by silica gel chromatography, eluting with methanol:ethyl acetate (0:1 to 1:4) to give 7-(3-fluoroazetidin-1-yl)-*N*-(*trans*-4-(2-hydroxypropan-2-yl)cyclohexyl)-1,8-naphthyridine-3-carboxamide **1t** (0.0748 g, 0.184 mmol, 69.3% yield). ¹H NMR (400 MHz, CD₃SOCD₃) δ 1.04 (s, 6H), 1.04–1.24 (m, 3H), 1.30 (q, *J* = 12 Hz, 2H), 1.83 (br d, *J* = 11 Hz, 2H), 1.92 (br d, *J* = 11 Hz, 2H), 3.66–3.78 (m, 1H), 4.03 (s, 1H), 4.22 (br dd, *J* = 24, 11 Hz, 2H), 4.42–4.58 (m, 2H), 5.46–5.68 (m, 1H), 6.88 (d, *J* = 9 Hz, 1H), 8.14 (d, *J* = 9 Hz, 1H), 8.36 (d, *J* = 8 Hz, 1H), 8.56 (s, 1H), 9.13 (s, 1H); LC-MS (LC-ES) C₂₁H₂₇N₄O₂ M + H = 387; *t*_R = 0.48 min, 100% purity.

Ethyl 7-(2-methylazetidin-1-yl)-1,8-naphthyridine-3-carboxylate **6i**



N,N-Diisopropylethylamine (0.987 mL, 5.67 mmol) was added to ethyl 7-chloro-1,8-naphthyridine-3-carboxylate **17c** (0.3352 g, 1.416 mmol) in *N*-methyl-2-pyrrolidone (4.72 mL) at room temperature. Then 2-methylazetidine hydrochloride (0.457 g, 4.25 mmol) was added and the reaction mixture was heated at 100 °C in the microwave for one hour. The reaction mixture was diluted in dichloromethane, washed with saturated sodium bicarbonate, dried over magnesium sulfate, filtered, and concentrated. The resulting residue was purified by RP HPLC, eluting with acetonitrile:water with 0.1% ammonium hydroxide (5:95 to 100:0), then further purified by silica gel chromatography, eluting with methanol:ethyl acetate (0:1 to 1:19) to give ethyl 7-(2-methylazetidin-1-yl)-1,8-naphthyridine-3-carboxylate **6i** (0.3815 g, 1.336 mmol, 94% yield). ¹H NMR (400 MHz, CD₃SOCD₃) δ 1.34 (t, *J* = 7 Hz, 3H), 1.53 (d, *J* = 6 Hz, 3H), 1.94–2.06 (m, 1H), 2.46–2.60 (m, 1H), 4.03 (q, *J* = 7 Hz, 1H), 4.14 (q, *J* = 6 Hz, 1H), 4.34 (q, *J* = 7 Hz, 2H), 4.58 (h, *J* = 6 Hz, 1H), 6.81 (d, *J* = 9 Hz, 1H), 8.16 (d, *J* = 9 Hz, 1H), 8.65 (s, 1H), 9.12 (s, 1H); LC-MS (LC-ES) M + H = 272.

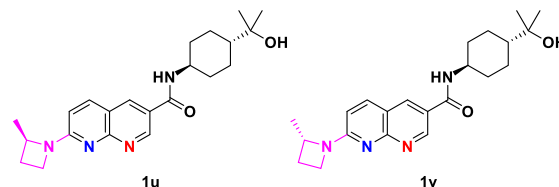
7-(2-Methylazetidin-1-yl)-1,8-naphthyridine-3-carboxylic acid lithium salt **7p**



Lithium hydroxide (0.101 g, 4.22 mmol) was added to ethyl 7-(2-methylazetidin-1-yl)-1,8-naphthyridine-3-carboxylate **6i** (0.3815 g, 1.406 mmol) in methanol (5.6 mL) and water (1.4 mL) at room

temperature and the reaction mixture was stirred three hours at 60 °C. The reaction mixture was concentrated to give 7-(2-methylazetidin-1-yl)-1,8-naphthyridine-3-carboxylic acid lithium salt **7p** (0.3698 g, 1.404 mmol, 100% yield). ¹H NMR (400 MHz, CD₃SOCD₃) δ 1.51 (d, *J* = 6 Hz, 3H), 1.94–2.06 (m, 1H), 2.42–2.54 (m, 1H), 3.94 (q, *J* = 8 Hz, 1H), 4.06 (q, *J* = 8 Hz, 1H), 4.50 (h, *J* = 6 Hz, 1H), 6.69 (d, *J* = 9 Hz, 1H), 8.03 (d, *J* = 9 Hz, 1H), 8.39 (s, 1H), 9.15 (s, 1H); LC-MS (LC-ES) M + H = 244.

N-(*trans*-4-(2-Hydroxypropan-2-yl)cyclohexyl)-7-((*R*)-2-methylazetidin-1-yl)-1,8-naphthyridine-3-carboxamide **1u** and *N*-(*trans*-4-(2-Hydroxypropan-2-yl)cyclohexyl)-7-((*S*)-2-methylazetidin-1-yl)-1,8-naphthyridine-3-carboxamide **1v**



N,N-Diisopropylethylamine (0.444 mL, 2.54 mmol) was added to 7-(2-methylazetidin-1-yl)-1,8-naphthyridine-3-carboxylic acid lithium salt **7p** (0.1061 g, 0.424 mmol) in *N,N*-dimethylformamide (1.4 mL) at room temperature. Then, 2-(*trans*-4-aminocyclohexyl)propan-2-ol **8a** (0.080 g, 0.509 mmol, PharmaBlock) was added and the reaction mixture was stirred for five minutes. Then, *n*-propylphosphonic acid anhydride (0.505 mL, 0.848 mmol) was added and the reaction mixture was stirred for sixty-four hours. The reaction mixture was concentrated. The resulting residue was purified by RP HPLC, eluting with acetonitrile: water with 0.1% ammonium hydroxide (5:95 to 100:0), then further purified by silica gel chromatography, eluting with methanol:ethyl acetate (0:1 to 1:4) to give racemic *N*-(*trans*-4-(2-hydroxypropan-2-yl)cyclohexyl)-7-(2-methylazetidin-1-yl)-1,8-naphthyridine-3-carboxamide (0.0514 g, 0.128 mmol, 30.1% yield). ¹H NMR (400 MHz, CD₃SOCD₃) δ 1.04 (s, 6H), 1.04–1.24 (m, 3H), 1.30 (q, *J* = 12 Hz, 2H), 1.52 (d, *J* = 6 Hz, 3H), 1.83 (br d, *J* = 12 Hz, 2H), 1.91 (br d, *J* = 11 Hz, 2H), 1.96–2.06 (m, 1H), 2.46–2.58 (m, 1H), 3.64–3.78 (m, 1H), 4.00 (q, *J* = 8 Hz, 1H), 4.03 (s, 1H), 4.11 (q, *J* = 8 Hz, 1H), 4.56 (h, *J* = 7 Hz, 1H), 6.79 (d, *J* = 9 Hz, 1H), 8.07 (d, *J* = 9 Hz, 1H), 8.32 (d, *J* = 8 Hz, 1H), 8.52 (s, 1H), 9.09 (s, 1H); LC-MS (LC-ES) M + H = 383. Racemic *N*-(*trans*-4-(2-hydroxypropan-2-yl)cyclohexyl)-7-(2-methylazetidin-1-yl)-1,8-naphthyridine-3-carboxamide (0.1238 g, 0.324 mmol) was separated into its enantiomers on a chiral IC column eluting with methanol:hexanes (3:2) with 1% diethylamine to give *N*-(*trans*-4-(2-hydroxypropan-2-yl)cyclohexyl)-7-((*R*)-2-methylazetidin-1-yl)-1,8-naphthyridine-3-carboxamide **1u** (0.028 g, 0.070 mmol, 21.49% yield) as the first diastereomer (>99% ee) to elute and *N*-(*trans*-4-(2-hydroxypropan-2-yl)cyclohexyl)-7-((*S*)-2-methylazetidin-1-yl)-1,8-naphthyridine-3-carboxamide **1v** (0.035 g, 0.087 mmol, 26.9% yield) as the last diastereomer to elute (86.6% ee). The structures were assigned by vibrational circular dichroism.

N-(*trans*-4-(2-Hydroxypropan-2-yl)cyclohexyl)-7-((*R*)-2-methylazetidin-1-yl)-1,8-naphthyridine-3-carboxamide **1u**

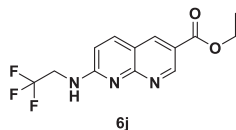
¹H NMR (400 MHz, CD₃SOCD₃) δ 1.04 (s, 6H), 1.04–1.24 (m, 3H), 1.30 (q, *J* = 12 Hz, 2H), 1.52 (d, *J* = 6 Hz, 3H), 1.83 (br d, *J* = 12 Hz, 2H), 1.91 (br d, *J* = 11 Hz, 2H), 1.96–2.06 (m, 1H), 2.46–2.58 (m, 1H), 3.64–3.78 (m, 1H), 4.00 (q, *J* = 8 Hz, 1H), 4.02 (s, 1H), 4.11 (q, *J* = 8 Hz, 1H), 4.56 (h, *J* = 6 Hz, 1H), 6.79 (d, *J* = 9 Hz, 1H), 8.07 (d, *J* = 9 Hz, 1H), 8.31 (d, *J* = 8 Hz, 1H), 8.52 (s, 1H), 9.10 (s, 1H); LC-MS (LC-ES) C₂₂H₃₀N₄O₂ M + H = 383; *t*_R = 0.52 min, 100% purity.

N-(*trans*-4-(2-Hydroxypropan-2-yl)cyclohexyl)-7-((*S*)-2-methylazetidin-1-yl)-1,8-naphthyridine-3-carboxamide **1v**

¹H NMR (400 MHz, CD₃SOCD₃) δ 1.04 (s, 6H), 1.04–1.24 (m, 3H), 1.30 (q, *J* = 12 Hz, 2H), 1.52 (d, *J* = 6 Hz, 3H), 1.83 (br d, *J* = 11 Hz, 2H), 1.91 (br d, *J* = 12 Hz, 2H), 1.96–2.06 (m, 1H), 2.46–2.58 (m, 1H), 3.64–3.78 (m, 1H), 4.00 (q, *J* = 8 Hz, 1H), 4.02 (s, 1H), 4.11 (q, *J* = 8 Hz, 1H), 4.56 (h, *J* = 6 Hz, 1H), 6.78 (d, *J* = 9 Hz, 1H), 8.07 (d, *J* = 9 Hz, 1H),

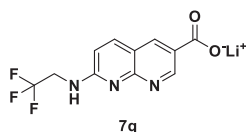
8.31 (d, $J = 8$ Hz, 1H), 8.51 (s, 1H), 9.09 (s, 1H); LC-MS (LC-ES) $C_{22}H_{30}N_4O_2$ M + H = 383; $t_R = 0.52$ min, 99% purity.

Ethyl 7-((2,2,2-trifluoroethyl)amino)-1,8-naphthyridine-3-carboxylate **6j**



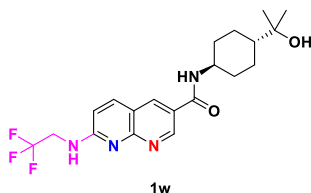
N,N-Diisopropylethylamine (1.199 mL, 6.88 mmol) was added to ethyl 7-chloro-1,8-naphthyridine-3-carboxylate **17c** (0.4071 g, 1.720 mmol) in *N*-methyl-2-pyrrolidone (5.73 mL) at room temperature. Then 2,2,2-trifluoroethanamine (0.511 g, 5.16 mmol) was added and the reaction mixture was heated at 100 °C in the microwave for five hours. The reaction mixture was diluted in dichloromethane, washed with saturated sodium bicarbonate, dried over magnesium sulfate, filtered, and concentrated. The residue was purified by RP HPLC, eluting with acetonitrile:water with 0.1% ammonium hydroxide (5:95 to 100:0), then further purified by silica gel chromatography, eluting with ethyl acetate:hexanes (2:3 to 1:0) to give ethyl 7-((2,2,2-trifluoroethyl)amino)-1,8-naphthyridine-3-carboxylate **6j** (0.1719 g, 0.546 mmol, 31.7% yield). 1H NMR (400 MHz, CD_3SOCD_3) δ 1.36 (t, $J = 7$ Hz, 3H), 4.36 (q, $J = 7$ Hz, 2H), 4.36–4.46 (m, 2H), 7.04 (d, $J = 7$ Hz, 1H), 8.20 (d, $J = 9$ Hz, 1H), 8.34 (br s, 1H), 8.70 (s, 1H), 9.16 (s, 1H); LC-MS (LC-ES) M + H = 300.

7-((2,2,2-Trifluoroethyl)amino)-1,8-naphthyridine-3-carboxylic acid lithium salt **7q**



Lithium hydroxide (0.041 g, 1.723 mmol) was added to ethyl 7-((2,2,2-trifluoroethyl)amino)-1,8-naphthyridine-3-carboxylate **6j** (0.1719 g, 0.574 mmol) in methanol (2.3 mL) and water (0.57 mL) at room temperature and the reaction mixture was stirred sixteen hours at 60 °C. The reaction mixture was concentrated to give 7-((2,2,2-trifluoroethyl)amino)-1,8-naphthyridine-3-carboxylic acid lithium salt **7q** (0.2390 g, 0.816 mmol, 142% yield). 1H NMR (400 MHz, CD_3SOCD_3) δ 4.35 (p, $J = 7$ Hz, 2H), 6.90 (d, $J = 9$ Hz, 1H), 7.83 (br s, 1H), 8.02 (d, $J = 9$ Hz, 1H), 8.36 (s, 1H), 9.12 (s, 1H); LC-MS (LC-ES) M + H = 272.

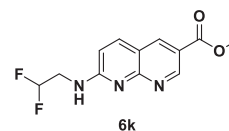
N-(*trans*-4-(2-Hydroxypropan-2-yl)cyclohexyl)-7-((2,2,2-trifluoroethyl)amino)-1,8-naphthyridine-3-carboxamide **1w**



N,N-Diisopropylethylamine (0.216 mL, 1.234 mmol) was added to 7-((2,2,2-trifluoroethyl)amino)-1,8-naphthyridine-3-carboxylic acid lithium salt **7q** (0.0572 g, 0.206 mmol) in *N,N*-dimethylformamide (0.69 mL) at room temperature. Then, 2-(*trans*-4-aminocyclohexyl)propan-2-ol **8a** (0.039 g, 0.247 mmol, PharmaBlock) was added and the reaction mixture was stirred for five minutes. Then, *n*-propylphosphonic acid anhydride (0.245 mL, 0.411 mmol) was added and the reaction mixture was stirred for sixteen hours. The reaction mixture was concentrated. The resulting residue was purified by RP HPLC, eluting with acetonitrile:water with 0.1% ammonium hydroxide (5:95 to 100:0), then further purified by silica gel chromatography, eluting with methanol:ethyl acetate (0:1 to 1:4) to give *N*-(*trans*-4-(2-hydroxypropan-

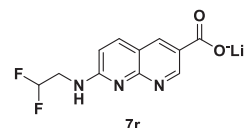
2-yl)cyclohexyl)-7-((2,2,2-trifluoroethyl)amino)-1,8-naphthyridine-3-carboxamide **1w** (0.0219 g, 0.051 mmol, 24.65% yield). 1H NMR (400 MHz, CD_3SOCD_3) δ 1.04 (s, 6H), 1.04–1.24 (m, 3H), 1.30 (q, $J = 12$ Hz, 2H), 1.83 (br d, $J = 13$ Hz, 2H), 1.92 (br d, $J = 11$ Hz, 2H), 3.66–3.78 (m, 1H), 4.02 (s, 1H), 4.38 (p, $J = 8$ Hz, 2H), 7.01 (d, $J = 9$ Hz, 1H), 8.09 (d, $J = 9$ Hz, 1H), 8.17 (t, $J = 7$ Hz, 1H), 8.36 (d, $J = 8$ Hz, 1H), 8.55 (s, 1H), 9.12 (s, 1H); LC-MS (LC-ES) $C_{20}H_{25}F_3N_4O_2$ M + H = 411; $t_R = 0.56$ min, 98% purity.

Ethyl 7-((2,2-difluoroethyl)amino)-1,8-naphthyridine-3-carboxylate **6k**



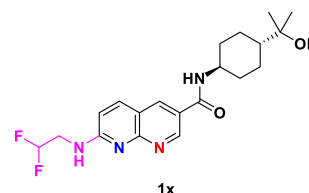
N,N-Diisopropylethylamine (1.224 mL, 7.03 mmol) was added to ethyl 7-chloro-1,8-naphthyridine-3-carboxylate **17c** (0.4158 g, 1.757 mmol) in *N*-methyl-2-pyrrolidone (5.86 mL) at room temperature. Then 2,2-difluoroethanamine (0.427 g, 5.27 mmol) was added and the reaction mixture was heated at 100 °C in the microwave for three hours. The reaction mixture was diluted in dichloromethane, washed with saturated sodium bicarbonate, dried over magnesium sulfate, filtered, and concentrated. The resulting residue was purified by RP HPLC, eluting with acetonitrile:water with 0.1% ammonium hydroxide (5:95 to 100:0) to give ethyl 7-((2,2-difluoroethyl)amino)-1,8-naphthyridine-3-carboxylate **6k** (0.4796 g, 1.620 mmol, 92% yield). 1H NMR (400 MHz, CD_3SOCD_3) δ 1.35 (t, $J = 7$ Hz, 3H), 3.84–3.98 (m, 2H), 4.36 (q, $J = 7$ Hz, 2H), 6.24 (t, $J = 56$ Hz, 1H), 7.00 (d, $J = 9$ Hz, 1H), 8.14 (d, $J = 9$ Hz, 1H), 8.18 (br s, 1H), 8.66 (s, 1H), 9.14 (s, 1H); LC-MS (LC-ES) M + H = 282.

7-((2,2-Difluoroethyl)amino)-1,8-naphthyridine-3-carboxylic acid lithium salt **7r**



Lithium hydroxide (0.123 g, 5.12 mmol) was added to ethyl 7-((2,2-difluoroethyl)amino)-1,8-naphthyridine-3-carboxylate **6k** (0.4796 g, 1.705 mmol) in methanol (6.8 mL) and water (1.7 mL) at room temperature and the reaction mixture was stirred three hours at 60 °C. The reaction mixture was concentrated to give 7-((2,2-difluoroethyl)amino)-1,8-naphthyridine-3-carboxylic acid lithium salt **7r** (0.4567 g, 1.668 mmol, 98% yield). 1H NMR (400 MHz, CD_3SOCD_3) δ 3.71 (t, $J = 16$ Hz, 2H), 6.53 (t, $J = 57$ Hz, 1H), 6.57 (d, $J = 9$ Hz, 1H), 7.54 (d, $J = 7$ Hz, 1H), 8.10 (s, 1H), 8.91 (s, 1H); LC-MS (LC-ES) M + H = 254.

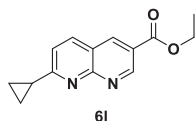
7-((2,2-Difluoroethyl)amino)-*N*-(*trans*-4-(2-hydroxypropan-2-yl)cyclohexyl)-1,8-naphthyridine-3-carboxamide **1x**



N,N-Diisopropylethylamine (0.269 mL, 1.543 mmol) was added to 7-((2,2-difluoroethyl)amino)-1,8-naphthyridine-3-carboxylic acid lithium salt **7r** (0.0669 g, 0.257 mmol) in *N,N*-dimethylformamide (0.86 mL) at room temperature. Then, 2-(*trans*-4-aminocyclohexyl)propan-2-ol **8a** (0.049 g, 0.309 mmol, PharmaBlock) was added and the reaction mixture was stirred for five minutes. Then, *n*-propylphosphonic acid anhydride (0.306 mL, 0.514 mmol) was added and the reaction mixture

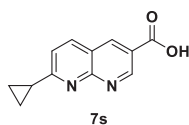
was stirred for sixteen hours. The reaction mixture was concentrated. The resulting residue was purified by RP HPLC, eluting with acetonitrile: water with 0.1% ammonium hydroxide (5:95 to 100:0), then further purified by silica gel chromatography, eluting with methanol:ethyl acetate (0:1 to 1:4) to give 7-((2,2-difluoroethyl)amino)-*N*-(*trans*-4-(2-hydroxypropan-2-yl)cyclohexyl)-1,8-naphthyridine-3-carboxamide **1x** (0.0611 g, 0.148 mmol, 57.5% yield). ^1H NMR (400 MHz, CD_3SOCD_3) δ 1.04 (s, 6H), 1.04–1.24 (m, 3H), 1.31 (q, $J = 11$ Hz, 2H), 1.83 (br d, $J = 12$ Hz, 2H), 1.92 (br d, $J = 12$ Hz, 2H), 3.66–3.80 (m, 1H), 3.91 (br t, $J = 15$ Hz, 2H), 4.01 (s, 1H), 6.23 (t, $J = 57$ Hz, 1H), 6.98 (d, $J = 9$ Hz, 1H), 8.00 (br s, 1H), 8.04 (d, $J = 9$ Hz, 1H), 8.32 (d, $J = 8$ Hz, 1H), 8.52 (s, 1H), 9.10 (s, 1H); LC-MS (LC-ES) $\text{C}_{20}\text{H}_{26}\text{F}_2\text{N}_4\text{O}_2$ $M + H = 393$; $t_R = 0.50$ min, 99% purity.

Ethyl 7-cyclopropyl-1,8-naphthyridine-3-carboxylate **6l**



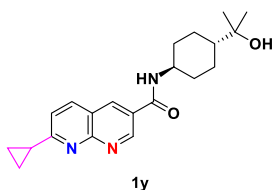
Cyclopropylboronic acid (3.16 g, 36.8 mmol) was added to a solution of ethyl 7-chloro-1,8-naphthyridine-3-carboxylate **17c** (3 g, 12.27 mmol), dicyclohexyl(2',6'-dimethoxy-[1,1'-biphenyl]-2-yl)phosphine (0.504 g, 1.227 mmol), tris(dibenzylideneacetone)dipalladium(0) (2.247 g, 2.453 mmol), and 2 M sodium carbonate (15.33 mL, 30.7 mmol) in toluene (30 mL) at room temperature under nitrogen and the reaction mixture was purged with argon for 10 min. The resulting reaction mixture was heated to 110 °C and stirred for sixteen hours. On completion, the reaction mixture was cooled, filtered through a Celite® pad, and the filtrate was evaporated under reduced pressure. The residue was purified via neutral alumina column chromatography, eluting with ethyl acetate:petroleum ether (1:1) to afford ethyl 7-cyclopropyl-1,8-naphthyridine-3-carboxylate **6l** (700 mg, 2.58 mmol, 21% yield) as an off white solid. ^1H NMR (400 MHz, CDCl_3) δ 1.12–1.23 (m, 2H), 1.43–1.53 (m, 5H), 2.25–2.36 (m, 1H), 4.48 (q, $J = 7$ Hz, 2H), 7.46 (d, $J = 8$ Hz, 1H), 8.11 (d, $J = 8$ Hz, 1H), 8.78 (d, $J = 2$ Hz, 1H), 9.56 (d, $J = 2$ Hz, 1H); LC-MS (LC-ES) $M + H = 243$.

7-Cyclopropyl-1,8-naphthyridine-3-carboxylic acid **7s**



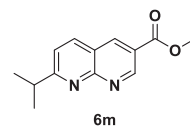
Sodium hydroxide (17.58 mL, 35.2 mmol) was added to a solution of ethyl 7-cyclopropyl-1,8-naphthyridine-3-carboxylate **6l** (7.1 g, 29.3 mmol) in tetrahydrofuran (30 mL) at room temperature and reaction mixture was stirred for fifteen hours. Then, the reaction mixture was concentrated, acidified with diluted hydrochloric acid and the precipitated solid was filtered, washed with water, and dried to give a crude solid. This material was washed with *n*-pentane (500 mL) and diethyl ether (500 mL), then dried to give 7-cyclopropyl-1,8-naphthyridine-3-carboxylic acid **7s** (5.33 g, 23.89 mmol, 82% yield). ^1H NMR (400 MHz, CD_3SOCD_3) δ 1.04–1.16 (m, 4H), 2.22–2.35 (m, 1H), 7.50 (d, $J = 8$ Hz, 1H), 8.31 (d, $J = 8$ Hz, 1H), 8.59 (s, 1H), 9.36 (s, 1H); LC-MS (LC-ES) $M - H = 213$.

7-Cyclopropyl-*N*-((*trans*-4-(2-hydroxypropan-2-yl)cyclohexyl)-1,8-naphthyridine-3-carboxamide **1y**



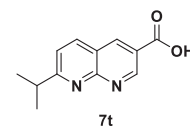
N,N-Diisopropylethylamine (1.977 mL, 11.32 mmol) was added to 7-cyclopropyl-1,8-naphthyridine-3-carboxylic acid **7s** (0.6061 g, 2.83 mmol) in dichloromethane (14.15 mL) at room temperature. Then, 2-(*trans*-4-aminocyclohexyl)propan-2-ol **8a** (0.667 g, 4.24 mmol, Pharmablock) was added and the reaction mixture was stirred for five minutes. Then, *n*-propylphosphonic acid anhydride (3.03 mL, 5.09 mmol) was added and the reaction mixture was stirred for sixteen hours. The reaction mixture was concentrated. The resulting residue was purified by RP HPLC, eluting with acetonitrile:water with 0.1% ammonium hydroxide (5:95 to 100:0), then further purified by silica gel chromatography, eluting with methanol:ethyl acetate (0:1 to 1:4) to give 7-cyclopropyl-*N*-((*trans*-4-(2-hydroxypropan-2-yl)cyclohexyl)-1,8-naphthyridine-3-carboxamide **1y** (0.5820 g, 1.564 mmol, 55.3% yield). ^1H NMR (400 MHz, CD_3SOCD_3) δ 1.04 (s, 6H), 1.06–1.24 (m, 7H), 1.32 (q, $J = 11$ Hz, 2H), 1.83 (br d, $J = 11$ Hz, 2H), 1.93 (br d, $J = 11$ Hz, 2H), 2.32–2.40 (m, 1H), 3.75 (dt, $J = 8, 4, 4$ Hz, 1H), 4.06 (s, 1H), 7.63 (d, $J = 9$ Hz, 1H), 8.39 (d, $J = 8$ Hz, 1H), 8.57 (br d, $J = 8$ Hz, 1H), 8.78 (d, $J = 2$ Hz, 1H), 9.32 (d, $J = 2$ Hz, 1H); ^{13}C NMR (400 MHz, CD_3SOCD_3) δ 12.20 (2C), 18.41, 26.54 (2C), 27.52 (2C), 32.89 (2C), 48.41, 49.41, 70.97, 119.98, 122.73, 127.43, 137.20, 138.51, 152.13, 156.68, 164.03, 169.15; LC-MS (LC-ES) $\text{C}_{21}\text{H}_{27}\text{N}_3\text{O}_2$ $M + H = 354$, $t_R = 0.65$ min, 100% purity; HRMS $\text{C}_{21}\text{H}_{27}\text{N}_3\text{O}_2$ Calculated: $M + H = 354.2171$; Measured: $M + H = 354.2182$; Elemental Analysis for $\text{C}_{21}\text{H}_{27}\text{N}_3\text{O}_2$ C Theoretical 71.3%, Measured 71.0%; H Theoretical 7.7%, Measured 8.0%; N Theoretical 11.9%, Measured 11.6%.

Ethyl 7-isopropyl-1,8-naphthyridine-3-carboxylate **6m**



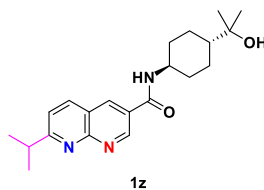
[1,1'-Bis(diphenylphosphino)ferrocene]dichloropalladium(II) dichloromethane complex (0.282 g, 0.345 mmol) was added to ethyl 7-chloro-1,8-naphthyridine-3-carboxylate **17c** (0.797 g, 3.37 mmol), followed by copper(I) iodide (0.136 g, 0.714 mmol). Then, tetrahydrofuran (35 mL) was added and the reaction mixture was purged with nitrogen. Isopropylzinc(II) bromide (12.0 mL, 6.00 mmol) was added and the reaction mixture was stirred for 30 min, then quenched with ethanol and concentrated. 1 M Potassium carbonate (25 mL) and dichloromethane (50 mL) were added and the reaction mixture was filtered through Celite®, extracted with dichloromethane, dried over magnesium sulfate, filtered, and concentrated. The residue was purified via silica gel chromatography, eluting with methanol:dichloromethane (0:1 to 1:12) with 10% ammonium hydroxide to give impure ethyl 7-isopropyl-1,8-naphthyridine-3-carboxylate **6m** (0.885 g, 108% yield) as a dark red–orange gum. LC-MS (LC-ES) $M + H = 245$.

7-Isopropyl-1,8-naphthyridine-3-carboxylic acid **7t**



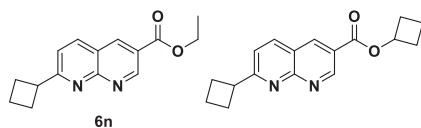
1 M Sodium hydroxide (5.0 mL, 5.00 mmol) was added to impure ethyl 7-isopropyl-1,8-naphthyridine-3-carboxylate **6m** (0.823 g, 3.37 mmol) in methanol (25 mL) and the reaction mixture was stirred for four hours, then quenched with 1 M hydrochloric acid (5 mL) and concentrated. The residue was purified by reverse phase HPLC, eluting with acetonitrile:water (0:1 to 1:4) with 0.1% trifluoroacetic acid to give 7-isopropyl-1,8-naphthyridine-3-carboxylic acid **7t** (0.137 g, 0.634 mmol, 19% yield) as a tan-yellow solid. ^1H NMR (400 MHz, CD_3SOCD_3) δ 1.35 (d, $J = 7$ Hz, 6H), 3.29 (h, $J = 7$ Hz, 1H), 7.72 (d, $J = 9$ Hz, 1H), 8.59 (d, $J = 9$ Hz, 1H), 9.02 (d, $J = 2$ Hz, 1H), 9.42 (d, $J = 2$ Hz, 1H), 13.56 (br s, 1H); LC-MS (LC-ES) $M - H = 217$.

N-((*trans*-4-(2-Hydroxypropan-2-yl)cyclohexyl)-7-isopropyl-1,8-

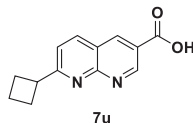
naphthyridine-3-carboxamide **1z**

2-(*trans*-4-Aminocyclohexyl)propan-2-ol **8a** (0.110 g, 0.699 mmol, PharmaBlock) was added to 7-isopropyl-1,8-naphthyridine-3-carboxylic acid **7t** (0.135 g, 0.624 mmol) in tetrahydrofuran (6 mL). Then, *N,N*-diisopropylethylamine (0.13 mL, 0.746 mmol) was added, followed by 1-[bis(dimethylamino)methylene]-1*H*-1,2,3-triazolo[4,5-*b*]pyridinium 3-oxide hexafluorophosphate (0.286 g, 0.752 mmol) and the reaction mixture was stirred for three hours, then quenched with 1 M aqueous potassium carbonate:tetrahydrofuran (1:1, 10 mL). The layers were separated, and the organic layer was washed with saturated sodium chloride (5 mL), dried over magnesium sulfate, filtered, and concentrated. The residue was purified by silica gel chromatography, eluting with ethanol:ethyl acetate (1:3):hexanes (0:1 to 1:0) to give *N*-(*trans*-4-(2-hydroxypropan-2-yl)cyclohexyl)-7-isopropyl-1,8-naphthyridine-3-carboxamide **1z** (0.176 g, 0.495 mmol, 79% yield) as an off-white powder. ¹H NMR (400 MHz, CD₃SOCD₃) δ 1.05 (s, 6H), 1.08–1.24 (m, 3H), 1.34 (q, *J* = 12 Hz, 2H), 1.35 (d, *J* = 7 Hz, 6H), 1.84 (br d, *J* = 12 Hz, 2H), 1.94 (br d, *J* = 12 Hz, 2H), 3.28 (h, *J* = 7 Hz, 1H), 3.70–3.84 (m, 1H), 4.07 (s, 1H), 7.67 (d, *J* = 8 Hz, 1H), 8.48 (d, *J* = 8 Hz, 1H), 8.62 (d, *J* = 8 Hz, 1H), 8.84 (d, *J* = 2 Hz, 1H), 9.38 (d, *J* = 2 Hz, 1H); LC-MS (LC-ES) C₂₁H₂₉N₃O₂ M + H = 356; *t_R* = 0.70 min, 100% purity.

Ethyl 7-cyclobutyl-1,8-naphthyridine-3-carboxylate **6n** and Cyclobutyl 7-cyclobutyl-1,8-naphthyridine-3-carboxylate

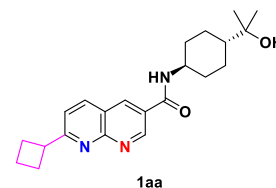


[1,1'-Bis(diphenylphosphino)ferrocene]dichloropalladium (II)-dichloromethane adduct (0.168 g, 0.206 mmol) was added to ethyl 7-chloro-1,8-naphthyridine-3-carboxylate **17c** (0.476 g, 2.011 mmol), followed by tetrahydrofuran (20 mL) and the reaction mixture was purged with nitrogen. Then, cyclobutylzinc(II) bromide (4.5 mL, 2.250 mmol, 0.5 M in tetrahydrofuran) was added and the reaction mixture was heated at 60 °C for 90 min. Then, additional cyclobutylzinc(II) bromide (0.8 mL, 0.400 mmol, 0.5 M in tetrahydrofuran) was added. After 30 min, the reaction was allowed to cool to room temperature, combined with material from another reaction and purified via silica gel chromatography, eluting with (3:1 ethyl acetate:ethanol):hexanes (0:1 to 1:1 to 1:0) to give material that was further purified via silica gel chromatography, eluting with (9:1 methanol:ammonium hydroxide):dichloromethane (0:1 to 1:15) to give a mixture of ethyl 7-cyclobutyl-1,8-naphthyridine-3-carboxylate **6n** and cyclobutyl 7-cyclobutyl-1,8-naphthyridine-3-carboxylate (0.421 g, ~1.643 mmol, ~65% combined yield) as a tan-orange powder. LC-MS (LC-ES) M + H = 257; LC-MS (LC-ES) M + H = 283.

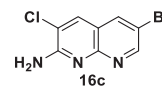
7-Cyclobutyl-1,8-naphthyridine-3-carboxylic acid **7u**

1 N Sodium hydroxide (3.2 mL, 3.20 mmol) was added to the mixed ester ethyl/cyclobutyl 7-cyclobutyl-1,8-naphthyridine-3-carboxylate **6n** (0.421 g, 1.643 mmol) in methanol (10 mL) and the reaction mixture was stirred for 2.5 h. Then, the reaction was quenched with 1 N

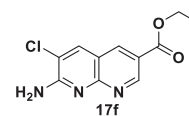
hydrochloric acid (3.2 mL) and concentrated to ~ 6 mL volume. The solids were filtered off and rinsed with water, air-dried, and then dried under vacuum to give 7-cyclobutyl-1,8-naphthyridine-3-carboxylic acid **7u** (0.294 g, 1.288 mmol, 78% yield) as an orange-yellow powder. ¹H NMR (400 MHz, CD₃SOCD₃) δ 1.84–1.96 (m, 1H), 2.00–2.14 (m, 1H), 2.32–2.48 (m, 4H), 3.91 (p, *J* = 8 Hz, 1H), 7.59 (d, *J* = 8 Hz, 1H), 8.53 (d, *J* = 8 Hz, 1H), 8.98 (br s, 1H), 9.41 (d, *J* = 2 Hz, 1H), 13.59 (br s, 1H); LC-MS (LC-ES) M + H = 229.

7-Cyclobutyl-*N*-(*trans*-4-(2-hydroxypropan-2-yl)cyclohexyl)-1,8-naphthyridine-3-carboxamide **1aa**

2-(*trans*-4-Aminocyclohexyl)propan-2-ol **8a** (0.040 g, 0.254 mmol, PharmaBlock) was added to 7-cyclobutyl-1,8-naphthyridine-3-carboxylic acid **7u** (0.057 g, 0.250 mmol) in *N,N*-dimethylformamide (2.5 mL). Then, *N,N*-diisopropylethylamine (0.05 mL, 0.287 mmol) was added, followed by 1-[bis(dimethylamino)methylene]-1*H*-1,2,3-triazolo[4,5-*b*]pyridinium 3-oxide hexafluorophosphate (0.117 g, 0.308 mmol) and the reaction mixture was stirred for five hours and concentrated. Dichloromethane and methanol were added to the residue and it was purified via silica gel chromatography, eluting with (3:1 ethyl acetate:ethanol):hexanes (0:1 to 7:3) to give a material which was triturated/sonicated with ethyl acetate and the solids collected by filtration, air-dried, then dried under vacuum overnight to give 7-cyclobutyl-*N*-(*trans*-4-(2-hydroxypropan-2-yl)cyclohexyl)-1,8-naphthyridine-3-carboxamide **1aa** (0.068 g, 0.185 mmol, 74.1% yield) as a cream colored powder. ¹H NMR (400 MHz, CD₃SOCD₃) δ 1.04 (s, 6H), 1.06–1.24 (m, 3H), 1.32 (q, *J* = 12 Hz, 2H), 1.84 (br d, *J* = 12 Hz, 2H), 1.86–1.98 (m, 3H), 2.00–2.14 (m, 1H), 2.30–2.48 (m, 4H), 3.70–3.82 (m, 1H), 3.90 (p, *J* = 9 Hz, 1H), 4.06 (s, 1H), 7.58 (d, *J* = 8 Hz, 1H), 8.45 (d, *J* = 8 Hz, 1H), 8.61 (d, *J* = 8 Hz, 1H), 8.82 (d, *J* = 2 Hz, 1H), 9.37 (d, *J* = 2 Hz, 1H); LC-MS (LC-ES) C₂₂H₂₉N₃O₂ M + H = 368; *t_R* = 0.72 min, 100% purity.

6-Bromo-3-chloro-1,8-naphthyridin-2-amine **16c**

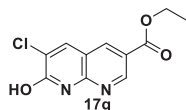
Hydrogen peroxide (51.6 mL, 505 mmol, 30 wt% in water) was added to a solution of 6-bromo-1,8-naphthyridin-2-amine **16b** (15 g, 63.1 mmol) in concentrated hydrochloric acid (60 mL) at 27 °C in a sealed tube. The resultant reaction mixture was stirred for 30 h at 27 °C. On completion, the reaction mixture was neutralized with 50% sodium hydroxide solution (100 mL) to pH = ~8. The precipitated solid compound was filtered and dried under vacuum to give impure material, which was purified via neutral alumina column chromatography, eluting with methanol:dichloromethane (1:99) to afford 6-bromo-3-chloro-1,8-naphthyridin-2-amine **16c** (6.5 g, 15.7 mmol, 24.9% yield) as an off-white solid. ¹H NMR (400 MHz, CD₃SOCD₃) δ 7.31 (br s, 2H), 8.22–8.24 (m, 1H), 8.37 (d, *J* = 3 Hz, 1H), 8.76 (d, *J* = 3 Hz, 1H); LC-MS (LC-ES) M + H = 258.

Ethyl 7-amino-6-chloro-1,8-naphthyridine-3-carboxylate **17f**

[1,1'-Bis(diphenylphosphino)ferrocene]dichloropalladium(II) dichloromethane adduct (1.283 g, 1.571 mmol) and triethylamine (4.38 mL, 31.4 mmol) were added to a solution of 6-bromo-3-chloro-1,8-

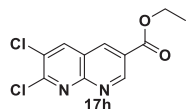
naphthyridin-2-amine **16c** (6.5 g, 15.71 mmol) in ethanol (100 mL) in a steel bomb at 27 °C. The reaction mixture was stirred at 100 °C under a carbon monoxide atmosphere (80 psi) for two hours. On completion, the reaction mixture was filtered through Celite® and the filtrate was concentrated under reduced pressure to give impure material. This material was purified via neutral alumina column chromatography, eluting with methanol:dichloromethane (1:19) to afford ethyl 7-amino-6-chloro-1,8-naphthyridine-3-carboxylate **17f** (2 g, 7.22 mmol, 45.9% yield) as an off-white solid. ¹H NMR (400 MHz, CD₃SOCD₃) δ 1.35 (t, *J* = 7 Hz, 3H), 4.37 (q, *J* = 7 Hz, 2H), 7.60 (br s, 2H), 8.45 (s, 1H), 8.68 (d, *J* = 2 Hz, 1H), 9.17 (d, *J* = 2 Hz, 1H); LC-MS (LC-ES) *M* + *H* = 252.

Ethyl 6-chloro-7-hydroxy-1,8-naphthyridine-3-carboxylate **17g**



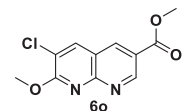
Aqueous sulfuric acid (~12 mL in 200 mL water) (200 mL, 400 mmol) was added dropwise to ethyl 7-amino-6-chloro-1,8-naphthyridine-3-carboxylate **17f** (4 g, 15.89 mmol) at 0 °C, followed by the addition of 2 M sodium nitrite in water (15.9 mL, 31.8 mmol) dropwise at 0 °C. The resultant reaction mixture was allowed to warm to 27 °C and stirred for sixteen hours. On completion, the reaction mixture was filtered and dried under vacuum to give an impure material. This material was washed with diethyl ether (50 mL) and dried under vacuum to afford ethyl 6-chloro-7-hydroxy-1,8-naphthyridine-3-carboxylate **17g** (3.8 g, 10.17 mmol, 64% yield) as an off white solid. ¹H NMR (400 MHz, CD₃SOCD₃) δ 1.35 (t, *J* = 7 Hz, 3H), 4.37 (q, *J* = 7 Hz, 2H), 8.49 (s, 1H), 8.68 (d, *J* = 2 Hz, 1H), 9.02 (d, *J* = 2 Hz, 1H), 13.07 (br s, 1H); LC-MS (LC-ES) *M* + *H* = 253.

Ethyl 6,7-dichloro-1,8-naphthyridine-3-carboxylate **17h**



Phosphorous oxychloride (6.0 mL, 64.3 mmol) was added in dropwise to a solution of ethyl 6-chloro-7-hydroxy-1,8-naphthyridine-3-carboxylate **17g** (5.6 g, 16.07 mmol) and *N,N*-diisopropylethylamine (5.61 mL, 32.1 mmol) in 1,4-dioxane (50 mL) at 0 °C. The resulting reaction mixture was heated to 80 °C and stirred for five hours. On completion, the reaction mixture was quenched with ice water (250 mL) and extracted with ethyl acetate (300 mL, 2X). The combined organic layers were washed with brine (250 mL) and evaporated under reduced pressure to give an impure material, which was purified by neutral alumina column chromatography, eluting with ethyl acetate:petroleum ether (3:2) to afford ethyl 6,7-dichloro-1,8-naphthyridine-3-carboxylate **17h** (2.39 g, 8.37 mmol, 52.1% yield) as an off-white solid. ¹H NMR (400 MHz, CDCl₃) δ 1.47 (t, *J* = 7 Hz, 3H), 4.51 (q, *J* = 7 Hz, 2H), 8.38 (s, 1H), 8.82 (d, *J* = 2 Hz, 1H), 9.64 (d, *J* = 2 Hz, 1H); LC-MS (LC-ES) *M* + *H* = 271.

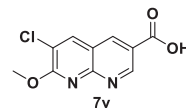
Methyl 6-chloro-7-methoxy-1,8-naphthyridine-3-carboxylate **6o**



Sodium methoxide (25% in methanol, 0.65 mL, 2.84 mmol) was added to ethyl 6,7-dichloro-1,8-naphthyridine-3-carboxylate **17h** (0.154 g, 0.568 mmol) in methanol (10 mL) at room temperature and stirred for twenty-four hours. It was combined with a smaller scale reaction and concentrated to ~4 mL volume. The solids were filtered off and rinsed with methanol (2 mL) then air-dried, followed by drying under vacuum to give methyl 6-chloro-7-methoxy-1,8-naphthyridine-3-

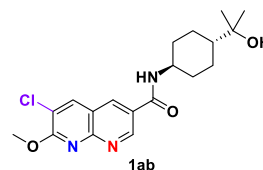
carboxylate **6o** (0.125 g, 0.495 mmol, 82% combined yield) as a tan powder. ¹H NMR (400 MHz, CD₃SOCD₃) δ 3.95 (s, 3H), 4.15 (s, 3H), 8.80 (s, 1H), 8.98 (d, *J* = 2 Hz, 1H), 9.35 (d, *J* = 2 Hz, 1H); LC-MS (LC-ES) *M* + *H* = 253.

6-Chloro-7-methoxy-1,8-naphthyridine-3-carboxylic acid **7v**



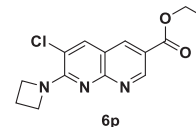
1 N Sodium hydroxide (0.50 mL, 0.500 mmol) was added to the methyl 6-chloro-7-methoxy-1,8-naphthyridine-3-carboxylate **6o** (0.125 g, 0.495 mmol) in tetrahydrofuran (5 mL) at room temperature and the reaction mixture was stirred for five hours. Then, more 1 N sodium hydroxide (0.50 mL, 0.500 mmol) was added and the reaction mixture was stirred for nineteen hours. The reaction mixture was acidified with 1 N hydrochloric acid (1.0 mL) and a precipitate formed. The solids were filtered off and rinsed with water, and air-dried, then dried under vacuum to give 6-chloro-7-methoxy-1,8-naphthyridine-3-carboxylic acid **7v** (0.097 g, 0.406 mmol, 82% yield) as a cream colored powder. ¹H NMR (400 MHz, CD₃SOCD₃) δ 4.14 (s, 3H), 8.78 (s, 1H), 8.93 (d, *J* = 2 Hz, 1H), 9.33 (d, *J* = 2 Hz, 1H), 13.58 (br s, 1H); LC-MS (LC-ES) *M* + *H* = 239.

6-Chloro-*N*-(*trans*-4-(2-hydroxypropan-2-yl)cyclohexyl)-7-methoxy-1,8-naphthyridine-3-carboxamide **1ab**



2-(*trans*-4-Aminocyclohexyl)propan-2-ol **8a** (0.061 g, 0.388 mmol, PharmaBlock) was added to 6-chloro-7-methoxy-1,8-naphthyridine-3-carboxylic acid **7v** (0.096 g, 0.402 mmol) in *N,N*-dimethylformamide (4 mL) at room temperature. Then, *N,N*-diisopropylethylamine (0.09 mL, 0.517 mmol) was added to the suspension, followed by 1-[bis(dimethylamino)methylene]-1*H*-1,2,3-triazolo[4,5-*b*]pyridinium 3-oxide hexafluorophosphate (0.189 g, 0.497 mmol) and the reaction mixture was stirred for fourteen hours. The reaction mixture was concentrated, and the residue was purified via silica gel chromatography, eluting with ethyl acetate:ethanol (3:1):hexanes (0:1 to 3:1). Ethyl acetate (2 mL) was added to the solid residue and it was triturated/sonicated, then filtered and dried to give 6-chloro-*N*-(*trans*-4-(2-hydroxypropan-2-yl)cyclohexyl)-7-methoxy-1,8-naphthyridine-3-carboxamide **1ab** (0.119 g, 0.315 mmol, 81% yield) as an off white powder. ¹H NMR (400 MHz, CD₃SOCD₃) δ 1.04 (s, 6H), 1.06–1.24 (m, 3H), 1.31 (q, *J* = 12 Hz, 2H), 1.83 (br d, *J* = 11 Hz, 2H), 1.93 (br d, *J* = 10 Hz, 2H), 3.68–3.80 (m, 1H), 4.06 (s, 1H), 4.12 (s, 3H), 8.60 (d, *J* = 8 Hz, 1H), 8.69 (s, 1H), 8.75 (d, *J* = 2 Hz, 1H), 9.30 (d, *J* = 2 Hz, 1H); LC-MS (LC-ES) C₁₉H₂₄N₃O₃ *M* + *H* = 378; *t*_R = 0.79 min, 100% purity.

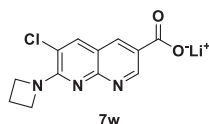
Ethyl 7-(azetidin-1-yl)-6-chloro-1,8-naphthyridine-3-carboxylate **6p**



N,N-Diisopropylethylamine (0.264 mL, 1.515 mmol) was added to ethyl 6,7-dichloro-1,8-naphthyridine-3-carboxylate **17h** (0.1027 g, 0.379 mmol) in *N*-methyl-2-pyrrolidone (1.263 mL) at room temperature. Then, azetidine hydrochloride (0.071 g, 0.758 mmol) was added and the reaction mixture was heated at 100 °C in the microwave for one hour. The reaction mixture was diluted in dichloromethane, washed with saturated sodium bicarbonate, dried over magnesium sulfate,

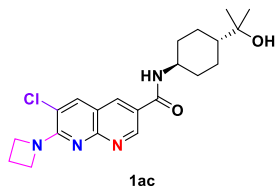
filtered, and concentrated. The residue was purified by RP HPLC, eluting with acetonitrile:water with 0.1% ammonium hydroxide (5:95 to 100:0), then further purified by silica gel chromatography, eluting with ethyl acetate:hexanes (1:4 to 4:1) to give ethyl 7-(azetidin-1-yl)-6-chloro-1,8-naphthyridine-3-carboxylate **6p** (0.0783 g, 0.255 mmol, 67.3% yield). ^1H NMR (400 MHz, CD_3SOCD_3) δ 1.34 (t, $J = 7$ Hz, 3H), 2.33 (p, $J = 8$ Hz, 2H), 4.35 (q, $J = 7$ Hz, 2H), 4.38–4.54 (m, 4H), 8.40 (s, 1H), 8.68 (d, $J = 2$ Hz, 1H), 9.15 (d, $J = 2$ Hz, 1H); LC-MS (LC-ES) $M + H = 292$.

Lithium 7-(azetidin-1-yl)-6-chloro-1,8-naphthyridine-3-carboxylate **7w**



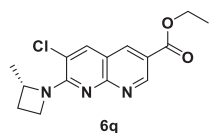
Lithium hydroxide (0.019 g, 0.805 mmol) was added to ethyl 7-(azetidin-1-yl)-6-chloro-1,8-naphthyridine-3-carboxylate **6p** (0.0783 g, 0.268 mmol) in methanol (1.1 mL) and water (0.27 mL) at room temperature and the reaction mixture was stirred three hours at 60 °C. The reaction mixture was concentrated to give lithium 7-(azetidin-1-yl)-6-chloro-1,8-naphthyridine-3-carboxylate **7w** (0.0653 g, 0.230 mmol, 86% yield). ^1H NMR (400 MHz, CD_3SOCD_3) δ 2.30 (p, $J = 8$ Hz, 2H), 4.34 (t, $J = 8$ Hz, 4H), 8.27 (s, 1H), 8.40 (d, $J = 2$ Hz, 1H), 9.17 (d, $J = 2$ Hz, 1H); LC-MS (LC-ES) $M + H = 264$.

7-(Azetidin-1-yl)-6-chloro-*N*-(*trans*-4-(2-hydroxypropan-2-yl)cyclohexyl)-1,8-naphthyridine-3-carboxamide **1ac**



N,N-Diisopropylethylamine (0.169 mL, 0.969 mmol) was added to lithium 7-(azetidin-1-yl)-6-chloro-1,8-naphthyridine-3-carboxylate **7w** (0.0653 g, 0.242 mmol) in *N,N*-dimethylformamide (0.81 mL) at room temperature. Then, 2-(*trans*-4-aminocyclohexyl)propan-2-ol **8a** (0.050 g, 0.315 mmol, PharmaBlock) was added and the reaction mixture was stirred for five minutes. Then, *n*-propylphosphonic acid anhydride (0.288 mL, 0.484 mmol) was added and the reaction mixture was stirred for sixteen hours. The reaction mixture was concentrated. The resulting residue was purified by RP HPLC, eluting with acetonitrile:water with 0.1% ammonium hydroxide (5:95 to 100:0), then further purified by silica gel chromatography, eluting with methanol:ethyl acetate (0:1 to 1:4) to give 7-(azetidin-1-yl)-6-chloro-*N*-(*trans*-4-(2-hydroxypropan-2-yl)cyclohexyl)-1,8-naphthyridine-3-carboxamide **1ac** (0.0312 g, 0.074 mmol, 30.4% yield). ^1H NMR (400 MHz, CD_3SOCD_3) δ 1.03 (s, 6H), 1.04–1.24 (m, 3H), 1.30 (q, $J = 12$ Hz, 2H), 1.82 (br d, $J = 12$ Hz, 2H), 1.91 (br d, $J = 10$ Hz, 2H), 2.32 (p, $J = 8$ Hz, 2H), 3.66–3.78 (m, 1H), 4.05 (s, 1H), 4.41 (t, $J = 7$ Hz, 4H), 8.30 (s, 1H), 8.43 (d, $J = 8$ Hz, 1H), 8.52 (d, $J = 2$ Hz, 1H), 9.13 (d, $J = 2$ Hz, 1H); LC-MS (LC-ES) $\text{C}_{21}\text{H}_{27}\text{ClN}_4\text{O}_2$ $M + H = 403$; $t_R = 0.59$ min, 100% purity.

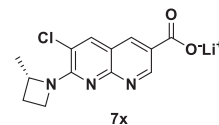
Ethyl (S)-6-chloro-7-(2-methylazetidin-1-yl)-1,8-naphthyridine-3-carboxylate **6q**



N,N-Diisopropylethylamine (1.930 mL, 11.08 mmol) was added to ethyl 6,7-dichloro-1,8-naphthyridine-3-carboxylate **17h** (0.7511 g, 2.77 mmol) in *N*-methyl-2-pyrrolidone (5.54 mL) at room temperature.

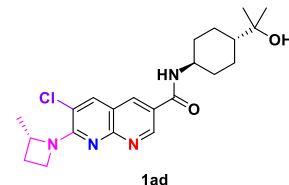
Then (S)-2-methylazetidin-1-ium ((1*R*,4*S*)-7,7-dimethyl-2-oxobicyclo [2.2.1]heptan-1-yl)methanesulfonate⁶³ (1.261 g, 4.16 mmol) was added and the reaction mixture was heated at 100 °C in the microwave for one hour. The reaction mixture was diluted in dichloromethane, washed with saturated sodium bicarbonate, dried over magnesium sulfate, filtered, and concentrated. The residue was purified by RP HPLC, eluting with acetonitrile:water with 0.1% ammonium hydroxide (5:95:100:0), then further purified by silica gel chromatography, eluting with ethyl acetate:hexanes (1:4 to 4:1) to give ethyl (S)-6-chloro-7-(2-methylazetidin-1-yl)-1,8-naphthyridine-3-carboxylate **6q** (0.7191 g, 2.234 mmol, 81% yield). ^1H NMR (400 MHz, CD_3SOCD_3) δ 1.35 (t, $J = 7$ Hz, 3H), 1.50 (d, $J = 6$ Hz, 3H), 1.92–2.02 (m, 1H), 2.44–2.56 (m, 1H), 4.31 (dt, $J = 9, 7$ Hz, 1H), 4.36 (q, $J = 7$ Hz, 2H), 4.56 (dt, $J = 9, 6$ Hz, 1H), 4.80 (h, $J = 6$ Hz, 1H), 8.43 (s, 1H), 8.70 (d, $J = 2$ Hz, 1H), 9.16 (d, $J = 2$ Hz, 1H); LC-MS (LC-ES) $M + H = 306$.

Lithium (S)-6-chloro-7-(2-methylazetidin-1-yl)-1,8-naphthyridine-3-carboxylate **7x**



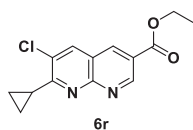
Lithium hydroxide (0.068 g, 2.82 mmol) was added to ethyl (S)-6-chloro-7-(2-methylazetidin-1-yl)-1,8-naphthyridine-3-carboxylate **6q** (0.7191 g, 2.352 mmol) in methanol (9.4 mL) and water (2.4 mL) at room temperature and the reaction mixture was stirred sixteen hours at 45 °C. The reaction mixture was concentrated to give lithium (S)-6-chloro-7-(2-methylazetidin-1-yl)-1,8-naphthyridine-3-carboxylate **7x** (0.6877 g, 2.303 mmol, 98% yield). ^1H NMR (400 MHz, CD_3SOCD_3) δ 1.45 (d, $J = 6$ Hz, 3H), 1.90–2.00 (m, 1H), 2.38–2.50 (m, 1H), 4.11 (dt, $J = 9, 6$ Hz, 1H), 4.47 (dt, $J = 9, 6$ Hz, 1H), 4.74 (h, $J = 8$ Hz, 1H), 8.30 (s, 1H), 8.41 (d, $J = 2$ Hz, 1H), 9.17 (d, $J = 2$ Hz, 1H); LC-MS (LC-ES) $M + H = 278$.

6-Chloro-*N*-(*trans*-4-(2-hydroxypropan-2-yl)cyclohexyl)-7-((S)-2-methylazetidin-1-yl)-1,8-naphthyridine-3-carboxamide **1ad**



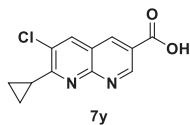
N,N-Diisopropylethylamine (0.162 mL, 0.927 mmol) was added to lithium (S)-6-chloro-7-(2-methylazetidin-1-yl)-1,8-naphthyridine-3-carboxylate **7x** (0.0657 g, 0.232 mmol) in *N,N*-dimethylformamide (0.77 mL) at room temperature. Then, 2-(*trans*-4-aminocyclohexyl)propan-2-ol **8a** (0.055 g, 0.347 mmol, PharmaBlock) was added and the reaction mixture was stirred for five minutes. Then, *n*-propylphosphonic acid anhydride (0.276 mL, 0.463 mmol) was added and the reaction mixture was stirred for sixteen hours. The reaction mixture was concentrated. The resulting residue was purified by RP HPLC, eluting with acetonitrile:water with 0.1% ammonium hydroxide (5:95 to 100:0), then further purified by silica gel chromatography, eluting with methanol:ethyl acetate (0:1 to 1:4) to give 6-chloro-*N*-(*trans*-4-(2-hydroxypropan-2-yl)cyclohexyl)-7-((S)-2-methylazetidin-1-yl)-1,8-naphthyridine-3-carboxamide **1ad** (0.0560 g, 0.128 mmol, 55.1% yield). ^1H NMR (400 MHz, CD_3SOCD_3) δ 1.04 (s, 6H), 1.06–1.24 (m, 3H), 1.30 (q, $J = 12$ Hz, 2H), 1.48 (d, $J = 6$ Hz, 3H), 1.83 (br d, $J = 11$ Hz, 2H), 1.91 (br d, $J = 10$ Hz, 2H), 1.90–2.02 (m, 1H), 2.42–2.54 (m, 1H), 3.66–3.78 (m, 1H), 4.05 (s, 1H), 4.24 (dt, $J = 9, 7$ Hz, 1H), 4.53 (dt, $J = 9, 6$ Hz, 1H), 4.79 (h, $J = 8$ Hz, 1H), 8.33 (s, 1H), 8.44 (d, $J = 8$ Hz, 1H), 8.54 (d, $J = 2$ Hz, 1H), 9.14 (d, $J = 2$ Hz, 1H); LC-MS (LC-ES) $\text{C}_{22}\text{H}_{29}\text{ClN}_4\text{O}_2$ $M + H = 417$; $t_R = 0.68$ min, 100% purity.

Ethyl 6-chloro-7-cyclopropyl-1,8-naphthyridine-3-carboxylate **6r**



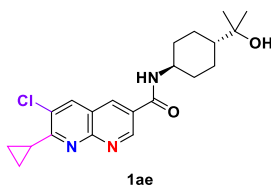
Potassium cyclopropyltrifluoroborate (0.157 g, 1.061 mmol) was added to ethyl 6,7-dichloro-1,8-naphthyridine-3-carboxylate **17h** (0.273 g, 1.007 mmol) at room temperature. Then cesium carbonate (0.988 g, 3.03 mmol) was added, followed by the addition of [1,1'-bis(diphenylphosphino)ferrocene]dichloropalladium (II)-dichloromethane adduct (0.083 g, 0.102 mmol). Then, toluene (20 mL) and water (2 mL) were added and nitrogen was bubbled through the reaction mixture for ~ 5 min. Then, the reaction mixture was heated at 100 °C for five hours. The organics were decanted from the aqueous layer and the aqueous washed with dichloromethane. The combined organics were concentrated, and the residue was purified by silica gel chromatography, eluting with (3:1 ethyl acetate:ethanol):hexanes (0:1 to 1:6) to give ethyl 6-chloro-7-cyclopropyl-1,8-naphthyridine-3-carboxylate **6r** (0.143 g, 0.543 mmol, 51% yield) as a lavender-gray solid. ¹H NMR (400 MHz, CD₃SOCD₃) δ 1.22–1.28 (m, 4H), 1.37 (t, *J* = 7 Hz, 3H), 2.74 (p, *J* = 6 Hz, 1H), 4.40 (q, *J* = 7 Hz, 2H), 8.80 (s, 1H), 8.99 (d, *J* = 2 Hz, 1H), 9.37 (d, *J* = 2 Hz, 1H); LC-MS (LC-ES) *M* + *H* = 277.

6-Chloro-7-cyclopropyl-1,8-naphthyridine-3-carboxylic acid **7y**



1 N Sodium hydroxide (3.2 mL, 3.20 mmol) was added to a solution of ethyl 6-chloro-7-cyclopropyl-1,8-naphthyridine-3-carboxylate **6r** (0.448 g, 1.619 mmol, from three batches) in methanol (10 mL) and the reaction mixture was stirred for sixty-four hours. Upon consumption of the starting material, the reaction was quenched with 1 N hydrochloric acid (3.2 mL), the solids were collected by filtration, washed with water (3X), air dried, and then dried under vacuum overnight to give 6-chloro-7-cyclopropyl-1,8-naphthyridine-3-carboxylic acid **7y** (0.382 g, 1.536 mmol, 95% yield) as a tan powder. ¹H NMR (400 MHz, CD₃SOCD₃) δ 1.20–1.28 (m, 4H), 2.74 (p, *J* = 6 Hz, 1H), 8.78 (s, 1H), 8.96 (d, *J* = 2 Hz, 1H), 9.36 (d, *J* = 2 Hz, 1H), 13.67 (br s, 1H); LC-MS (LC-ES) *M* + *H* = 249.

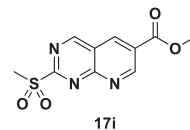
6-Chloro-7-cyclopropyl-*N*-((trans)-4-(2-hydroxypropan-2-yl)cyclohexyl)-1,8-naphthyridine-3-carboxamide **1ae**



2-(trans-4-Aminocyclohexyl)propan-2-ol **8a** (0.040 g, 0.254 mmol, PharmaBlock) and *N,N*-diisopropylethylamine (0.06 mL, 0.344 mmol) were added to the 6-chloro-7-cyclopropyl-1,8-naphthyridine-3-carboxylic acid **7y** (0.063 g, 0.253 mmol) in *N,N*-dimethylformamide (2.5 mL). Then, 1-[bis(dimethylamino)methylene]-1*H*-1,2,3-triazolo[4,5-*b*]pyridinium 3-oxide hexafluorophosphate (0.116 g, 0.305 mmol) was added and the reaction mixture was stirred for 100 min. Then the reaction mixture was concentrated. Dichloromethane and methanol were added to the residue and the mixture was purified by silica gel chromatography, eluting with (ethyl acetate:ethanol) (3:1):hexanes (0:1 to 1:3) to give a solid that was triturated/sonicated with ethyl acetate to give 6-chloro-7-cyclopropyl-*N*-((trans)-4-(2-hydroxypropan-2-yl)cyclohexyl)-1,8-naphthyridine-3-carboxamide **1ae** (0.82 g, 0.211 mmol, 83% yield) as a white powder. ¹H NMR (400 MHz, CD₃SOCD₃) δ 1.04 (s, 6H),

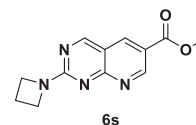
1.06–1.26 (m, 7H), 1.31 (q, *J* = 12 Hz, 2H), 1.83 (br d, *J* = 11 Hz, 2H), 1.93 (br d, *J* = 10 Hz, 2H), 2.68–2.78 (m, 1H), 3.68–3.80 (m, 1H), 4.06 (s, 1H), 8.64 (d, *J* = 8 Hz, 1H), 8.68 (s, 1H), 8.77 (d, *J* = 2 Hz, 1H), 9.34 (d, *J* = 2 Hz, 1H); LC-MS (LC-ES) C₂₁H₂₆ClN₃O₂ *M* + *H* = 388; *t*_R = 0.89 min, 100% purity.

Ethyl 2-(methylsulfonyl)pyrido[2,3-*d*]pyrimidine-6-carboxylate **17i**



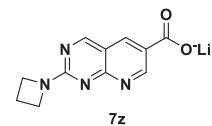
To a stirred, cooled (0 °C) solution of ethyl 2-(methylthio)pyrido[2,3-*d*]pyrimidine-6-carboxylate **17d** (200 mg, 0.802 mmol) in dichloromethane (10 mL) was added 3-chloroperoxybenzoic acid (360 mg, 1.606 mmol). The mixture was stirred for three hours, then quenched with saturated aqueous sodium bicarbonate, extracted with dichloromethane (2X), washed with brine, dried over sodium sulfate, filtered, and concentrated to give impure ethyl 2-(methylsulfonyl)pyrido[2,3-*d*]pyrimidine-6-carboxylate **17i** (175 mg, 78% yield), which was carried forward into the next reaction. LC-MS (LC-ES) *M* + *H* = 282.

Ethyl 2-(azetidin-1-yl)pyrido[2,3-*d*]pyrimidine-6-carboxylate **6s**



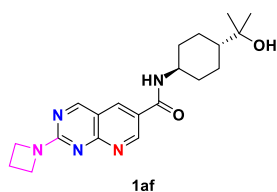
To crude ethyl 2-(methylsulfonyl)pyrido[2,3-*d*]pyrimidine-6-carboxylate **17i** (98 mg, 0.348 mmol) and azetidine hydrochloride (65 mg, 0.695 mmol) was added *N*-methyl-2-pyrrolidone (1.5 mL), followed by *N,N*-diisopropylethylamine (0.25 mL, 1.431 mmol), and the reaction mixture was heated with stirring in a microwave at 100 °C for two hours. After cooling to room temperature, the mixture was loaded onto a pre-packed Celite® cartridge and purified by reverse phase chromatography, eluting with acetonitrile:water with 0.1% ammonium hydroxide (0:1 to 4:1) to give ethyl 2-(azetidin-1-yl)pyrido[2,3-*d*]pyrimidine-6-carboxylate **6s** (10 mg, 0.039 mmol, 11.1% yield) as a yellow solid. ¹H NMR (400 MHz, CD₃OD) δ 1.47 (t, *J* = 7 Hz, 3H), 2.52 (p, *J* = 8 Hz, 2H), 4.38 (t, *J* = 8 Hz, 4H), 4.47 (q, *J* = 7 Hz, 2H), 8.86 (d, *J* = 2 Hz, 1H), 9.27 (s, 1H), 9.37 (d, *J* = 2 Hz, 1H); LC-MS (LC-ES) *M* + *H* = 259.

Lithium 2-(azetidin-1-yl)pyrido[2,3-*d*]pyrimidine-6-carboxylate **7z**



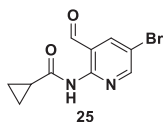
To a stirred solution of ethyl 2-(azetidin-1-yl)pyrido[2,3-*d*]pyrimidine-6-carboxylate **6s** (17 mg, 0.066 mmol) in methanol (1 mL) at room temperature was added 1 M aqueous lithium hydroxide (0.20 mL, 0.200 mmol). The mixture was stirred for three hours, then methanol (1 mL) and 1 M aqueous lithium hydroxide (0.1 mL, 0.100 mmol) were added and the reaction mixture was stirred for 90 min. Then, the reaction mixture was heated at 50 °C for 1 h, cooled, and concentrated to give lithium 2-(azetidin-1-yl)pyrido[2,3-*d*]pyrimidine-6-carboxylate **7z** (25 mg, 0.106 mmol, 161% yield). ¹H NMR (400 MHz, CD₃SOCD₃) δ 2.35 (p, *J* = 8 Hz, 2H), 4.16 (t, *J* = 8 Hz, 4H), 8.50 (d, *J* = 2 Hz, 1H), 9.23 (s, 1H), 9.29 (d, *J* = 2 Hz, 1H); LC-MS (LC-ES) *M* + *H* = 231.

2-(Azetidin-1-yl)-*N*-((trans)-4-(2-hydroxypropan-2-yl)cyclohexyl)pyrido[2,3-*d*]pyrimidine-6-carboxamide **1af**



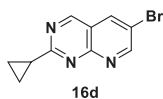
To a thick, stirred suspension of lithium 2-(azetidin-1-yl)pyrido[2,3-d]pyrimidine-6-carboxylate **7z** (15 mg, 0.064 mmol) and 2-((trans-4-aminocyclohexyl)propan-2-ol **8a** (15 mg, 0.095 mmol, PharmaBlock) in *N,N*-dimethylformamide (1 mL) was added *N,N*-diisopropylethylamine (0.055 mL, 0.318 mmol), followed by *n*-propylphosphonic acid anhydride (0.075 mL, 0.127 mmol). The mixture became homogeneous and was allowed to stir overnight. The mixture was loaded onto a pre-packed Celite® cartridge and purified by reverse phase chromatography, eluting with acetonitrile:water with 0.1% ammonium hydroxide (0:1 to 4:1), then repurified by silica gel chromatography, eluting with ethyl acetate:ethanol (3:1):hexanes (1:9 to 3:1), then repurified by silica gel chromatography, eluting with methanol:dichloromethane (0:1 to 1:9) to give 2-(azetidin-1-yl)-*N*-((trans-4-(2-hydroxypropan-2-yl)cyclohexyl)pyrido[2,3-d]pyrimidine-6-carboxamide **1af** (18.5 mg, 0.052 mmol, 21% yield) as a yellow solid. ¹H NMR (400 MHz, CD₃SOCD₃) δ 1.04 (s, 6H), 1.04–1.24 (m, 3H), 1.29 (q, *J* = 12 Hz, 2H), 1.83 (br d, *J* = 12 Hz, 2H), 1.91 (br d, *J* = 12 Hz, 2H), 2.37 (p, *J* = 8 Hz, 2H), 3.66–3.78 (m, 1H), 4.21 (t, *J* = 7 Hz, 4H), 8.41 (d, *J* = 8 Hz, 1H), 8.67 (d, *J* = 2 Hz, 1H), 9.25 (d, *J* = 2 Hz, 1H), 9.29 (s, 1H); LC-MS (LC-ES) C₂₀H₂₇N₅O₂ M + H = 370; t_R = 0.57 min, 100% purity.

N-(5-Bromo-3-formylpyridin-2-yl)cyclopropanecarboxamide **25**



Cyclopropanecarbonyl chloride (1 mL, 11.02 mmol) was added to a stirred solution of 2-amino-5-bromonicotinaldehyde **24** (1 g, 4.97 mmol) and pyridine (2 mL, 24.73 mmol) in dichloromethane (20 mL) and the mixture was stirred for 30 min. The mixture was evaporated to dryness under reduced pressure and placed in vacuo for ~ 15 min to give a brown foam. This material was dissolved in tetrahydrofuran (30 mL) and methanol (10 mL) and then 1 N aqueous sodium hydroxide (15 mL, 15.00 mmol) was added dropwise. The mixture was stirred for 10 min and the mixture was concentrated under reduced pressure. The remaining material was triturated with water to give a solid which was collected via vacuum filtration, washed with water and dried in vacuo overnight to give *N*-(5-bromo-3-formylpyridin-2-yl)cyclopropanecarboxamide **25** (1.21 g, 4.50 mmol, 90% yield) as a tan solid. ¹H NMR (400 MHz, CD₃SOCD₃) δ 0.80–0.92 (m, 4H), 1.98–2.08 (m, 1H), 8.19 (d, *J* = 2 Hz, 1H), 8.76 (d, *J* = 2 Hz, 1H), 9.56 (s, 1H), 11.27 (br s, 1H); LC-MS (LC-ES) M + H = 269.

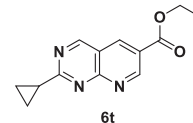
6-Bromo-2-cyclopropylpyrido[2,3-d]pyrimidine **16d**



7 M Ammonia (30 mL, 210 mmol) in methanol was added to *N*-(5-bromo-3-formylpyridin-2-yl)cyclopropanecarboxamide **25** (1.20 g, 4.46 mmol) suspended in methanol (20 mL). The mixture quickly became homogeneous. The reaction vessel was sealed, and the mixture was heated at 80 °C overnight, then, the mixture was cooled and concentrated under reduced pressure. The remaining material was dissolved in dichloromethane and purified via silica gel chromatography, eluting with ethyl acetate:hexanes (1:9 to 9:1) to give 6-bromo-2-cyclopropylpyrido[2,3-d]pyrimidine **16d** (745 mg, 2.98 mmol, 66.8%

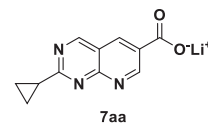
yield) as a yellow solid. ¹H NMR (400 MHz, CD₃SOCD₃) δ 1.14–1.22 (m, 4H), 2.36–2.44 (m, 1H), 8.87 (d, *J* = 3 Hz, 1H), 9.24 (d, *J* = 3 Hz, 1H), 9.51 (s, 1H); LC-MS (LC-ES) M + H = 250.

Ethyl 2-cyclopropylpyrido[2,3-d]pyrimidine-6-carboxylate **6t**



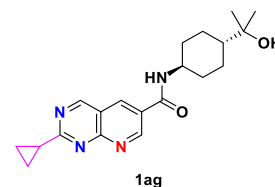
A stirred mixture of 6-bromo-2-cyclopropylpyrido[2,3-d]pyrimidine **16d** (100 mg, 0.400 mmol), [1,1'-bis(diphenylphosphino)ferrocene] dichloropalladium(II) dichloromethane adduct (50 mg, 0.061 mmol) and *N,N*-diisopropylethylamine (0.35 mL, 2.004 mmol) in ethanol (5 mL) was purged with nitrogen for 3 min, followed by purging with carbon monoxide for ~ 5 min. The mixture was stirred under a carbon monoxide balloon and heated at 80 °C overnight. After cooling to room temperature, the mixture was filtered through a pad of Celite®, rinsing with ethanol. The filtrate was evaporated to dryness under reduced pressure and the remaining dark material was dissolved in a minimal amount of dichloromethane and purified via silica chromatography, eluting with ethyl acetate:ethanol (3:1): hexanes (1:19 to 1:1) to give ethyl 2-cyclopropylpyrido[2,3-d]pyrimidine-6-carboxylate **6t** (63 mg, 0.259 mmol, 64.8% yield) as a white solid. ¹H NMR (400 MHz, CD₃SOCD₃) δ 1.20–1.26 (m, 4H), 1.38 (t, *J* = 7 Hz, 3H), 2.38–2.48 (m, 1H), 4.41 (q, *J* = 7 Hz, 2H), 9.15 (d, *J* = 2 Hz, 1H), 9.55 (d, *J* = 2 Hz, 1H), 9.73 (s, 1H); LC-MS (LC-ES) M + H = 244.

Lithium 2-cyclopropylpyrido[2,3-d]pyrimidine-6-carboxylate **7aa**



To a stirred solution of ethyl 2-cyclopropylpyrido[2,3-d]pyrimidine-6-carboxylate **6t** (62 mg, 0.255 mmol) in methanol (4 mL) was added 1 M aqueous lithium hydroxide (0.80 mL, 0.800 mmol). The mixture was stirred for two hours, then concentrated, slurried with methanol and re-concentrated (2X) to give crude lithium 2-cyclopropylpyrido[2,3-d]pyrimidine-6-carboxylate **7aa** (77 mg, 0.348 mmol, >100% yield) which was carried forward to the next reaction. ¹H NMR (400 MHz, CD₃SOCD₃) δ 1.10–1.18 (m, 4H), 2.32–2.42 (m, 1H), 8.74 (d, *J* = 2 Hz, 1H), 9.54 (s, 1H), 9.55 (d, *J* = 2 Hz, 1H); LC-MS (LC-ES) M + H = 216.

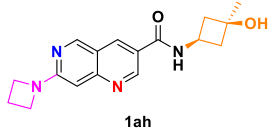
2-Cyclopropyl-*N*-(trans-4-(2-hydroxypropan-2-yl)cyclohexyl)pyrido[2,3-d]pyrimidine-6-carboxamide **1ag**



To a stirred solution of lithium 2-cyclopropylpyrido[2,3-d]pyrimidine-6-carboxylate **7aa** (75 mg, 0.253 mmol maximum) and 2-((trans-4-aminocyclohexyl)propan-2-ol **8a** (60 mg, 0.382 mmol, PharmaBlock) in *N,N*-dimethylformamide (2 mL) was added *N,N*-diisopropylethylamine (0.23 mL, 1.317 mmol), followed by *n*-propylphosphonic acid anhydride (0.30 mL, 0.509 mmol) and the reaction mixture was allowed to stir overnight. The reaction mixture was purified by reverse phase chromatography, eluting with acetonitrile–water with 0.1% ammonium hydroxide (0:1 to 4:1) to give 2-cyclopropyl-*N*-(trans-4-(2-hydroxypropan-2-yl)cyclohexyl)pyrido[2,3-d]pyrimidine-6-carboxamide **1ag** (62 mg, 0.175 mmol, 69.1% yield) as a white solid. ¹H NMR (400 MHz, CD₃SOCD₃) δ 1.04 (s, 6H), 0.90–1.22 (m, 7H), 1.31 (q, *J* = 12 Hz, 2H), 1.84 (br d, *J* = 12 Hz, 2H), 1.94 (br d, *J* = 10 Hz, 2H), 2.36–2.46 (m, 1H),

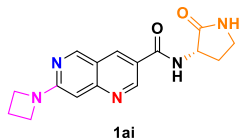
3.68–3.80 (m, 1H), 4.06 (s, 1H), 8.68 (d, $J = 8$ Hz, 1H), 8.94 (d, $J = 2$ Hz, 1H), 9.51 (d, $J = 2$ Hz, 1H), 9.63 (s, 1H); LC-MS (LC-ES) $C_{20}H_{26}N_4O_2$ M + H = 355; $t_R = 0.56$ min, 100% purity.

7-(Azetidin-1-yl)-*N*-((1*s*,3*s*)-3-hydroxy-3-methylcyclobutyl)-1,6-naphthyridine-3-carboxamide **1ah**



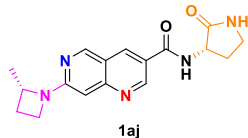
N,N-Diisopropylethylamine (0.301 mL, 1.722 mmol) was added to 7-(azetidin-1-yl)-1,6-naphthyridine-3-carboxylic acid lithium salt **7i** (0.0678 g, 0.287 mmol) in *N,N*-dimethylformamide (0.96 mL) at room temperature. Then, (1*s*,3*s*)-3-amino-1-methylcyclobutanol hydrochloride **8b** (0.047 g, 0.344 mmol, AstaTech) was added and the reaction mixture was stirred for five minutes. Then, *n*-propylphosphonic acid anhydride (0.342 mL, 0.574 mmol) was added and the reaction mixture was stirred for sixteen hours. The reaction mixture was concentrated. The resulting residue was purified by RP HPLC, eluting with acetonitrile: water with 0.1% ammonium hydroxide (5:95 to 100:0) to give 7-(azetidin-1-yl)-*N*-((1*s*,3*s*)-3-hydroxy-3-methylcyclobutyl)-1,6-naphthyridine-3-carboxamide **1ah** (0.0370 g, 0.113 mmol, 39.2% yield). 1H NMR (400 MHz, CD_3SOCD_3) δ 1.27 (s, 3H), 2.11 (t, $J = 10$ Hz, 2H), 2.30 (t, $J = 8$ Hz, 2H), 2.39 (p, $J = 7$ Hz, 2H), 4.02 (h, $J = 7$ Hz, 1H), 4.08 (t, $J = 7$ Hz, 4H), 4.97 (s, 1H), 6.54 (s, 1H), 8.71 (s, 1H), 8.74 (d, $J = 9$ Hz, 1H), 9.03 (s, 1H), 9.18 (s, 1H); LC-MS (LC-ES) $C_{17}H_{20}N_4O_2$ M + H = 313; $t_R = 0.40$ min, 100% purity.

(*S*)-7-(Azetidin-1-yl)-*N*-(2-oxopyrrolidin-3-yl)-1,6-naphthyridine-3-carboxamide **1ai**



N,N-Diisopropylethylamine (0.209 mL, 1.194 mmol) was added to 7-(azetidin-1-yl)-1,6-naphthyridine-3-carboxylic acid lithium salt **7i** (0.0470 g, 0.199 mmol) in *N,N*-dimethylformamide (0.663 mL) at room temperature. Then, (*S*)-3-aminopyrrolidin-2-one **8c** (0.028 g, 0.279 mmol, AstaTech) was added and the reaction mixture was stirred for five minutes. Then, *n*-propylphosphonic acid anhydride (0.237 mL, 0.398 mmol) was added and the reaction mixture was stirred for sixteen hours. The reaction mixture was concentrated. The resulting residue was purified by RP HPLC, eluting with acetonitrile: water with 0.1% ammonium hydroxide (5:95 to 100:0) to give (*S*)-7-(azetidin-1-yl)-*N*-(2-oxopyrrolidin-3-yl)-1,6-naphthyridine-3-carboxamide **1ai** (0.0358 g, 0.109 mmol, 54.9% yield). 1H NMR (400 MHz, CD_3SOCD_3) δ 2.01 (p, $J = 10$ Hz, 1H), 2.32–2.44 (m, 3H), 3.25 (q, $J = 9$ Hz, 2H), 4.09 (t, $J = 7$ Hz, 4H), 4.59 (q, $J = 9$ Hz, 1H), 6.55 (s, 1H), 7.86 (s, 1H), 8.73 (s, 1H), 8.85 (d, $J = 8$ Hz, 1H), 9.06 (s, 1H), 9.20 (s, 1H); LC-MS (LC-ES) $C_{16}H_{17}N_5O_2$ M + H = 312; $t_R = 0.35$ min, 100% purity.

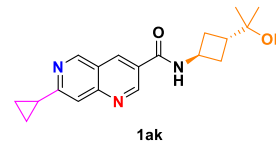
7-((*S*)-2-Methylazetidin-1-yl)-*N*-((*S*)-2-oxopyrrolidin-3-yl)-1,6-naphthyridine-3-carboxamide **1aj**



N,N-Diisopropylethylamine (0.293 mL, 1.678 mmol) was added to lithium 7-(2-methylazetidin-1-yl)-1,6-naphthyridine-3-carboxylate **7k** (0.0697 g, 0.280 mmol) in *N,N*-dimethylformamide (0.93 mL) at room temperature. Then, (*S*)-3-aminopyrrolidin-2-one **8c** (0.039 g, 0.392 mmol, AstaTech) was added and the reaction mixture was stirred

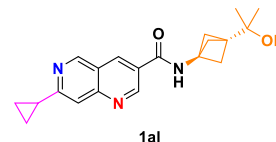
for five minutes. Then, *n*-propylphosphonic acid anhydride (0.333 mL, 0.559 mmol) was added and the reaction mixture was stirred for sixteen hours. The reaction mixture was concentrated. The resulting residue was purified by RP HPLC, eluting with acetonitrile: water with 0.1% ammonium hydroxide (5:95 to 100:0) to give 7-((*S*)-2-methylazetidin-1-yl)-*N*-((*S*)-2-oxopyrrolidin-3-yl)-1,6-naphthyridine-3-carboxamide **1aj** (0.0520 g, 0.152 mmol, 54.3% yield). 1H NMR (400 MHz, CD_3SOCD_3) δ 1.51 (d, $J = 6$ Hz, 3H), 1.94–2.12 (m, 2H), 2.32–2.44 (m, 1H), 2.44–2.54 (m, 1H), 3.20–3.32 (m, 2H), 3.88 (q, $J = 8$ Hz, 1H), 4.05 (q, $J = 8$ Hz, 1H), 4.45 (q, $J = 7$ Hz, 1H), 4.59 (q, $J = 9$ Hz, 1H), 6.55 (s, 1H), 7.86 (s, 1H), 8.73 (s, 1H), 8.86 (d, $J = 8$ Hz, 1H), 9.06 (s, 1H), 9.20 (s, 1H); LC-MS (LC-ES) $C_{17}H_{19}N_5O_2$ M + H = 326; $t_R = 0.42$ min, 100% purity.

7-Cyclopropyl-*N*-(*trans*-3-(2-hydroxypropan-2-yl)cyclobutyl)-1,6-naphthyridine-3-carboxamide **1ak**



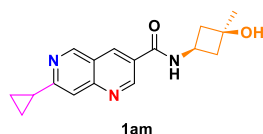
N,N-Diisopropylethylamine (0.122 mL, 0.700 mmol) was added to a stirred solution of 7-cyclopropyl-1,6-naphthyridine-3-carboxylic acid **7l** (75 mg, 0.350 mmol) in *N,N*-dimethylformamide (1.5 mL) at room temperature. Then, 1-[bis(dimethylamino)methylene]-1*H*-1,2,3-triazolo[4,5-*b*]pyridinium 3-oxide hexafluorophosphate (200 mg, 0.525 mmol) was added. After stirring for 15 min, 2-(*trans*-3-aminocyclobutyl)propan-2-ol hydrochloride **8d** (87 mg, 0.525 mmol, AstaTech) was added, followed by the addition of *N,N*-diisopropylethylamine (0.122 mL, 0.700 mmol) and the reaction mixture was stirred for fifteen hours. Then the reaction mixture was concentrated under vacuum to dryness. The resulting residue was triturated with acetonitrile to yield 7-cyclopropyl-*N*-(*trans*-3-(2-hydroxypropan-2-yl)cyclobutyl)-1,6-naphthyridine-3-carboxamide **1ak** (0.050 g, 0.149 mmol, 42.6% yield) as an off white solid. 1H NMR (400 MHz, CD_3SOCD_3) δ 1.05 (s, 6H), 1.00–1.10 (m, 4H), 2.02–2.12 (m, 2H), 2.20–2.38 (m, 4H), 4.27 (s, 1H), 4.37 (sex, $J = 7$ Hz, 1H), 7.86 (s, 1H), 8.92 (d, $J = 2$ Hz, 1H), 9.00 (d, $J = 7$ Hz, 1H), 9.33 (s, 1H), 9.39 (d, $J = 2$ Hz, 1H); LC-MS (LC-ES) $C_{19}H_{23}N_3O_2$ M + H = 326; $t_R = 0.62$ min, 100% purity.

7-Cyclopropyl-*N*-(3-(2-hydroxypropan-2-yl)bicyclo[1.1.1]pentan-1-yl)-1,6-naphthyridine-3-carboxamide **1al**



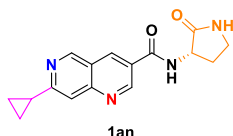
1-[Bis(dimethylamino)methylene]-1*H*-1,2,3-triazolo[4,5-*b*]pyridinium 3-oxide hexafluorophosphate (115 mg, 0.303 mmol) was added to a stirred solution of 7-cyclopropyl-1,6-naphthyridine-3-carboxylic acid **7l** (50 mg, 0.233 mmol) in *N,N*-dimethylformamide (1.0 mL) at room temperature, followed by the addition of *N,N*-diisopropylethylamine (0.122 mL, 0.700 mmol) and the reaction mixture was stirred for 15 min. Then, 2-(3-aminobicyclo[1.1.1]pentan-1-yl)propan-2-ol hydrochloride **8e** (45.6 mg, 0.257 mmol, PharmaBlock) was added and stirring was continued for 18 h. Then, the reaction mixture was concentrated under vacuum to yield 7-cyclopropyl-*N*-(3-(2-hydroxypropan-2-yl)bicyclo[1.1.1]pentan-1-yl)-1,6-naphthyridine-3-carboxamide **1al** (52 mg, 0.146 mmol, 63% yield) as an off white solid. 1H NMR (400 MHz, CD_3SOCD_3) δ 1.04–1.14 (m, 4H), 1.09 (s, 6H), 1.96 (s, 6H), 2.30–2.42 (m, 1H), 4.23 (s, 1H), 7.87 (s, 1H), 8.91 (d, $J = 2$ Hz, 1H), 9.32 (s, 2H), 9.38 (d, $J = 2$ Hz, 1H); LC-MS (LC-ES) $C_{20}H_{23}N_3O_2$ M + H = 338; $t_R = 0.67$ min, 100% purity.

7-Cyclopropyl-*N*-((1*s*,3*s*)-3-hydroxy-3-methylcyclobutyl)-1,6-naphthyridine-3-carboxamide **1am**



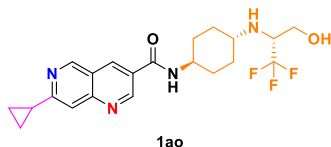
N,N-Diisopropylethylamine (0.122 mL, 0.700 mmol) was added to a stirred solution of 7-cyclopropyl-1,6-naphthyridine-3-carboxylic acid **71** (75 mg, 0.350 mmol) in *N,N*-dimethylformamide (1.5 mL) at room temperature. Then, 1-[bis(dimethylamino)methylene]-1*H*-1,2,3-triazolo[4,5-*b*]pyridinium 3-oxide hexafluorophosphate (200 mg, 0.525 mmol) was added. After stirring for 15 min, (1*S*,3*S*)-3-amino-1-methylcyclobutan-1-ol hydrochloride **8b** (72.3 mg, 0.525 mmol, AstaTech) was added, followed by the addition of *N,N*-diisopropylethylamine (0.122 mL, 0.700 mmol) and the reaction mixture was stirred for fifteen hours. Then, the reaction mixture was concentrated to dryness under vacuum. The resulting residue was triturated with acetonitrile to give 7-cyclopropyl-*N*-((1*S*,3*S*)-3-hydroxy-3-methylcyclobutyl)-1,6-naphthyridine-3-carboxamide **1am** (0.050 g, 0.160 mmol, 45.6% yield) as an off white solid. ¹H NMR (400 MHz, CD₃SOCD₃) δ 1.00–1.12 (m, 4H), 1.28 (s, 3H), 2.12 (dt, *J* = 9, 2 Hz, 2H), 2.26–2.38 (m, 3H), 4.02 (sex, *J* = 8 Hz, 1H), 5.03 (s, 1H), 7.85 (s, 1H), 8.92 (d, *J* = 2 Hz, 1H), 8.98 (d, *J* = 7 Hz, 1H), 9.32 (s, 1H), 9.38 (d, *J* = 2 Hz, 1H); LC-MS (LC-ES) C₁₇H₁₉N₃O₂ M + H = 298; *t*_R = 0.52 min, 100% purity.

(*S*)-7-Cyclopropyl-*N*-(2-oxopyrrolidin-3-yl)-1,6-naphthyridine-3-carboxamide **1an**



1-[Bis(dimethylamino)methylene]-1*H*-1,2,3-triazolo[4,5-*b*]pyridinium 3-oxide hexafluorophosphate (200 mg, 0.525 mmol) was added to a stirred solution of 7-cyclopropyl-1,6-naphthyridine-3-carboxylic acid **71** (75 mg, 0.350 mmol) in *N,N*-dimethylformamide (1.5 mL) at room temperature. Then *N,N*-diisopropylethylamine (0.092 mL, 0.525 mmol) was added. After stirring for 15 min, (*S*)-3-aminopyrrolidin-2-one **8c** (52.6 mg, 0.525 mmol, AstaTech) was added to the reaction mixture, followed by the addition of *N,N*-diisopropylethylamine (0.092 mL, 0.525 mmol) and the reaction mixture was stirred for eight hours. Then, the reaction mixture was concentrated under vacuum. The resulting residue was triturated with acetonitrile to give (*S*)-7-cyclopropyl-*N*-(2-oxopyrrolidin-3-yl)-1,6-naphthyridine-3-carboxamide **1an** (0.075 g, 0.240 mmol, 68.7% yield) as an off white solid. ¹H NMR (400 MHz, CD₃SOCD₃) δ 1.00–1.14 (m, 4H), 2.03 (quin, *J* = 11 Hz, 1H), 2.30–2.44 (m, 2H), 3.20–3.30 (m, 2H), 4.62 (q, *J* = 10 Hz, 1H), 7.87 (s, 1H), 7.94 (s, 1H), 8.93 (d, *J* = 2 Hz, 1H), 9.10 (d, *J* = 8 Hz, 1H), 9.34 (s, 1H), 9.40 (d, *J* = 2 Hz, 1H); LC-MS (LC-ES) C₁₆H₁₆N₄O₂ M + H = 297; *t*_R = 0.44 min, 100% purity.

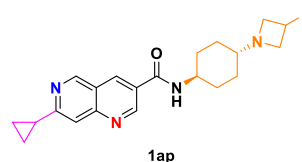
7-Cyclopropyl-*N*-((*trans*-4-(((*R*)-1,1,1-trifluoro-3-hydroxypropan-2-yl)amino)cyclohexyl)-1,6-naphthyridine-3-carboxamide **1ao**



N,N-Diisopropylethylamine (0.092 mL, 0.525 mmol) was added to a stirred solution of 7-cyclopropyl-1,6-naphthyridine-3-carboxylic acid **71** (75 mg, 0.350 mmol) in *N,N*-dimethylformamide (1.5 mL) at room temperature. Then, 1-[bis(dimethylamino)methylene]-1*H*-1,2,3-triazolo[4,5-*b*]pyridinium 3-oxide hexafluorophosphate (200 mg, 0.525 mmol) was added. After stirring for 15 min, (*R*)-2-((*trans*-4-

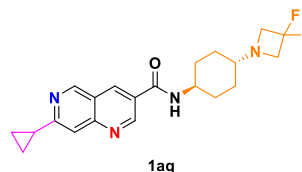
aminocyclohexyl)amino)-3,3,3-trifluoropropan-1-ol⁵¹ **8f** (103 mg, 0.455 mmol) in *N,N*-dimethylformamide (0.5 mL) was added, followed by the addition of *N,N*-diisopropylethylamine (0.092 mL, 0.525 mmol) and the reaction mixture was stirred for eight hours. Then, the reaction mixture was concentrated to dryness under vacuum. The resulting residue was purified via reverse phase chromatography, eluting with acetonitrile:water with 0.1% ammonium hydroxide (0:1 to 1:0) to give 7-cyclopropyl-*N*-((*trans*-4-(((*R*)-1,1,1-trifluoro-3-hydroxypropan-2-yl)amino)cyclohexyl)-1,6-naphthyridine-3-carboxamide **1ao** (0.035 g, 0.079 mmol, 22.5% yield) as an off white solid. ¹H NMR (400 MHz, CD₃SOCD₃) δ 1.02–1.10 (m, 4H), 1.12 (q, *J* = 13 Hz, 2H), 1.36 (q, *J* = 13 Hz, 2H), 1.84–2.00 (m, 4H), 2.30–2.38 (m, 1H), 2.44–2.56 (m, 1H), 3.22–3.34 (m, 2H), 3.44–3.52 (m, 1H), 3.58–3.66 (m, 1H), 3.72–3.84 (m, 1H), 5.01 (t, *J* = 6 Hz, 1H), 7.86 (s, 1H), 8.62 (d, *J* = 8 Hz, 1H), 8.88 (d, *J* = 2 Hz, 1H), 9.33 (s, 1H), 9.37 (d, *J* = 2 Hz, 1H); LC-MS (LC-ES) C₂₁H₂₅F₃N₄O M + H = 423; *t*_R = 0.47 min, 100% purity.

7-Cyclopropyl-*N*-(*trans*-4-(3-fluoroazetidin-1-yl)cyclohexyl)-1,6-naphthyridine-3-carboxamide **1ap**



N,N-Diisopropylethylamine (0.092 mL, 0.525 mmol) was added to 7-cyclopropyl-1,6-naphthyridine-3-carboxylic acid **71** (75 mg, 0.350 mmol) in *N,N*-dimethylformamide (1.5 mL) at room temperature. Then, 1-[bis(dimethylamino)methylene]-1*H*-1,2,3-triazolo[4,5-*b*]pyridinium 3-oxide hexafluorophosphate (200 mg, 0.525 mmol) was added. After stirring for 15 min, *trans*-4-(3-fluoroazetidin-1-yl)cyclohexan-1-amine⁵² **8g** (0.0724 g, 0.420 mmol) was added, followed by the addition of *N,N*-diisopropylethylamine (0.092 mL, 0.525 mmol) and the reaction mixture was stirred for fifteen hours. Then, the reaction mixture was concentrated under vacuum to dryness. The resulting residue was purified via reverse phase chromatography, eluting with acetonitrile:water with 0.1% ammonium hydroxide (0:1 to 1:0) to give 7-cyclopropyl-*N*-(*trans*-4-(3-fluoroazetidin-1-yl)cyclohexyl)-1,6-naphthyridine-3-carboxamide **1ap** (0.070 g, 0.180 mmol, 51.6% yield) as an off white solid. ¹H NMR (400 MHz, CD₃SOCD₃) δ 1.01 (q, *J* = 13 Hz, 2H), 1.02–1.10 (m, 4H), 1.35 (q, *J* = 14 Hz, 2H), 1.77 (br d, *J* = 11 Hz, 2H), 1.88 (br d, *J* = 10 Hz, 2H), 1.96–2.08 (m, 1H), 2.30–2.38 (m, 1H), 2.96–3.10 (m, 2H), 3.46–3.58 (m, 2H), 3.70–3.82 (m, 1H), 5.10 (dquin, *J* = 58, 5 Hz, 1H), 7.86 (s, 1H), 8.63 (d, *J* = 8 Hz, 1H), 8.88 (d, *J* = 2 Hz, 1H), 9.33 (s, 1H), 9.37 (d, *J* = 2 Hz, 1H); LC-MS (LC-ES) C₂₁H₂₅FN₄O M + H = 369; *t*_R = 0.38 min, 98% purity.

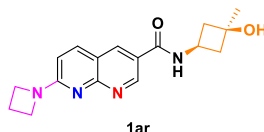
7-Cyclopropyl-*N*-(*trans*-4-(3,3-difluoroazetidin-1-yl)cyclohexyl)-1,6-naphthyridine-3-carboxamide **1aq**



N,N-Diisopropylethylamine (0.092 mL, 0.525 mmol) was added to 7-cyclopropyl-1,6-naphthyridine-3-carboxylic acid **71** (75 mg, 0.350 mmol) in *N,N*-dimethylformamide (1.5 mL) at room temperature. Then, 1-[bis(dimethylamino)methylene]-1*H*-1,2,3-triazolo[4,5-*b*]pyridinium 3-oxide hexafluorophosphate (200 mg, 0.525 mmol) was added. After stirring for 15 min, *trans*-4-(3,3-difluoroazetidin-1-yl)cyclohexan-1-amine⁵³ **8h** (87 mg, 0.455 mmol) was added, followed by the addition of *N,N*-diisopropylethylamine (0.092 mL, 0.525 mmol) and the reaction mixture was stirred for fifteen hours. Then, the reaction mixture was purified via reverse phase chromatography, eluting with acetonitrile:

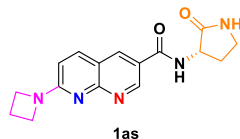
water with 0.1% ammonium hydroxide (0:1 to 1:0) to give 7-cyclopropyl-*N*-(*trans*-4-(3,3-difluoroazetidin-1-yl)cyclohexyl)-1,6-naphthyridine-3-carboxamide **1aq** (0.095 g, 0.234 mmol, 66.7% yield) as an off white solid. ¹H NMR (400 MHz, CD₃SOCD₃) δ 1.00–1.10 (m, 4H), 1.07 (q, *J* = 11 Hz, 2H), 1.36 (q, *J* = 14 Hz, 2H), 1.77 (br d, *J* = 11 Hz, 2H), 1.89 (br d, *J* = 10 Hz, 2H), 2.13 (t, *J* = 11 Hz, 1H), 2.30–2.38 (m, 1H), 3.54 (t, *J* = 12 Hz, 4H), 3.72–3.84 (m, 1H), 7.85 (s, 1H), 8.63 (d, *J* = 8 Hz, 1H), 8.88 (d, *J* = 2 Hz, 1H), 9.33 (s, 1H), 9.37 (d, *J* = 2 Hz, 1H); LC-MS (LC-ES) C₂₁H₂₄F₂N₄O M + H = 387; t_R = 0.39 min, 100% purity.

7-(Azetidin-1-yl)-*N*-((1*s*,3*s*)-3-hydroxy-3-methylcyclobutyl)-1,8-naphthyridine-3-carboxamide **1ar**



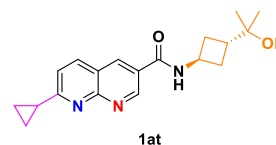
N,N-Diisopropylethylamine (0.321 mL, 1.837 mmol) was added to 7-(azetidin-1-yl)-1,8-naphthyridine-3-carboxylic acid lithium salt **7n** (0.0723 g, 0.306 mmol) in *N,N*-dimethylformamide (1.02 mL) at room temperature. Then, (1*s*,3*s*)-3-amino-1-methylcyclobutanol hydrochloride **8b** (0.059 g, 0.429 mmol, AstaTech) was added and the reaction mixture was stirred for five minutes. Then, *n*-propylphosphonic acid anhydride (0.364 mL, 0.612 mmol) was added and the reaction mixture was stirred for sixty-four hours. The reaction mixture was concentrated. The resulting residue was purified by RP HPLC, eluting with acetonitrile:water with 0.1% ammonium hydroxide (5:95 to 100:0) to give 7-(azetidin-1-yl)-*N*-((1*s*,3*s*)-3-hydroxy-3-methylcyclobutyl)-1,8-naphthyridine-3-carboxamide **1ar** (0.0611 g, 0.186 mmol, 60.7% yield). ¹H NMR (400 MHz, CD₃SOCD₃) δ 1.27 (s, 3H), 2.11 (t, *J* = 8 Hz, 2H), 2.30 (t, *J* = 8 Hz, 2H), 2.39 (p, *J* = 7 Hz, 2H), 3.99 (h, *J* = 8 Hz, 1H), 4.16 (t, *J* = 7 Hz, 4H), 4.96 (br s, 1H), 6.78 (d, *J* = 9 Hz, 1H), 8.07 (d, *J* = 9 Hz, 1H), 8.53 (s, 1H), 8.69 (d, *J* = 5 Hz, 1H), 9.11 (s, 1H); LC-MS (LC-ES) C₁₇H₂₀N₄O₂ M + H = 313; t_R = 0.32 min, 99% purity.

(*S*)-7-(Azetidin-1-yl)-*N*-(2-oxopyrrolidin-3-yl)-1,8-naphthyridine-3-carboxamide **1as**



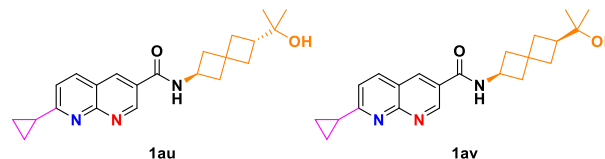
N,N-Diisopropylethylamine (0.299 mL, 1.712 mmol) was added to 7-(azetidin-1-yl)-1,8-naphthyridine-3-carboxylic acid lithium salt **7n** (0.0674 g, 0.285 mmol) in *N,N*-dimethylformamide (0.951 mL) at room temperature. Then, (*S*)-3-aminopyrrolidin-2-one **8c** (0.040 g, 0.400 mmol, AstaTech) was added and the reaction mixture was stirred for five minutes. Then, *n*-propylphosphonic acid anhydride (0.340 mL, 0.571 mmol) was added and the reaction mixture was stirred for sixteen hours. The reaction mixture was concentrated. The resulting residue was purified by RP HPLC, eluting with acetonitrile:water with 0.1% ammonium hydroxide (5:95 to 100:0) to give (*S*)-7-(azetidin-1-yl)-*N*-(2-oxopyrrolidin-3-yl)-1,8-naphthyridine-3-carboxamide **1as** (0.0578 g, 0.176 mmol, 61.8% yield). ¹H NMR (400 MHz, CD₃SOCD₃) δ 2.01 (p, *J* = 11 Hz, 1H), 2.30–2.44 (m, 3H), 3.25 (q, *J* = 9 Hz, 2H), 4.17 (t, *J* = 7 Hz, 4H), 4.59 (q, *J* = 9 Hz, 1H), 6.79 (d, *J* = 9 Hz, 1H), 7.85 (s, 1H), 8.09 (d, *J* = 9 Hz, 1H), 8.55 (s, 1H), 8.79 (d, *J* = 8 Hz, 1H), 9.12 (s, 1H); LC-MS (LC-ES) C₁₆H₁₇N₅O₂ M + H = 312; t_R = 0.27 min, 99% purity.

7-Cyclopropyl-*N*-(*trans*-3-(2-hydroxypropan-2-yl)cyclobutyl)-1,8-naphthyridine-3-carboxamide **1at**



N,N-Diisopropylethylamine (0.280 mL, 1.602 mmol) was added to 7-cyclopropyl-1,8-naphthyridine-3-carboxylic acid **7s** (0.0858 g, 0.401 mmol) in *N,N*-dimethylformamide (1.3 mL) at room temperature. Then, 2-(*trans*-3-aminocyclobutyl)propan-2-ol hydrochloride **8d** (0.066 g, 0.401 mmol, AstaTech) was added and the reaction mixture was stirred for five minutes. Then, *n*-propylphosphonic acid anhydride (0.477 mL, 0.801 mmol) was added and the reaction mixture was stirred for sixteen hours. The reaction mixture was concentrated. The resulting residue was purified by RP HPLC, eluting with acetonitrile:water with 0.1% ammonium hydroxide (5:95 to 100:0), then further purified by silica gel chromatography, eluting with methanol:ethyl acetate (0:1 to 3:2) to give 7-cyclopropyl-*N*-(*trans*-3-(2-hydroxypropan-2-yl)cyclobutyl)-1,8-naphthyridine-3-carboxamide **1at** (0.0630 g, 0.184 mmol, 45.9% yield). ¹H NMR (400 MHz, CD₃SOCD₃) δ 1.05 (s, 6H), 1.08–1.20 (m, 4H), 2.02–2.12 (m, 2H), 2.18–2.42 (m, 4H), 4.26 (s, 1H), 4.37 (h, *J* = 7 Hz, 1H), 7.64 (d, *J* = 8 Hz, 1H), 8.39 (d, *J* = 8 Hz, 1H), 8.81 (d, *J* = 2 Hz, 1H), 8.96 (d, *J* = 7 Hz, 1H), 9.34 (d, *J* = 2 Hz, 1H); LC-MS (LC-ES) C₁₉H₂₃N₃O₂ M + H = 326; t_R = 0.57 min, 93% purity.

(*S*)-7-cyclopropyl-*N*-(6-(2-hydroxypropan-2-yl)spiro[3.3]heptan-2-yl)-1,8-naphthyridine-3-carboxamide **1au** and (*R*)-7-cyclopropyl-*N*-(6-(2-hydroxypropan-2-yl)spiro[3.3]heptan-2-yl)-1,8-naphthyridine-3-carboxamide **1av**



N,N-Diisopropylethylamine (0.255 mL, 1.460 mmol) was added to 7-cyclopropyl-1,8-naphthyridine-3-carboxylic acid **7s** (0.0782 g, 0.365 mmol) in *N,N*-dimethylformamide (1.2 mL) at room temperature. Then, racemic 2-(6-aminospiro[3.3]heptan-2-yl)propan-2-ol⁴³ **8i** (0.062 g, 0.365 mmol) was added and the reaction mixture was stirred for five minutes. Then, *n*-propylphosphonic acid anhydride (0.435 mL, 0.730 mmol) was added and the reaction mixture was stirred for sixteen hours. The reaction mixture was concentrated. The resulting residue was purified by RP HPLC, eluting with acetonitrile:water with 0.1% ammonium hydroxide (5:95 to 100:0), then further purified by silica gel chromatography, eluting with methanol:ethyl acetate (0:1 to 1:4) to give racemic 7-cyclopropyl-*N*-(6-(2-hydroxypropan-2-yl)spiro[3.3]heptan-2-yl)-1,8-naphthyridine-3-carboxamide (0.0886 g, 0.230 mmol, 63.1% yield). Racemic 7-cyclopropyl-*N*-(6-(2-hydroxypropan-2-yl)spiro[3.3]heptan-2-yl)-1,8-naphthyridine-3-carboxamide (0.0750 g, 0.205 mmol) was separated into its enantiomers on a chiral IG column, eluting with ethanol:heptane (2:3) with 0.1% isopropylamine to give (*S*)-7-cyclopropyl-*N*-(6-(2-hydroxypropan-2-yl)spiro[3.3]heptan-2-yl)-1,8-naphthyridine-3-carboxamide **1au** (0.0302 g, 0.079 mmol, 38.3% yield) as the first enantiomer to elute and (*R*)-7-cyclopropyl-*N*-(6-(2-hydroxypropan-2-yl)spiro[3.3]heptan-2-yl)-1,8-naphthyridine-3-carboxamide **1av** (0.0294 g, 0.076 mmol, 37.2% yield) as the last enantiomer to elute. The structures were assigned by vibrational circular dichroism.

(*S*)-7-cyclopropyl-*N*-(6-(2-hydroxypropan-2-yl)spiro[3.3]heptan-2-yl)-1,8-naphthyridine-3-carboxamide **1au**

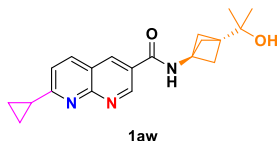
¹H NMR (400 MHz, CD₃SOCD₃) δ 0.94 (s, 3H), 0.95 (s, 3H), 1.10–1.20 (m, 4H), 1.66–1.76 (m, 1H), 1.86–2.02 (m, 4H), 2.06–2.22 (m, 3H), 2.30–2.46 (m, 2H), 4.01 (s, 1H), 4.33 (h, *J* = 8 Hz, 1H), 7.64 (d, *J* = 9 Hz, 1H), 8.38 (d, *J* = 8 Hz, 1H), 8.78 (d, *J* = 2 Hz, 1H), 8.90 (d, *J* = 8 Hz, 1H), 9.31 (d, *J* = 2 Hz, 1H); LC-MS (LC-ES) C₂₂H₂₇N₃O₂ M + H =

366; t_R = 5.8 min, 99.5% ee.

(R)-7-cyclopropyl-*N*-(6-(2-hydroxypropan-2-yl)spiro[3.3]heptan-2-yl)-1,8-naphthyridine-3-carboxamide **1av**

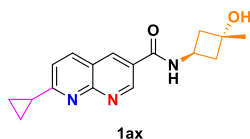
^1H NMR (400 MHz, CD_3SOCD_3) δ 0.94 (s, 3H), 0.95 (s, 3H), 1.10–1.20 (m, 4H), 1.66–1.76 (m, 1H), 1.86–2.02 (m, 4H), 2.06–2.22 (m, 3H), 2.30–2.46 (m, 2H), 4.01 (s, 1H), 4.33 (h, J = 8 Hz, 1H), 7.64 (d, J = 9 Hz, 1H), 8.38 (d, J = 8 Hz, 1H), 8.78 (d, J = 2 Hz, 1H), 8.90 (d, J = 8 Hz, 1H), 9.31 (d, J = 2 Hz, 1H); LC-MS (LC-ES) $\text{C}_{22}\text{H}_{27}\text{N}_3\text{O}_2$ $M + H$ = 366; t_R = 8.6 min, 99.5% ee.

7-Cyclopropyl-*N*-(3-(2-hydroxypropan-2-yl)bicyclo[1.1.1]pentan-1-yl)-1,8-naphthyridine-3-carboxamide **1aw**



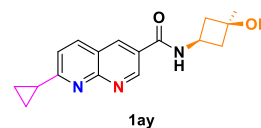
1-[Bis(dimethylamino)methylene]-1*H*-1,2,3-triazolo[4,5-*b*]pyridinium 3-oxide hexafluorophosphate (115 mg, 0.303 mmol) was added to a stirred solution of 7-cyclopropyl-1,8-naphthyridine-3-carboxylic acid **7s** (50 mg, 0.233 mmol) in *N,N*-dimethylformamide (1.0 mL), followed by the addition of *N,N*-diisopropylethylamine (0.163 mL, 0.934 mmol) at room temperature. The reaction mixture was stirred for 15 min and then 2-(3-aminobicyclo[1.1.1]pentan-1-yl)propan-2-ol hydrochloride **8e** (45.6 mg, 0.257 mmol, PharmaBlock) was added and stirring was continued for 18 h. Then the reaction mixture was concentrated under vacuum to yield a crude mixture. This residue was purified by reverse phase HPLC, eluting with acetonitrile:water (0:1 to 1:0) with 0.1% ammonium hydroxide to give 7-Cyclopropyl-*N*-(3-(2-hydroxypropan-2-yl)bicyclo[1.1.1]pentan-1-yl)-1,8-naphthyridine-3-carboxamide **1aw** (0.057 g, 0.160 mmol, 69% yield) as an off white solid. ^1H NMR (400 MHz, CD_3SOCD_3) δ 1.09 (s, 6H), 1.12–1.22 (m, 4H), 1.95 (s, 6H), 2.30–2.44 (m, 1H), 4.24 (s, 1H), 7.65 (d, J = 8 Hz, 1H), 8.38 (d, J = 8 Hz, 1H), 8.80 (d, J = 2 Hz, 1H), 9.29 (s, 1H), 9.32 (d, J = 2 Hz, 1H); LC-MS (LC-ES) $\text{C}_{20}\text{H}_{23}\text{N}_3\text{O}_2$ $M + H$ = 338; t_R = 0.61 min, 96% purity.

7-Cyclopropyl-*N*-((1*r*,3*r*)-3-hydroxy-3-methylcyclobutyl)-1,8-naphthyridine-3-carboxamide **1ax**



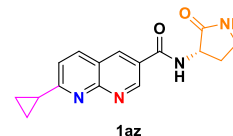
N,N-Diisopropylethylamine (0.288 mL, 1.647 mmol) was added to 7-cyclopropyl-1,8-naphthyridine-3-carboxylic acid **7s** (0.0882 g, 0.412 mmol) in *N,N*-dimethylformamide (1.4 mL) at room temperature. Then, (1*r*,3*r*)-3-amino-1-methylcyclobutan-1-ol **8j** (0.042 g, 0.412 mmol, AstaTech) was added and the reaction mixture was stirred for five minutes. Then, *n*-propylphosphonic acid anhydride (0.490 mL, 0.823 mmol) was added and the reaction mixture was stirred for sixteen hours. The reaction mixture was concentrated. The resulting residue was purified by RP HPLC, eluting with acetonitrile:water with 0.1% ammonium hydroxide (5:95 to 100:0), then further purified by silica gel chromatography, eluting with methanol:ethyl acetate (0:1 to 2:3) to give 7-cyclopropyl-*N*-((1*r*,3*r*)-3-hydroxy-3-methylcyclobutyl)-1,8-naphthyridine-3-carboxamide **1ax** (0.0986 g, 0.315 mmol, 77% yield). ^1H NMR (400 MHz, CD_3SOCD_3) δ 1.10–1.20 (m, 4H), 1.29 (s, 3H), 2.04–2.14 (m, 2H), 2.26–2.42 (m, 3H), 4.54 (h, J = 8 Hz, 1H), 4.89 (s, 1H), 7.64 (d, J = 8 Hz, 1H), 8.39 (d, J = 8 Hz, 1H), 8.78 (d, J = 2 Hz, 1H), 8.91 (d, J = 7 Hz, 1H), 9.32 (d, J = 2 Hz, 1H); LC-MS (LC-ES) $\text{C}_{17}\text{H}_{19}\text{N}_3\text{O}_2$ $M + H$ = 298; t_R = 0.44 min, 95% purity.

7-Cyclopropyl-*N*-((1*s*,3*s*)-3-hydroxy-3-methylcyclobutyl)-1,8-naphthyridine-3-carboxamide **1ay**



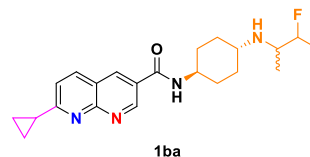
N,N-Diisopropylethylamine (0.249 mL, 1.428 mmol) was added to 7-cyclopropyl-1,8-naphthyridine-3-carboxylic acid **7s** (0.0765 g, 0.357 mmol) in *N,N*-dimethylformamide (1.2 mL) at room temperature. Then, (1*s*,3*s*)-3-amino-1-methylcyclobutan-1-ol **8b** (0.036 g, 0.357 mmol, AstaTech) was added and the reaction mixture was stirred for five minutes. Then, *n*-propylphosphonic acid anhydride (0.425 mL, 0.714 mmol) was added and the reaction mixture was stirred for sixty-six hours. The reaction mixture was concentrated. The resulting residue was purified by RP HPLC, eluting with acetonitrile:water with 0.1% ammonium hydroxide (5:95 to 100:0), then further purified by silica gel chromatography, eluting with methanol:ethyl acetate (0:1 to 2:3) to give 7-cyclopropyl-*N*-((1*s*,3*s*)-3-hydroxy-3-methylcyclobutyl)-1,8-naphthyridine-3-carboxamide **1ay** (0.0710 g, 0.227 mmol, 63.5% yield). ^1H NMR (400 MHz, CD_3SOCD_3) δ 1.08–1.20 (m, 4H), 1.28 (s, 3H), 2.13 (t, J = 8 Hz, 2H), 2.28–2.42 (m, 3H), 4.02 (h, J = 8 Hz, 1H), 5.02 (s, 1H), 7.64 (d, J = 8 Hz, 1H), 8.38 (d, J = 8 Hz, 1H), 8.81 (d, J = 2 Hz, 1H), 8.95 (d, J = 7 Hz, 1H), 9.33 (d, J = 2 Hz, 1H); LC-MS (LC-ES) $\text{C}_{17}\text{H}_{19}\text{N}_3\text{O}_2$ $M + H$ = 298; t_R = 0.44 min, 96% purity.

(*S*)-7-Cyclopropyl-*N*-(2-oxopyrrolidin-3-yl)-1,8-naphthyridine-3-carboxamide **1az**



N,N-Diisopropylethylamine (0.265 mL, 1.520 mmol) was added to 7-cyclopropyl-1,8-naphthyridine-3-carboxylic acid **7s** (0.0814 g, 0.380 mmol) in *N,N*-dimethylformamide (1.3 mL) at room temperature. Then, (*S*)-3-aminopyrrolidin-2-one **8c** (0.038 g, 0.380 mmol, AstaTech) was added and the reaction mixture was stirred for five minutes. Then, *n*-propylphosphonic acid anhydride (0.452 mL, 0.760 mmol) was added and the reaction mixture was stirred for sixteen hours. The reaction mixture was concentrated. The resulting residue was purified by RP HPLC, eluting with acetonitrile:water with 0.1% ammonium hydroxide (5:95 to 100:0), then further purified by silica gel chromatography, eluting with methanol:ethyl acetate (0:1 to 3:2) to give (*S*)-7-cyclopropyl-*N*-(2-oxopyrrolidin-3-yl)-1,8-naphthyridine-3-carboxamide **1az** (0.0510 g, 0.164 mmol, 43.0% yield). ^1H NMR (400 MHz, CD_3SOCD_3) δ 1.10–1.22 (m, 4H), 1.96–2.10 (m, 1H), 2.32–2.44 (m, 2H), 3.20–3.30 (m, 2H), 4.62 (q, J = 9 Hz, 1H), 7.66 (d, J = 8 Hz, 1H), 7.93 (s, 1H), 8.41 (d, J = 8 Hz, 1H), 8.83 (d, J = 2 Hz, 1H), 9.06 (d, J = 8 Hz, 1H), 9.35 (d, J = 2 Hz, 1H); LC-MS (LC-ES) $\text{C}_{16}\text{H}_{16}\text{N}_4\text{O}_2$ $M + H$ = 297; t_R = 0.37 min, 95% purity.

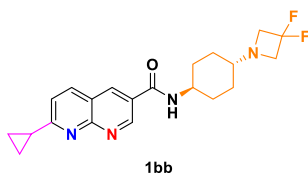
Racemic 7-Cyclopropyl-*N*-(*trans*-4-((1,1-difluoropropan-2-yl)amino)cyclohexyl)-1,8-naphthyridine-3-carboxamide **1ba**



N,N-Diisopropylethylamine (0.384 mL, 2.201 mmol) was added to 7-cyclopropyl-1,8-naphthyridine-3-carboxylic acid **7s** (0.1179 g, 0.550 mmol) in *N,N*-dimethylformamide (1.8 mL) at room temperature. Then, *trans*-*N*1-(1,1-difluoropropan-2-yl)cyclohexane-1,4-diamine⁵² **8k** (0.106 g, 0.550 mmol) was added and the reaction mixture was stirred for five minutes. Then, *n*-propylphosphonic acid anhydride (0.655 mL,

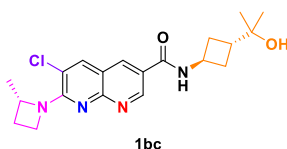
1.101 mmol) was added and the reaction mixture was stirred for sixty-six hours. The reaction mixture was concentrated. The resulting residue was purified by RP HPLC, eluting with acetonitrile:water with 0.1% ammonium hydroxide (5:95 to 100:0), then further purified by silica gel chromatography, eluting with methanol:ethyl acetate (0:1 to 3:2), then further purified by silica gel chromatography, eluting with methanol:dichloromethane (0:1 to 2:3) to give racemic 7-cyclopropyl-*N*-(*trans*-4-((1,1-difluoropropan-2-yl)amino)cyclohexyl)-1,8-naphthyridine-3-carboxamide **1ba** (0.0523 g, 0.128 mmol, 23.24% yield). ¹H NMR (400 MHz, CD₃SOCD₃) δ 1.02 (d, *J* = 6 Hz, 3H), 1.06–1.20 (m, 6H), 1.30–1.46 (m, 2H), 1.82–2.00 (m, 4H), 2.30–2.40 (m, 1H), 2.42–2.50 (m, 1H), 2.90–3.08 (m, 1H), 3.68–3.84 (m, 1H), 5.77 (dt, *J* = 57, 4 Hz, 1H), 7.63 (d, *J* = 8 Hz, 1H), 8.39 (d, *J* = 8 Hz, 1H), 8.58 (d, *J* = 8 Hz, 1H), 8.78 (d, *J* = 2 Hz, 1H), 9.31 (d, *J* = 2 Hz, 1H); LC-MS (LC-ES) C₂₁H₂₆N₄O M + H = 389; t_R = 0.41 min, 100% purity.

7-Cyclopropyl-*N*-(*trans*-4-(3,3-difluoroazetidin-1-yl)cyclohexyl)-1,8-naphthyridine-3-carboxamide **1bb**



N,N-Diisopropylethylamine (0.239 mL, 1.369 mmol) was added to 7-cyclopropyl-1,8-naphthyridine-3-carboxylic acid **7s** (0.0733 g, 0.342 mmol) in *N,N*-dimethylformamide (1.1 mL) at room temperature. Then, *trans*-4-(3,3-difluoroazetidin-1-yl)cyclohexan-1-amine⁵³ **8h** (0.065 g, 0.342 mmol) was added and the reaction mixture was stirred for five minutes. Then, *n*-propylphosphonic acid anhydride (0.407 mL, 0.684 mmol) was added and the reaction mixture was stirred for sixteen hours. The reaction mixture was concentrated. The resulting residue was purified by RP HPLC, eluting with acetonitrile:water with 0.1% ammonium hydroxide (5:95 to 100:0), then further purified by silica gel chromatography, eluting with methanol:ethyl acetate (0:1 to 2:3) to give 7-cyclopropyl-*N*-(*trans*-4-(3,3-difluoroazetidin-1-yl)cyclohexyl)-1,8-naphthyridine-3-carboxamide **1bb** (0.0596 g, 0.147 mmol, 42.8% yield). ¹H NMR (400 MHz, CD₃SOCD₃) δ 1.07 (q, *J* = 14 Hz, 2H), 1.08–1.20 (m, 4H), 1.36 (q, *J* = 14 Hz, 2H), 1.77 (br d, *J* = 12 Hz, 2H), 1.88 (br d, *J* = 11 Hz, 2H), 2.06–2.18 (m, 1H), 2.28–2.42 (m, 1H), 3.54 (t, *J* = 12 Hz, 4H), 3.72–3.84 (m, 1H), 7.63 (d, *J* = 8 Hz, 1H), 8.39 (d, *J* = 8 Hz, 1H), 8.59 (d, *J* = 8 Hz, 1H), 8.78 (d, *J* = 2 Hz, 1H), 9.32 (d, *J* = 2 Hz, 1H); LC-MS (LC-ES) C₂₁H₂₄F₂N₄O M + H = 387, t_R = 0.41 min, 98% purity.

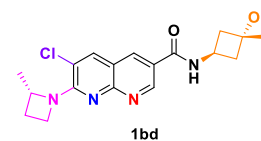
6-Chloro-*N*-(*trans*-3-(2-hydroxypropan-2-yl)cyclobutyl)-7-((*S*)-2-methylazetidin-1-yl)-1,8-naphthyridine-3-carboxamide **1bc**



N,N-Diisopropylethylamine (0.152 mL, 0.872 mmol) was added to lithium (S)-6-chloro-7-(2-methylazetidin-1-yl)-1,8-naphthyridine-3-carboxylate **7x** (0.0618 g, 0.218 mmol) in *N,N*-dimethylformamide (0.73 mL) at room temperature. Then, 2-(*trans*-3-aminocyclobutyl)propan-2-ol hydrochloride **8d** (0.043 g, 0.261 mmol, AstaTech) was added and the reaction mixture was stirred for five minutes. Then, *n*-propylphosphonic acid anhydride (0.259 mL, 0.436 mmol) was added and the reaction mixture was stirred for sixteen hours. The reaction mixture was concentrated. The resulting residue was purified by RP HPLC, eluting with acetonitrile:water with 0.1% ammonium hydroxide (5:95 to 100:0), then further purified by silica gel chromatography, eluting with methanol:ethyl acetate (0:1 to 2:3) to give 6-chloro-*N*-(*trans*-3-(2-hydroxypropan-2-yl)cyclobutyl)-7-((*S*)-2-methylazetidin-1-

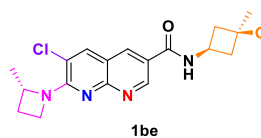
yl)-1,8-naphthyridine-3-carboxamide **1bc** (0.0627 g, 0.153 mmol, 70.3% yield). ¹H NMR (400 MHz, CD₃SOCD₃) δ 1.04 (s, 6H), 1.48 (d, *J* = 6 Hz, 3H), 1.90–2.10 (m, 3H), 2.18–2.34 (m, 3H), 2.42–2.54 (m, 1H), 4.24 (s, 1H), 4.24 (dt, *J* = 9, 7 Hz, 1H), 4.34 (h, *J* = 7 Hz, 1H), 4.53 (dt, *J* = 9, 6 Hz, 1H), 4.79 (h, *J* = 8 Hz, 1H), 8.33 (s, 1H), 8.56 (d, *J* = 2 Hz, 1H), 8.83 (d, *J* = 7 Hz, 1H), 9.17 (d, *J* = 2 Hz, 1H); LC-MS (LC-ES) C₂₀H₂₅ClN₄O₂ M + H = 389; t_R = 0.64 min, 98% purity.

6-Chloro-*N*-(1*r*,3*S*)-3-hydroxy-3-methylcyclobutyl)-7-((*S*)-2-methylazetidin-1-yl)-1,8-naphthyridine-3-carboxamide **1bd**



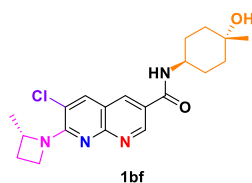
N,N-Diisopropylethylamine (0.165 mL, 0.942 mmol) was added to lithium (S)-6-chloro-7-(2-methylazetidin-1-yl)-1,8-naphthyridine-3-carboxylate **7x** (0.0668 g, 0.236 mmol) in *N,N*-dimethylformamide (0.78 mL) at room temperature. Then, (1*r*,3*r*)-3-amino-1-methylcyclobutan-1-ol **8j** (0.029 g, 0.283 mmol, AstaTech) was added and the reaction mixture was stirred for five minutes. Then, *n*-propylphosphonic acid anhydride (0.280 mL, 0.471 mmol) was added and the reaction mixture was stirred for sixteen hours. The reaction mixture was concentrated. The resulting residue was purified by RP HPLC, eluting with acetonitrile:water with 0.1% ammonium hydroxide (5:95 to 100:0), then further purified by silica gel chromatography, eluting with methanol:ethyl acetate (0:1 to 1:4) to give 6-chloro-*N*-(1*r*,3*S*)-3-hydroxy-3-methylcyclobutyl)-7-((*S*)-2-methylazetidin-1-yl)-1,8-naphthyridine-3-carboxamide **1bd** (0.0712 g, 0.187 mmol, 80% yield). ¹H NMR (400 MHz, CD₃SOCD₃) δ 1.28 (s, 3H), 1.48 (d, *J* = 6 Hz, 3H), 1.92–2.02 (m, 1H), 2.04–2.12 (m, 2H), 2.24–2.34 (m, 2H), 2.42–2.54 (m, 1H), 4.24 (dt, *J* = 9, 7 Hz, 1H), 4.46–4.58 (m, 2H), 4.79 (h, *J* = 8 Hz, 1H), 4.87 (s, 1H), 8.32 (s, 1H), 8.53 (d, *J* = 2 Hz, 1H), 8.78 (d, *J* = 7 Hz, 1H), 9.14 (d, *J* = 2 Hz, 1H); LC-MS (LC-ES) C₁₈H₂₁ClN₄O₂ M + H = 361; t_R = 0.56 min, 100% purity.

6-Chloro-*N*-(1*s*,3*R*)-3-hydroxy-3-methylcyclobutyl)-7-((*S*)-2-methylazetidin-1-yl)-1,8-naphthyridine-3-carboxamide **1be**



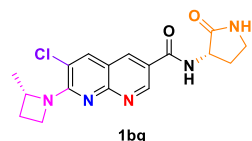
N,N-Diisopropylethylamine (0.150 mL, 0.859 mmol) was added to lithium (S)-6-chloro-7-(2-methylazetidin-1-yl)-1,8-naphthyridine-3-carboxylate **7x** (0.0609 g, 0.215 mmol) in *N,N*-dimethylformamide (0.72 mL) at room temperature. Then, (1*s*,3*s*)-3-amino-1-methylcyclobutan-1-ol **8b** (0.026 g, 0.258 mmol, AstaTech) was added and the reaction mixture was stirred for five minutes. Then, *n*-propylphosphonic acid anhydride (0.256 mL, 0.429 mmol) was added and the reaction mixture was stirred for sixteen hours. The reaction mixture was concentrated. The resulting residue was purified by RP HPLC, eluting with acetonitrile:water with 0.1% ammonium hydroxide (5:95 to 100:0), then further purified by silica gel chromatography, eluting with methanol:ethyl acetate (0:1 to 2:3) to give 6-chloro-*N*-(1*s*,3*R*)-3-hydroxy-3-methylcyclobutyl)-7-((*S*)-2-methylazetidin-1-yl)-1,8-naphthyridine-3-carboxamide **1be** (0.0686 g, 0.181 mmol, 84% yield). ¹H NMR (400 MHz, CD₃SOCD₃) δ 1.27 (s, 3H), 1.48 (d, *J* = 6 Hz, 3H), 1.90–2.02 (m, 1H), 2.06–2.16 (m, 2H), 2.26–2.34 (m, 2H), 2.42–2.54 (m, 1H), 4.00 (h, *J* = 7 Hz, 1H), 4.24 (dt, *J* = 9, 7 Hz, 1H), 4.53 (dt, *J* = 9, 6 Hz, 1H), 4.78 (h, *J* = 8 Hz, 1H), 5.00 (s, 1H), 8.32 (s, 1H), 8.55 (d, *J* = 2 Hz, 1H), 8.81 (d, *J* = 7 Hz, 1H), 9.16 (d, *J* = 2 Hz, 1H); LC-MS (LC-ES) C₁₈H₂₁ClN₄O₂ M + H = 361; t_R = 0.56 min, 100% purity.

6-Chloro-*N*-(1*r*,4*S*)-4-hydroxy-4-methylcyclohexyl)-7-((*S*)-2-methylazetidin-1-yl)-1,8-naphthyridine-3-carboxamide **1bf**



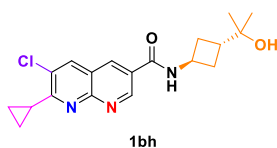
N,N-Diisopropylethylamine (0.158 mL, 0.907 mmol) was added to lithium (S)-6-chloro-7-(2-methylazetidin-1-yl)-1,8-naphthyridine-3-carboxylate **7x** (0.0643 g, 0.227 mmol) in *N,N*-dimethylformamide (0.76 mL) at room temperature. Then, (1*r*,4*r*)-4-amino-1-methylcyclohexan-1-ol **8l** (0.044 g, 0.340 mmol, AstaTech) was added and the reaction mixture was stirred for five minutes. Then, *n*-propylphosphonic acid anhydride (0.270 mL, 0.453 mmol) was added and the reaction mixture was stirred for sixteen hours. The reaction mixture was concentrated. The resulting residue was purified by RP HPLC, eluting with acetonitrile:water with 0.1% ammonium hydroxide (5:95 to 100:0), then further purified by silica gel chromatography, eluting with methanol:ethyl acetate (0:1 to 3:7) to give 6-chloro-*N*-((1*r*,4*S*)-4-hydroxy-4-methylcyclohexyl)-7-((*S*)-2-methylazetidin-1-yl)-1,8-naphthyridine-3-carboxamide **1bf** (0.0712 g, 0.174 mmol, 77% yield). ¹H NMR (400 MHz, CD₃SOCD₃) δ 1.15 (s, 3H), 1.48 (d, *J* = 6 Hz, 3H), 1.38–1.54 (m, 4H), 1.54–1.62 (m, 2H), 1.72–1.82 (m, 2H), 1.90–2.02 (m, 1H), 2.42–2.54 (m, 1H), 3.76–3.88 (m, 1H), 4.24 (dt, *J* = 9, 7 Hz, 1H), 4.31 (s, 1H), 4.53 (dt, *J* = 9, 6 Hz, 1H), 4.79 (h, *J* = 8 Hz, 1H), 8.33 (s, 1H), 8.39 (d, *J* = 8 Hz, 1H), 8.53 (d, *J* = 2 Hz, 1H), 9.13 (d, *J* = 2 Hz, 1H); LC-MS (LC-ES) C₂₀H₂₅ClN₄O₂ M + H = 389; *t*_R = 0.60 min, 100% purity.

6-Chloro-7-((*S*)-2-methylazetidin-1-yl)-*N*-((*S*)-2-oxopyrrolidin-3-yl)-1,8-naphthyridine-3-carboxamide **1bg**



N,N-Diisopropylethylamine (0.166 mL, 0.951 mmol) was added to lithium (S)-6-chloro-7-(2-methylazetidin-1-yl)-1,8-naphthyridine-3-carboxylate **7x** (0.0674 g, 0.238 mmol) in *N,N*-dimethylformamide (0.79 mL) at room temperature. Then, (S)-3-aminopyrrolidin-2-one **8c** (0.029 g, 0.285 mmol, AstaTech) was added and the reaction mixture was stirred for five minutes. Then, *n*-propylphosphonic acid anhydride (0.283 mL, 0.475 mmol) was added and the reaction mixture was stirred for sixteen hours. The reaction mixture was concentrated. The resulting residue was purified by RP HPLC, eluting with acetonitrile:water with 0.1% ammonium hydroxide (5:95 to 100:0), then further purified by silica gel chromatography, eluting with methanol:ethyl acetate (0:1 to 3:2) to give 6-chloro-7-((*S*)-2-methylazetidin-1-yl)-*N*-((*S*)-2-oxopyrrolidin-3-yl)-1,8-naphthyridine-3-carboxamide **1bg** (0.0604 g, 0.159 mmol, 67.1% yield). ¹H NMR (400 MHz, CD₃SOCD₃) δ 1.49 (d, *J* = 6 Hz, 3H), 1.92–2.08 (m, 2H), 2.30–2.42 (m, 1H), 2.42–2.54 (m, 1H), 3.18–3.28 (m, 2H), 4.26 (dt, *J* = 9, 7 Hz, 1H), 4.54 (dt, *J* = 9, 6 Hz, 1H), 4.60 (dt, *J* = 9, 8 Hz, 1H), 4.79 (h, *J* = 8 Hz, 1H), 7.91 (br s, 1H), 8.36 (s, 1H), 8.58 (d, *J* = 2 Hz, 1H), 8.93 (d, *J* = 8 Hz, 1H), 9.17 (d, *J* = 2 Hz, 1H); LC-MS (LC-ES) C₁₇H₁₈ClN₅O₂ M + H = 360; *t*_R = 0.50 min, 100% purity.

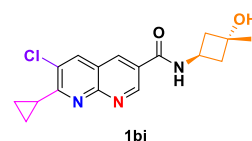
6-Chloro-7-cyclopropyl-*N*-(*trans*-3-(2-hydroxypropan-2-yl)cyclobutyl)-1,8-naphthyridine-3-carboxamide **1bh**



2-(*trans*-3-Aminocyclobutyl)propan-2-ol hydrochloride **8d** (0.037 g, 0.223 mmol, AstaTech) was added to 6-chloro-7-cyclopropyl-1,8-naph-

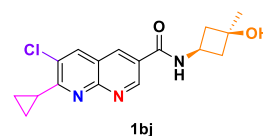
thyridine-3-carboxylic acid **7y** (0.053 g, 0.213 mmol) in *N,N*-dimethylformamide (2.5 mL). Then, *N,N*-diisopropylethylamine (0.10 mL, 0.574 mmol) was added, followed by 1-[bis(dimethylamino)methylene]-1*H*-1,2,3-triazolo[4,5-*b*]pyridinium 3-oxide hexafluorophosphate (0.099 g, 0.260 mmol) and the reaction mixture was stirred for 2.5 h and concentrated. Dichloromethane and methanol were added to the residue and it was purified via silica gel chromatography, eluting with (3:1 ethyl acetate: ethanol):hexanes (0:1 to 3:2) to give a material which was dissolved in ethyl acetate. Once crystals formed, the mixture was partially concentrated via a stream of nitrogen and the solids collected by filtration, air-dried, then dried under vacuum overnight to give 6-chloro-7-cyclopropyl-*N*-(*trans*-3-(2-hydroxypropan-2-yl)cyclobutyl)-1,8-naphthyridine-3-carboxamide **1bh** (0.049 g, 0.136 mmol, 63.9% yield) as a pale yellow solid. ¹H NMR (400 MHz, CD₃SOCD₃) δ 1.04 (s, 6H), 1.20–1.26 (m, 4H), 2.00–2.12 (m, 2H), 2.20–2.36 (m, 3H), 2.68–2.78 (m, 1H), 4.26 (s, 1H), 4.36 (sex, *J* = 7 Hz, 1H), 8.68 (s, 1H), 8.79 (d, *J* = 2 Hz, 1H), 9.02 (d, *J* = 7 Hz, 1H), 9.36 (d, *J* = 2 Hz, 1H); LC-MS (LC-ES) C₁₉H₂₂ClN₃O₂ M + H = 360; *t*_R = 0.82 min, 99% purity.

6-Chloro-7-cyclopropyl-*N*-((1*r*,3*r*)-3-hydroxy-3-methylcyclobutyl)-1,8-naphthyridine-3-carboxamide **1bi**



(1*r*,3*r*)-3-Amino-1-methylcyclobutan-1-ol **8j** (0.029 g, 0.287 mmol, AstaTech) was added to 6-chloro-7-cyclopropyl-1,8-naphthyridine-3-carboxylic acid **7y** (0.055 g, 0.221 mmol) in *N,N*-dimethylformamide (2.5 mL). Then, *N,N*-diisopropylethylamine (0.05 mL, 0.287 mmol) was added, followed by 1-[bis(dimethylamino)methylene]-1*H*-1,2,3-triazolo[4,5-*b*]pyridinium 3-oxide hexafluorophosphate (0.105 g, 0.276 mmol) and the reaction mixture was stirred for 145 min and concentrated. Dichloromethane and methanol were added to the residue and it was purified via silica gel chromatography, eluting with (3:1 ethyl acetate: ethanol):hexanes (0:1 to 7:3) to give a material which was dissolved in ethyl acetate. Once crystals formed, the mixture was partially concentrated via a stream of nitrogen and the solids collected by filtration, air-dried, then dried under vacuum overnight to give 6-chloro-7-cyclopropyl-*N*-((1*r*,3*r*)-3-hydroxy-3-methylcyclobutyl)-1,8-naphthyridine-3-carboxamide **1bi** (0.040 g, 0.121 mmol, 54.5% yield) as an off-white powder. ¹H NMR (400 MHz, CD₃SOCD₃) δ 1.20–1.26 (m, 4H), 1.29 (s, 3H), 2.04–2.14 (m, 2H), 2.26–2.34 (m, 2H), 2.68–2.78 (m, 1H), 4.53 (sex, *J* = 8 Hz, 1H), 4.90 (s, 1H), 8.68 (s, 1H), 8.77 (d, *J* = 2 Hz, 1H), 8.97 (d, *J* = 7 Hz, 1H), 9.34 (d, *J* = 2 Hz, 1H); LC-MS (LC-ES) C₁₇H₁₈ClN₃O₂ M + H = 332; *t*_R = 0.73 min, 100% purity.

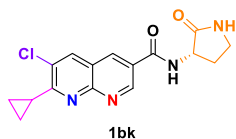
6-Chloro-7-cyclopropyl-*N*-((1*s*,3*s*)-3-hydroxy-3-methylcyclobutyl)-1,8-naphthyridine-3-carboxamide **1bj**



(1*s*,3*s*)-3-Amino-1-methylcyclobutan-1-ol **8b** (0.027 g, 0.267 mmol, AstaTech) was added to 6-chloro-7-cyclopropyl-1,8-naphthyridine-3-carboxylic acid **7y** (0.053 g, 0.213 mmol) in *N,N*-dimethylformamide (2.5 mL). Then, *N,N*-diisopropylethylamine (0.05 mL, 0.287 mmol) was added, followed by 1-[bis(dimethylamino)methylene]-1*H*-1,2,3-triazolo[4,5-*b*]pyridinium 3-oxide hexafluorophosphate (0.097 g, 0.255 mmol) and the reaction mixture was stirred for 145 min and concentrated. Dichloromethane and methanol were added to the residue and it was purified via silica gel chromatography, eluting with (3:1 ethyl acetate: ethanol):hexanes (0:1 to 3:2) to give a material which was triturated/sonicated with ethyl acetate and the solids collected by filtration, air-dried, then dried under vacuum overnight to give 6-chloro-7-

cyclopropyl-*N*-(1*s*,3*s*)-3-hydroxy-3-methylcyclobutyl)-1,8-naphthyridine-3-carboxamide **1bj** (0.051 g, 0.154 mmol, 72.1% yield) as a cream-colored powder. ¹H NMR (400 MHz, CD₃SOCD₃) δ 1.20–1.26 (m, 4H), 1.28 (s, 3H), 2.08–2.18 (m, 2H), 2.28–2.36 (m, 2H), 2.68–2.78 (m, 1H), 4.01 (sex, *J* = 7 Hz, 1H), 5.02 (s, 1H), 8.67 (s, 1H), 8.79 (d, *J* = 2 Hz, 1H), 9.01 (d, *J* = 7 Hz, 1H), 9.35 (d, *J* = 2 Hz, 1H); LC-MS (LC-ES) C₁₇H₁₈ClN₃O₂ M + H = 332; t_R = 0.73 min, 100% purity.

(*S*)-6-Chloro-7-cyclopropyl-*N*-(2-oxopyrrolidin-3-yl)-1,8-naphthyridine-3-carboxamide **1bk**



(*S*)-3-Aminopyrrolidin-2-one **8c** (0.024 g, 0.240 mmol, AstaTech) was added to 6-chloro-7-cyclopropyl-1,8-naphthyridine-3-carboxylic acid **7y** (0.053 g, 0.213 mmol) in *N,N*-dimethylformamide (2.5 mL), followed by *N,N*-diisopropylethylamine (0.05 mL, 0.287 mmol). Then, 1-[bis(dimethylamino)methylene]-1*H*-1,2,3-triazolo[4,5-*b*]pyridinium 3-oxide hexafluorophosphate (0.105 g, 0.276 mmol) was added and the reaction mixture was stirred for 150 min and concentrated. Dichloromethane and methanol were added to the residue and it was purified via silica gel chromatography, eluting with (3:1 ethyl acetate:ethanol): hexanes (0:1 to 24:1) to give a material which was triturated/sonicated with ethyl acetate and the solids collected by filtration, air-dried, then dried under vacuum overnight to give (*S*)-6-chloro-7-cyclopropyl-*N*-(2-oxopyrrolidin-3-yl)-1,8-naphthyridine-3-carboxamide **1bk** (0.035 g, 0.106 mmol, 49.6% yield) as a pale tan powder. ¹H NMR (400 MHz, CD₃SOCD₃) δ 1.18–1.28 (m, 4H), 1.96–2.10 (m, 1H), 2.34–2.46 (m, 1H), 2.68–2.78 (m, 1H), 3.22–3.28 (m, 2H), 4.62 (q, *J* = 9 Hz, 1H), 7.94 (br s, 1H), 8.71 (s, 1H), 8.82 (d, *J* = 2 Hz, 1H), 9.13 (d, *J* = 8 Hz, 1H), 9.36 (d, *J* = 2 Hz, 1H); LC-MS (LC-ES) C₁₆H₁₅ClN₄O₂ M + H = 331; t_R = 0.66 min, 100% purity.

Expression and purification of H-PGDS protein. Full length human H-PGDS cDNA (Invitrogen Ultimate ORF IOH13026) was amplified by PCR with the addition of a 5' 6-His tag and TEV protease cleavage site. The PCR product was digested with *Nde*I and *Xho*I and ligated into pET22b+ (Merck Novagen®). Expression was carried out in *E. coli* strain BL21 (DE3*) using auto-induction Overnight Express™ Instant TB medium (Merck Novagen®) supplemented with 1% glycerol. The culture was first grown at 37 °C and the temperature was reduced to 25 °C when OD₆₀₀ reached 2.0. Cells were harvested by centrifugation after a further 18 h. 10 g of *E. coli* cell pellet was suspended to a total volume of 80 mL in lysis buffer (20 mM Tris-Cl pH 7.5, 300 mM NaCl, 20 mM imidazole, 5 mM β-mercaptoethanol, 10% glycerol). 1 mg/mL protease inhibitors (Protease Inhibitor Cocktail Set III, Merck Calbiochem®) and 1 mg/mL lysozyme were added to the cell suspension. The suspension was then sonicated for 5 min (UltraSonic Processor VCX 750, Cole-Parmer Instrument Co.) with a micro probe (50% amplitude, 10 s on/off) and then centrifuged at 100,000 g for 90 min (at 4 °C). The supernatant was loaded onto a Ni-NTA HiTrap® column (5 mL, GE Healthcare, pre-equilibrated in lysis buffer). The column was washed with 10 column volumes of lysis buffer and eluted with lysis buffer containing 500 mM imidazole. The pooled protein peak fractions were concentrated using a 10 kDa centrifugal filter at 3500 g and 4 °C (Amicon Ultra-15 centrifugal filter unit with Ultracel-10 membrane from Millipore). Further purification of the concentrated protein was carried out using gel filtration chromatography on a HiLoad® 26/600 Superdex™ 75 preparative grade column (GE Healthcare Life Sciences) using 50 mM Tris pH 7.5, 50 mM sodium chloride, 1 mM dithiothreitol, 1 mM magnesium chloride. Fractions containing the protein were pooled, concentrated as described above, and stored at –80 °C. For protein used in crystallography, the 6-His tag was removed with TEV protease prior to the gel filtration step.

Expression and purification of cyclooxygenase-2 (COX-2) protein. The full length human COX-2 gene (accession number L15326) was amplified by PCR to generate an *Eco*RI – *Hind*III fragment containing an in-frame FLAG tag. This was subcloned into pFastBac 1 (Invitrogen). The COX-2 FLAG plasmid was recombined into the baculovirus genome according to the BAC-to-BAC protocol described by Invitrogen. Transfection into *Spodoptera frugiperda* (Sf9) insect cells was performed using Cellfectin® (Invitrogen), according to the manufacturer's protocol. Super Sf9 cells were cultured in EX420 media (SAFC Biosciences) to a density of approximately 1.5 × 10⁶ cells/mL within a wave bioreactor. Recombinant virus was added at a Multiplicity of Infection (MOI) of 5 and the culture was allowed to continue for 3 days. Cells were harvested using a continuous feed centrifuge run at 2500 g at a rate of approximately 2 l/min with cooling. The resultant cell slurry was re-centrifuged in pots (2500 g, 20 min, 4 °C) and the cell paste was stored at –80 °C. 342 g of cell paste was re-suspended to a final volume of 1600 mL in a buffer of 20 mM Tris-Cl pH 7.4, 150 mM sodium chloride, 0.1 mM EDTA, 1.3% w/v *n*-octyl-β-D-glucopyranoside containing 20 Complete EDTA-free Protease Inhibitor Cocktail tablets (Roche Applied Science). The suspension was sonicated in 500 mL batches for 8 × 5 s at 10 u amplitude with the medium tip of an MSE probe sonicator and subsequently incubated at 4 °C for 90 min with gentle stirring. The lysate was centrifuged at 12000 rpm for 45 min at 4 °C in a Sorvall SLA1500 rotor. The supernatant (1400 mL) was added to 420 mL of 20 mM Tris-Cl pH 7.4, 150 mM NaCl, 0.1 mM EDTA to reduce the concentration of *n*-octyl-β-D-glucopyranoside to 1% w/v. The diluted supernatant was incubated overnight at 4 °C on a roller with 150 mL of anti-FLAG M2 agarose affinity gel (Aldrich-Sigma) which had been pre-equilibrated with 20 mM Tris-Cl pH 7.4, 150 mM sodium chloride, 0.1 mM EDTA, 1% w/v *n*-octyl-β-D-glucopyranoside (purification buffer). The anti-Flag M2 agarose beads were pelleted by centrifugation in 500 mL conical Corning centrifuge pots at 2000 rpm for 10 min at 4 °C in a Sorvall RC3 swing-out rotor. The supernatant (unbound fraction) was discarded and the beads were re-suspended to half the original volume in purification buffer and re-centrifuged as above. The beads were then packed into a BioRad Econo Column (5 cm diameter) and washed with 1500 mL of purification buffer at 4 °C. Bound proteins were eluted with 100 μg/mL triple FLAG peptide (Aldrich-Sigma) in purification buffer. Six fractions each of 0.5 column volume were collected. After each 0.5 column volume of purification buffer was added into the column the flow was held for 10 min before elution. Fractions containing COX-2 were pooled resulting in a protein concentration of ~ 1 mg/mL. The protein was further concentrated on Vivaspin 20 centrifugal concentrators (10 kDa cut-off) to 2.4 mg/mL and then stored at –80 °C.

Test compound plate preparation. Test compounds were diluted to 1 mM in DMSO and a 1:3, 11 point serial dilution was performed across a 384 well HiBase plate (Greiner Bio-one). 100 nL of this dilution series was then transferred into a 384 well v-base plate (Greiner Bio-one) using an Echo™ acoustic dispenser (Labcyte Inc) to create the assay plate. 100 nL of DMSO was added to each well in columns 6 and 18 for use as control columns.

H-PGDS RapidFire™ High Throughput Mass Spectrometry Assay. The H-PGDS RapidFire™ mass spectrometric assay monitors conversion of prostaglandin H₂ (PGH₂) to prostaglandin D₂ (PGD₂) by hematopoietic prostaglandin D synthase (H-PGDS). In the assay format described here, the substrate (PGH₂) is formed *in situ* by the action of cyclooxygenase-2 on arachidonic acid. This first step is set up to be fast and generates a burst of PGH₂ at ~ 10 μM. The PGH₂ is then further converted to PGD₂ by the H-PGDS enzyme. The reaction is quenched with tin (II) chloride in citric acid, which converts any remaining PGH₂ to the more stable PGF_{2α}. Plates are then read on the RapidFire™ high throughput solid phase extraction system (Agilent) which incorporates a solid phase extraction step coupled to a triple quadrupole mass spectrometer (AB SCIEX). Relative levels of PGD₂ and PGF_{2α}, which acts as a surrogate for substrate, are measured and a percent conversion calculated. Inhibitors are characterized as compounds which lower the

conversion of PGH₂ to PGD₂.

In a typical assay, 5 μ L of an enzyme solution containing 10 nM H-PGDS enzyme, 1.1 μ M COX-2 enzyme (COX-1 may be substituted for COX-2 in the assay, but the assay would then need to be reoptimized to determine appropriate reagent amounts, conditions, etc., for optimum production of PGH₂ from arachidonic acid) and 2 mM reduced glutathione (Sigma-Aldrich), diluted in a buffer of 50 mM Tris-Cl pH 7.4, 10 mM magnesium chloride and 0.1% Pluronic F-127 (all Sigma-Aldrich) was added to each well of the plate except column 18 using a Multidrop Combi® dispenser (Thermo Fisher Scientific). 5 μ L of enzyme solution without H-PGDS was added to each well in column 18 of the assay plate to generate 100% inhibition control wells.

Immediately after the addition of enzyme solution, 2.5 μ L of a cofactor solution containing 4 μ M Hemin (Sigma-Aldrich) diluted in buffer of 50 mM Tris-Cl pH 7.4 and 10 mM magnesium chloride (all Sigma-Aldrich), was added to each well using a Multidrop Combi® dispenser. 2.5 μ L of substrate solution containing 80 μ M arachidonic acid (Sigma-Aldrich) and 1 mM sodium hydroxide (Sigma-Aldrich) diluted in HPLC grade water (Sigma-Aldrich) was then added to each well using a Multidrop Combi® dispenser, to initiate the reaction.

The assay plates were incubated at room temperature for the duration of the linear phase of the reaction (usually 1 min 30 s – 2 min, this timing should be checked on a regular basis). Precisely after this time, the reaction was quenched by the addition of 30 μ L of quench solution containing 32.5 mM tin(II) chloride (Sigma-Aldrich) in 200 mM citric acid (adjusted to pH 3.0 with 0.1 mM sodium hydroxide solution) to all wells using a Multidrop Combi® dispenser (Thermo Fisher Scientific). The tin(II) chloride was initially prepared as a suspension at an equivalent of 600 mM in HPLC water (Sigma-Aldrich) and sufficient concentrated hydrochloric acid (Sigma-Aldrich) was added in small volumes until dissolved. The assay plates were centrifuged at 1000 rpm for 5 min prior to analysis.

The assay plates were analyzed using a RapidFire™ high throughput solid phase extraction system (Agilent) coupled to a triple quadrupole mass spectrometer (AB SCIEX) to measure relative peak areas of PGF_{2 α} and PGD₂ product. Peaks were integrated using the RapidFire™ integrator software before percentage conversion of substrate to PGD₂ product was calculated as shown below:

% Conversion = ((PGD₂ peak area) / (PGD₂ peak area + PGF_{2 α} peak area)) \times 100.

Data were further analyzed within ActivityBase software (IDBS) using a four parameter curve fit of the following form:

$$y = \frac{a - d}{1 + (x/c)^b} + d$$

where a is the minimum, b is the Hill slope, c is the IC₅₀ and d is the maximum. Data are presented as the mean IC₅₀.

H-PGDS Rat Basophilic Leukemia (RBL) cell inhibition assay. The cellular assay used for measuring inhibition of H-PGDS employed a rat model for testing compounds for inhibition of PGD₂ production. PGD₂ signal is generated through rat basophil leukemia (RBL) cells. These cells are adherent and will produce PGD₂ upon the addition of A23187 (Calcimycin, a calcium ionophore).

RBL cells were grown within T175 flasks for up to 15 passages. The cells were detached and plated into 96 well assay plates at a density of 5e⁴ cells/well in 100 μ L/well. After 30 min of equilibration at room temperature, the plated cells were allowed to sit in a 37 °C, 5% CO₂ incubator overnight. On the day of processing, compounds were serially diluted with a top concentration of 5e⁵ [M] for 10 doses at a 1:3 dilution scheme. The compounds were stamped into each plate at 2 μ L/well and were diluted with 38 μ L of HBSS. The next day, the cells had attached themselves to the bottom of the wells and were ready to be washed. (Washing the cells was performed due to the 10% FBS within the growth media.) After 3 \times 160 μ L washes with HBSS, 160 μ L of HBSS was left in the well and 20 μ L (out of the 40 μ L) of compounds were transferred into

the wells of the washed cells (160 μ L HBSS/cells + 20 μ L compound). The compound and cells were incubated together for 30 min at 37 °C/5% CO₂. After the incubation, the compound and cells had 20 μ L of A23187 added into the assay plate (180 μ L HBSS/cells/compound + 20 μ L A23187). The compound, cells and ionophore were incubated together for 30 min at 37 °C/5% CO₂. At the 25 min mark, the assay plates were removed from the incubator and spun in the centrifuge for 5 min at 1000 rpms. The assay was then quenched by transferring 90 μ L (out of 200 μ L) of supernatant into 40 μ L of acetonitrile with 20 ng/mL PGD₂-d₄ (internal standard).

The completed assay plate was then sampled and read on the RapidFire™ Mass Spectrometer (RF-MS). Samples could also be frozen (at –20 °C) for about 2 weeks before signal degrades. The RF-MS was tuned to capture the PGD₂ product at xic 351.2/271.2 and the PGD₂-d₄ spiked in product at xic 355.2/275.1 on an Agilent 4000 or 5500.

Step 1, Data transformation, *Peaks for PGD₂ and D₄-PGD₂ integrated and expressed as ratio PGD₂:D₄-PGD₂.*

```

[READ1/<READ1 + READ2> X 100
  READ1; PGD2 analyte
  READ2; D4-PGD2 analyte
[PGD2/<PGD2 + D4-PGD2> X 100

```

Step 2, Data Normalization (between 0 and 100), % Inhibition is calculated as 100-((unknown-col12)/(col11-col12)*100)*

```

100-100 < CMPD-CTRL2>/<CTRL1-CTRL2>
  CMPD; Transformed data from the compound
  CTRL1; Control 1
    Average of column 11
    Represents 0% inhibition from the compound
  CTRL2; Control 2
    Average of column 12
    Represents 100% inhibition from the compound
100-100 < Transformed data - Avg of column for 100% inhibition>/< Avg of column
for 0% inhibition - Avg of column for 100% inhibition>

```

l-PGDS RapidFire™ High Throughput Mass Spectrometry Assay.

This protocol describes an assay to measure conversion of PGH₂ to PGD₂ by lipocalin prostaglandin D synthase (l-PGDS, Cayman Chemicals) using high throughput mass spectrometry. In the assay format described here, the substrate (PGH₂) is obtained commercially (Cayman Chemicals). The PGH₂ is converted to PGD₂ by the l-PGDS enzyme. There is also non-PGDS dependent conversion of PGH₂ to PGD₂, and this conversion is accounted for in control wells of the assay plate where no l-PGDS is added. The assay is tuned to achieve approximately 25–30% conversion of the PGH₂ that is l-PGDS-dependent. The reaction is quenched in all wells with tin (II) chloride which converts any remaining PGH₂ to the more stable PGF_{2 α} . Plates are then analyzed on the RapidFire™ system (Agilent) which incorporates a solid phase extraction step coupled to an electrospray ionization triple quadrupole mass spectrometer (AB SCIEX). Relative levels of PGD₂ and PGF_{2 α} , which acts as a surrogate to substrate, are measured and a percent conversion calculated. Inhibitors are characterized as compounds which lower the conversion of PGH₂ to PGD₂. The data analysis was similar to the H-PGDS RapidFire™ assay above.

mPGES RapidFire™ High Throughput Mass Spectrometry Assay.

This protocol describes a functional assay to measure conversion of PGH₂ to PGE₂ by mPGES (Cayman Chemicals) using high throughput mass spectrometry. In the assay format described here, the substrate (PGH₂) is formed *in situ* by the action of cyclooxygenase-2 on arachidonic acid. This first step is set up to be fast and generates a burst of PGH₂ at ~ 10–20 μ M (~K_m of PGH₂ for mPGES-1). The reaction is quenched with tin (II) chloride, which converts any remaining PGH₂ to the more stable PGF_{2 α} . Plates are then analyzed on the RapidFire™ system, which incorporates a solid phase extraction step coupled to an electrospray ionization triple quadrupole mass spectrometer. Relative levels of PGE₂ and PGF_{2 α} , which acts as a surrogate to substrate, are measured and a percent conversion calculated. Inhibitors are characterized as compounds which lower the conversion of PGH₂ to PGE₂. The

data analysis was similar to the H-PGDS RapidFire™ assay above.

Binding Kinetic Parameters Determination – 1y. The equilibrium binding constant (K_d and active site concentration by tight binding) for **1y** was determined by titration (1 to 4 μ L additions of a 10 μ M **1y** stock) of the intrinsic tryptophan fluorescence in the presence of glutathione (1 mL assay buffer: 50 mM Tris-HCl, pH 7.5; 0.5 mM $MgCl_2$; 1 mM reduced glutathione; 50 nM H-PGDS in a quartz cuvette) using a Molecular Devices M2 Instrument; excitation 285 nm, emission 360 nm, with a 325 nm cut-off filter; PMT Precision set to HIGH; and number of reads set to 30 reads per well. Fluorescence intensity (RFU) was read and recorded after each addition (6 to 8 times), the high and low were discarded, and the average ($N =$) determined. The no enzyme control average was subtracted from the sample average at each inhibitor addition. The net average fluorescence intensity at each inhibitor concentration (adjusted for the small volume changes) was fitted to a modified tight binding equation to obtain the K_d and the active site concentration using GraFit7 (Erithacus):

$$Y = A - ((A - B) * ((K + E + X) - \sqrt{(K + E + X)^2 - 4 * E * X})) / (2 * E)$$

where Y = net average FI, X = final inhibitor concentration, A = FO (initial FI), B = Fc (FI of the total EI complex), E = binding site conc, $K = K_d$.

The on or association rate (k_{on}) of **1y** was determined by measuring changes in the intrinsic tryptophan fluorescence of human H-PGDS. Inhibitor was titrated (0.1 μ M – 0.8 μ M final concentrations) in buffer (50 mM Tris-HCl, pH 7.5; 0.5 mM $MgCl_2$; 1 mM reduced glutathione) with 2% DMSO. Enzyme (80 nM) was prepared in buffer at 2x final concentration. Inhibitor and enzyme were rapidly mixed using a stopped flow instrument (Applied Photophysics SX20) in fluorescence mode with 10 mm pathlength flow cell orientation, excitation at 285 nm, emission > 320 nm using a bandpass filter. Photomultiplier voltage was set to approximately 80% of the saturating voltage using the auto PM function in the software after mixing equal volumes of H-PGDS and buffer. After determining this operating voltage, 2x concentrations of enzyme and inhibitor were rapidly mixed 1:1 and data was collected with 10,000 data points per time course. Time intervals were selected based on ≥ 5 half times at each inhibitor concentration ($t_{1/2} = \ln(2)/k_{obs}$); data earlier than 0.002 sec (instrument dead time) was omitted; the time courses for tryptophan fluorescence quenching were fitted to an equation for single exponential decay ($y = A0 * \exp(k_{obs} * t) + C$) using the Applied Photophysics instrument software to determine the k_{obs} at each inhibitor concentration, where $A0$ is the change in FI, C is the final fluorescence intensity and t is time in seconds. The k_{obs} were re-fitted versus [Inhibitor] to a linear equation where the slope = k_{on} .

The k_{off} for **1y** was calculated from the K_d and k_{on} . The k_{obs} versus [Inhibitor] replots from the stopped-flow binding experiments were linear to 800 nM or > than 3000 times the K_d value suggesting that the binding mechanism was single step in this concentration range, with $K_d = k_{off}/k_{on}$ and k_{off} reliably calculated from $K_d * k_{on}$.

Artificial membrane permeability (AMP) assay

The permeability rate is measured across a phospholipid bilayer system. The lipid is egg phosphatidyl choline (1.8%) and cholesterol (1%) dissolved in *n*-decane. This is applied to the bottom of the micro-filtration filter inserts in a Transwell plate. Phosphate buffer (50 mM disodium phosphate with 0.5% 2-hydroxypropyl- β -cyclodextrin), pH 7.4 is added to the top and bottom of the plate. The lipids are allowed to form bilayers across the small holes in the filter. Permeation experiment is initiated by adding the compound to the bottom well and stopped at a pre-determined elapsed time. The compound permeates through the membrane to enter the acceptor well. The compound concentration in both the donor and acceptor compartments is determined by liquid chromatography after 3 h incubation at room temperature.^{64,65} The permeability (logPapp) measuring how fast molecules pass through the

black lipid membrane is expressed in nm/s.

Mouse liver microsomal assay. Dilute 10 mM dimethyl sulfoxide stock of new chemical entity (NCE) to an appropriate intermediate concentration such that the final test concentration in the incubation is 0.5 mM and final organic solvent content is limited to 0.25%. Thaw liver microsomes in a room temperature water bath and immediately place on ice until ready to use. Vortex the microsomes and dilute to appropriate concentration using 50 mM phosphate buffer, pH 7.4. Add diluted NCE (0.5 mM final NCE concentration). Add diluted microsomes (0.5 mg/mL final protein concentration). Pre-incubate the plate for 5 min at 37 °C with shaking before adding cofactor solution (Final concentration in the incubation system: β -nicotinamide adenine dinucleotide phosphate (0.44 mM); glucose 6-phosphate (5.2 mM); glucose-6-phosphate dehydrogenase (1.2 U/mL); sodium bicarbonate (0.4%); 5 mM magnesium chloride or 1 mM nicotinamide adenine dinucleotide phosphate). Start the reaction by adding prewarmed (37 °C) cofactor solution. Mix the reaction for ~ 30 s. Remove a fixed volume of microsomal incubation (e.g. 100 μ L) at 6 timepoints up to 45 min and place into a 96-deepwell plate containing 2 volumes of chilled acetonitrile (e.g. 200 μ L) containing Internal standard; reaction plate should be maintained at 37 °C with shaking during the entire incubation period. Precipitate protein by mixing and centrifugation (2000g, 15 min). Transfer resultant supernatant to a new 96-well plate for LC-MS/MS analysis. Metabolic stability expressed as the percentage of parent NCE remaining is calculated from the peak area of NCE remaining after incubation (t_x) compared to the time zero (t_0) incubation. The half-life ($t_{1/2}$) is calculated using the following equation: $t_{1/2} = -\ln(2)/k$, where k is the turn-over rate constant of the \ln % remaining vs. time regression. Intrinsic Clearance (Cl_{int}) is calculated from the half-life using the following equations:

$$Cl_{int} = (0.693 / t_{1/2} \text{ min}) \times (\text{mL of incubation/mg microsomal protein}) \times (\text{mg microsomal protein/gm liver}) \times (\text{gm liver/kg body wt}).$$

Constant used for mg microsomal protein/gm liver: (46-rat, 48-mouse, 36.7-dog, 39.7- human, 52.5-monkey, 52.5-minipig). Constants used to represent gm/liver/kg body weight: (36-rat, 51-mouse, 32.5-dog, 24.5- human, 30-monkey, 16.7-minipig).

Fasted State Simulated Intestinal Fluid Solubility (FaS-SIF) assay. This experiment determines the solubility of solid compounds in Fasted State-Simulated Intestinal Fluid (FaS-SIF) at pH 6.5 after 4 h equilibration at room temperature. 1 mL of FaS-SIF buffer (3 mM sodium taurocholate, 0.75 mM lecithin in sodium phosphate buffer at pH = 6.5) is added to manually weighed 1 mg of solid compound in a 4 mL vial.⁶⁶ The resulting suspension is shaken at 900 rpm for 4 h at room temperature and then transferred to a Multiscreen HTS, 96-well solubility filter plate. The residual solid is removed by filtration. The supernatant solution is quantified by HPLC-UV using single point calibration of a known concentration of the compound in DMSO. The dynamic range of the assay is 1–1000 μ g/mL.

Protein Binding assay (PB). Chemically bonded human serum albumin (HSA) HPLC stationary phase (Chiral Technologies, France) are used for measuring compounds' binding to plasma proteins, applying linear gradient elution up to 30% isopropanol.⁶⁷ The run time is 6 min, including the re-equilibration of the stationary phases with the 50 mM pH = 7.4 ammonium acetate buffer. The gradient retention times are standardized using a calibration set of mixtures as previously described.⁶⁸

pK_A determination. Sirius T3 (Sirius Analytical Inc, UK) instrument is used for pK_A determination of compounds. The pK_A determination is based on acid-base titration and the protonation/deprotonation of the molecule is measured either by UV spectroscopy or potentiometrically. The pK_A value is calculated from the pH where the 50–50% of the protonated and unprotonated form of the molecules are present. The UV-metric method provides pK_A results for samples with chromophores whose UV absorbance changes as a function of pH. It typically requires 5 μ L of a 10 mM solution of the samples and the UV absorbance is

monitored over 54 pH values in a buffered solution in about 5 min.

When the ionization center is far from the UV chromophore, the pH-metric method based on potentiometric acid-base titration is used. Usually 0.5–1 mg of solid material is required for the measurements. The pH of each point in the titration curve is calculated using mass-balance equations and the calculated points are fitted to the measured curve by refining the pK_A (s). The pK_A that provides the best fit is taken to be the measured pK_A .

For poorly soluble compounds, the co-solvent method using various concentrations of co-solvent (usually methanol) is applied. The pK_A in water is calculated from the Yasuda-Shedlovsky extrapolation.

Crystallization Conditions. Apo crystals were grown using the vapor diffusion method. Protein [10 mg/mL in 50 mM tris(hydroxymethyl)aminomethane hydrochloride at pH 7.5, 50 mM sodium chloride, 1 mM dithiothreitol, 15 mM glutathione, and 1 mM magnesium chloride] was mixed with an equal volume of precipitant solution (21% poly(ethylene glycol) 6000, 1% 1,4-dioxane, 5.5% glycerol, 10 mM dithiothreitol, and 60 mM tris(hydroxymethyl)aminomethane hydrochloride at pH 8.5). Rod-like crystals formed in 3–7 days at room temperature and were soaked for ~ 24 h with 0.5–2 mM inhibitor. X-ray diffraction data was collected on a RAXIS detector operating on a FRE + generator or at the Advanced Photon Source (APS, Ser-CAT 22ID) using an Eiger detector. Data were integrated and processed using either D*Trek or HKL2000. The structures were solved by molecular replacement using MOLREP. The phases were refined using the CCP4 suite and manual rebuilding using Coot.

All *in vivo* studies were conducted in accordance with the GSK Policy on the Care, Welfare and Treatment of Laboratory Animals. All protocols were reviewed and approved by the Institutional Animal Care and Use Committee of GSK.

Mast Cell Degranulation Assay. Nine-week-old C57BL/6J male mice were randomized by body weight into 8 treatment groups, then dosed (p.o.) with either vehicle or the H-PGDS inhibitor **1y** at doses of 0.003, 0.01, 0.03, 0.1, 0.3, and 1.0 mg/kg. One hour later, mice were anesthetized and injected (*i.p.*) with phosphate buffered saline (0.2 mL) or compound 48/80 solution (0.75 mg/mL, Sigma), followed by gentle massage of the abdomen. Mice were kept under anesthesia for 7 min before blood was collected by cardiac puncture for measurement of inhibitor concentration. Mice were then euthanized by cervical dislocation. The abdominal cavity was opened with a small incision and filled with phosphate buffered saline (2.0 mL) and the abdomen was gently massaged for several seconds. Lavage fluid (1 mL) was removed, spun down (12,000 rpm for 2 min) and the supernatant kept on dry ice and later used for measurement of PGD₂ levels using LC/MS/MS.

Lipopolysaccharide (LPS) Challenge Assay. Eleven-week-old male C57BL/6J mice were randomized by body weight into 8 groups (n = 6), then dosed (p.o.) with vehicle (0.5% HPML with 0.1% Tween 80), or H-PGDS inhibitor **1y** at 0.003, 0.01, 0.03, 0.1, 0.3, and 1.0 mg/kg. One hour later, mice were injected (*i.p.*) with PBS or 20 ng/kg LPS. Blood samples were withdrawn via cardiac puncture 30 min post LPS injection and animals were then euthanized and gastrocnemius were isolated. Blood and skeletal muscle drug and prostaglandin levels were determined using LC/MS/MS.

In Vivo Functional Response to Muscle Injury in C57BL/6N mice. Under anesthesia, the right hind limb of a mouse is restrained at the knee and the foot attached to a motorized footplate/force transducer. Needle electrodes are inserted into the upper limb, either side of the sciatic nerve and a current sufficient to elicit a maximal muscle contraction is applied. Muscle tension is produced by moving the footplate to lengthen the plantarflexor muscles while the limb is under maximal stimulation. This is repeated 60 times to fatigue the muscles of the lower limb. Anesthesia, limb immobilization, and limb stimulation are then repeated at regular intervals to measure maximal isometric force in the recovering limb. The mice were randomized into groups based on starting lean body mass, which is strongly correlated with muscle strength in animals (and humans). *In vivo* muscle force for each animal was

determined prior to injury (pre-injury maximal tetanic force), but animals were not randomized by this parameter. Muscles were then exercised using eccentric contractions, and subsequent force assessments were determined longitudinally over days/weeks (post-injury maximal tetanic force). The experimentalist performing the assessments was blinded to the treatment groups. 7 to 9 animals are tested for each test condition. Eccentric contraction-induced muscle fatigue in vehicle-treated male C57BL/6N mice, 10–12 weeks of age, significantly reduces (~35%) maximal isometric torque 24 h after injury and takes ~ 5 weeks for full functional restoration. In contrast, animals (PO) dosed with 3 and 10 mg/kg QD of the compound of **1y** beginning 10 min prior to eccentric contraction challenge exhibited an acceleration in the kinetics of recovery. And 3 and 10 mg/kg QD of the compound of **1y** also reduced the initial magnitude of the injury, as determined by isometric limb force 24 h following protocol initiation.

In Vivo Functional Response to Muscle Injury in mdx mice Eccentric contraction-induced muscle fatigue in vehicle-treated male mdx mice, 7 months of age, significantly reduced (~54%) maximal isometric torque 24 h after injury and never returned to full functional restoration. In contrast, animals (PO) dosed with 0.1, 1, 3, and 10 mg/kg QD of **1y** beginning 10 min prior to eccentric contraction challenge exhibited an acceleration in the kinetics of recovery.

Declaration of Competing Interest

The authors are employees of GlaxoSmithKline or Astex Pharmaceuticals.

This research did not receive any specific grant from funding agencies in the public, commercial, or not-for-profit sectors.

Acknowledgements

The authors would like to thank Nathalie Barrett, Philip J. Day, Bernadette H. Mouzon, Vaughan Leyden, and David Taylor for the cloning, expression, and purification of the H-PGDS protein that was used in the biochemical assays.

References

- Mah JK. An overview of recent therapeutics advances for Duchenne muscular dystrophy. *Meth Mol Biol.* 2018;1687:3–17.
- Tsuda T. Clinical manifestations and overall management strategies for Duchenne muscular dystrophy. *Meth Mol Biol.* 2018;1687:19–28.
- Ryder S, Leadley RM, Armstrong N, et al. The burden, epidemiology, costs and treatment for Duchenne muscular dystrophy: an evidence review. *Orphanet J Rare Dis.* 2017;12:79.
- Birnkrant DJ, Bushby K, Bann CM, et al. Diagnosis and management of Duchenne muscular dystrophy, part 1: diagnosis, and neuromuscular, rehabilitation, endocrine, and gastrointestinal and nutritional management. *The Lancet Neurol.* 2018;17:251–267.
- Reinig AM, Mirzaei S, Berlau DJ. Advances in the treatment of Duchenne muscular dystrophy: new and emerging pharmacotherapies. *Pharmacotherapy.* 2017;37:492–499.
- Salmaninejad A, Valilou SF, Bayat H, et al. Duchenne muscular dystrophy: an updated review of common available therapies. *Int J Neurosci.* 2018;128:854–864.
- Crone M, Mah JK. Current and emerging therapies for Duchenne muscular dystrophy. *Curr Treat Options Neurol.* 2018;20:31.
- Hoxha M. Duchenne muscular dystrophy: focus on arachidonic acid metabolites. *Biomed Pharmacother.* 2019;110:796–802.
- Okinaga T, Mohri I, Fujimura H, et al. Induction of hematopoietic prostaglandin D synthase in hyalinized necrotic muscle fibers: its implication in grouped necrosis. *Acta Neuropathol.* 2002;104:377–384.
- Song W-L, Wang M, Ricciotti E, et al. Tetranor PGDM, an abundant urinary metabolite reflects biosynthesis of prostaglandin D₂ in mice and humans. *J Biol Chem.* 2008;283:1179–1188.
- Nakagawa T, Takeuchi A, Kakiuchi R, et al. A prostaglandin D₂ metabolite is elevated in the urine of Duchenne muscular dystrophy patients and increases further from 8 years old. *Clin Chim Acta.* 2013;423:10–14.
- Mohri I, Aritake K, Taniguchi H, et al. Inhibition of prostaglandin D synthase suppresses muscular necrosis. *Am J Pathol.* 2009;174:1735–1744.
- Takeshita E, Komaki H, Shimizu-Motohashi Y, Ishiyama A, Sasaki M, Takeda S. A phase I study of TAS-205 in patients with Duchenne muscular dystrophy. *Ann Clin Trans Neurol.* 2018;5:1338–1349.

- 14 Smith WL, Urade Y, Jakobsson P-J. Enzymes of the cyclooxygenase pathways of prostanoid biosynthesis. *Chem Rev.* 2011;111:5821–5865.
- 15 Flanagan JU, Smythe ML. Sigma-class glutathione transferases. *Drug Metab Rev.* 2011;43:194–214.
- 16 Hirata T, Narumiya S. Prostanoid receptors. *Chem Rev.* 2011;111:6209–6230.
- 17 Feng X, Ramsden MK, Negri J, et al. Eosinophil production of prostaglandin D₂ in patients with aspirin-exacerbated respiratory disease. *J Allergy Clin Immunol.* 2016;138:1089–1097.
- 18 Hyo S, Kawata R, Kadoyama K, et al. Expression of prostaglandin D₂ synthase in activated eosinophils in nasal polyps. *Arch Otolaryngol Head Neck Surg.* 2007;133:693–700.
- 19 Mohri I, Taniike M, Taniguchi H, et al. Prostaglandin D₂-mediated microglia/astrocyte interaction enhances astrogliosis and demyelination in twitche. *J Neurosci.* 2006;26:4383–4393.
- 20 Sanchez D, Ganfornina MD, Gutierrez G, Marin A. Exon-intron structure and evolution of the lipocalin gene family. *Mol Biol Evol.* 2003;20:775–783.
- 21 Aritake K, Kado Y, Inoue T, Miyano M, Urade Y. Structural and functional characterization of HQL-79, an orally selective inhibitor of human hematopoietic prostaglandin D synthase. *J Biol Chem.* 2006;281:15277–15286.
- 22 Hesterkamp T, Barker J, Davenport A, Whittaker M. Fragment based drug discovery using fluorescence correlation spectroscopy techniques: challenges and solutions. *Curr Top Med Chem.* 2007;7:1582–1591.
- 23 Hohwy M, Spadola L, Lundquist B, et al. Novel prostaglandin D synthase inhibitors generated by fragment-based drug design. *J Med Chem.* 2008;51:2178–2186.
- 24 Carron CP, Trujillo JJ, Olson KL, et al. Discovery of an oral potent selective inhibitor of hematopoietic prostaglandin D synthase (HPGDS). *ACS Med Chem Lett.* 2010;1:59–63.
- 25 Weibeth FJ, Yu Y, Subotkowski W, Pemberton C. Demonstration on pilot-plant scale of the utility of 1,5,7-triazabicyclo[4.4.0]dec-5-ene (TBD) as a catalyst in the efficient amidation of an unactivated methyl ester. *Org Proc Res Dev.* 2012;16:1967–1969.
- 26 Thuraiaratnam S. Hematopoietic prostaglandin D synthase inhibitors. *Prog Med Chem.* 2012;51:97–133.
- 27 Zhang D, Hop CECA, Patilea-Vrana G, et al. Drug concentration asymmetry in tissues and plasma for small molecule-related therapeutic modalities. *Drug Metab Dispos.* 2019;47:1122–1143.
- 28 An G. Small-molecule compounds exhibiting target-mediated drug disposition (TMDD): a minireview. *J Clin Pharmacol.* 2017;57:137–150.
- 29 Dekeyser JG, Shou M. Species differences of drug-metabolizing enzymes. *Encyclopedia Drug Metab Interact.* 2012;1:121–158.
- 30 Kim M-S, Wang S, Shen Z, et al. Differences in the pharmacokinetics of peroxisome proliferator-activated receptor agonists in genetically obese Zucker and Sprague-Dawley rats: implications of decreased glucuronidation in obese Zucker rat. *Drug Metab Dispos.* 2004;32:909–914.
- 31 Wilkinson EM, Ilhan ZE, Herbst-Kralovetz MM. Microbiota-drug interactions: impact on metabolism and efficacy of therapeutics. *Maturitas.* 2018;112:53–63.
- 32 Shi S, Klotz U. Age-related changes in pharmacokinetics. *Curr Drug Metab.* 2011;12:601–610.
- 33 Rolan P, McKeown L. Gender as a source of variability in human pharmacokinetics and pharmacodynamics. *Inter Cong Ser.* 1999;1178:121–132.
- 34 Czerniak R. Gender-based differences in pharmacokinetics in laboratory animal models. *Int J Toxicol.* 2001;20:161–163.
- 35 Tsai D, Jamal J-A, Davis JS, Lipman J, Roberts JA. Interethnic differences in pharmacokinetics of antibacterials. *Clin Pharmacokinet.* 2015;54:243–260.
- 36 Poggesi I, Benedetti MS, Whomsley R, Le Lamer S, Molimard M, Watelet J-B. Pharmacokinetics in special populations. *Drug Metab Rev.* 2009;41:422–454.
- 37 McGonigle P, Ruggeri B. Animal models of human disease: challenges in enabling translation. *Biochem Pharmacol.* 2014;87:162–171.
- 38 Kaur N, Narang A, Bansal AK. Use of biorelevant dissolution and PBPK modeling to predict oral drug absorption. *Eur J Pharm Biopharm.* 2018;129:222–246.
- 39 Toutain P-L, Ferran A, Bousquet-Melou A. Species differences in pharmacokinetics and pharmacodynamics. *Handbook Exp Pharmacol.* 2010;199:19–48.
- 40 Feng MR, Zheng N, Zhang X, Huh YM, Yu J-Y. Interspecies pharmacokinetic scaling and the prediction of human pharmacokinetics using animal and cell models. *Encyclopedia Drug Metab Interact.* 2012;2:495–530.
- 41 Giordanetto F, Jin C, Willmore L, Feher M, Shaw DE. Fragment hits: What do they look like and how do they bind? *J Med Chem.* 2019;62:3381–3394.
- 42 Saxty G, Norton D, Affleck K, et al. Identification of orally bioavailable small-molecule inhibitors of hematopoietic prostaglandin D₂ synthase using X-ray fragment based drug discovery. *Med Chem Commun.* 2014;5:134–141.
- 43 Deaton DN, Do Y, Holt J, et al. The discovery of quinoline-3-carboxamides as hematopoietic prostaglandin D synthase (H-PGDS) inhibitors. *Bioorg Med Chem.* 2019;27:1456–1478.
- 44 Clark DE. Computational prediction of blood-brain barrier permeation. *Ann Rep Med Chem.* 2005;40:403–415.
- 45 Fong CW. Permeability of the blood-brain barrier: Molecular mechanism of transport of drugs and physiologically important compounds. *J Membr Biol.* 2015;248:651–669.
- 46 Abraham MH. The factors that influence permeation across the blood-brain barrier. *Eur J Med Chem.* 2004;39:235–240.
- 47 Seelig A. The role of size and charge for blood-brain barrier permeation of drugs and fatty acids. *J Mol Neurosci.* 2007;33:32–41.
- 48 Mahar Doan KM, Humphreys JE, Webster LO, et al. Passive permeability and P-glycoprotein-mediated efflux differentiate central nervous system (CNS) and non-CNS marketed drugs. *J Pharmacol Exp Ther.* 2002;303:1029–1037.
- 49 Hitchcock SA, Pennington LD. Structure - brain exposure relationships. *J Med Chem.* 2006;49:7559–7583.
- 50 van de Waterbeemd H, Camenisch G, Folkers G, Chretien JR, Raevsky OA. Estimation of blood-brain barrier crossing of drugs using molecular size and shape, and H-bonding descriptors. *J Drug Targeting.* 1998;6:151–165.
- 51 Cadilla R, Deaton D.N., Hancock A.P., et al. Quinoline-3-carboxamides as H-PGDS inhibitors. PCT Int. Appl. WO 103851, 2017; Chem. Abstr. 2017, 167, 113565.
- 52 Deaton D.N., Shearer B.G., Youngman M.A. Chemical compounds as H-PGDS inhibitors. PCT Int. Appl. WO 229629, 2018; Chem. Abstr. 2018, 170, 123921.
- 53 Deaton D.N., Guo Y., Hancock A.P., et al. Preparation of 1,3-disubstituted cyclobutane or azetidine derivatives as hematopoietic prostaglandin D synthase (H-PGDS) inhibitors. PCT Int. Appl. WO 069863, 2018; Chem. Abstr. 2018, 168, 450876.
- 54 Dahl G, Akerud T. Pharmacokinetics and the drug–target residence time concept. *Drug Discov Today.* 2013;18:697–707.
- 55 Trujillo JJ, Kiefer JR, Huang W, et al. Investigation of the binding pocket of human hematopoietic prostaglandin (PG) D₂ synthase (hH-PGDS): A tale of two waters. *Bioorg Med Chem Lett.* 2012;22:3795–3799.
- 56 Jakobsson P-J, Thorén S, Morgenstern R, Samuelsson B. Identification of human prostaglandin E synthase: a microsomal glutathione-dependent, inducible enzyme, constituting a potential novel drug target. *Proc Natl Acad Sci USA.* 1999;96:7220–7225.
- 57 Gillie DJ, Novick SJ, Donovan BT, Payne LA, Townsend C. Development of a high-throughput electrophysiological assay for the human ether-a-go-go related potassium channel hERG. *J Pharmacol Toxicol Methods.* 2013;67:33–44.
- 58 Rothchild AM. Mechanisms of histamine release by compound 48/80. *Br J Pharmacol.* 1970;38:253–262.
- 59 Grounds MD, Radley HG, Lynch GS, Nagaraju K, De Luca A. Towards developing standard operating procedures for pre-clinical testing in the mdx mouse model of Duchenne muscular dystrophy. *Neurobiol Dis.* 2008;31:1–19.
- 60 Boger DL, Ledebor MW, Kume M, Searcey M, Jin Q. Total synthesis and comparative evaluation of luzopeptin A-C and quinoxapeptin A-C. *J Am Chem Soc.* 1999;121:11375–11383.
- 61 Flynn D.L., Kaufman M.D., Vogeti L., et al. Preparation of naphthyridinylphenyl ureas as Raf inhibitors. PCT Int. Appl. WO 134298, 2013; Chem. Abstr. 2013, 159, 486154.
- 62 Reichardt C, Scheibelein W. Synthese 6-substituierter 2-amino-1,8-naphthyridine aus substituierten malonaldehyden. *Tetrahedron Lett.* 1977;18:2087–2090.
- 63 Dowling MS, Fernando DP, Hou J, Liu B, Smith AC. Two scalable syntheses of (S)-2-methylazetidine. *J Org Chem.* 2016;81:3031–3036.
- 64 Veber DF, Johnson SR, Chen H-Y, Smith BR, Ward KW, Kopple D. Molecular properties that influence the oral bioavailability of drug candidates. *J Med Chem.* 2002;45:2615–2623.
- 65 Kany M, Senner F, Gubernator K. Physicochemical high throughput screening: parallel artificial membrane permeation assay in the description of passive absorption processes. *J Med Chem.* 1998;41:1007–1010.
- 66 Sou T, Bergström CAS. Automated assays for thermodynamic (equilibrium) solubility determination. *Drug Disc Today: Tech.* 2018;27:11–19.
- 67 Bunally S, Young RJ. The role and impact of high throughput biomimetic measurements in drug discovery. *ADMET & DMPK.* 2018;6:74–84.
- 68 Valko K, Nunhuck S, Bevan C, Abraham MH, Reynolds DP. Fast gradient HPLC method to determine compounds binding to human serum albumin. Relationships with octanol/water and immobilized artificial membrane lipophilicity. *J Pharm Sci.* 2003;92:2236–2248.